

**Dissolvable Silk Films for Oral Mucosal  
Delivery of the Antimalarial Drug  
Mefloquine Hydrochloride**

A Thesis

Submitted by

Joy A. Ajayi-Carrier

In partial fulfillment of the requirements for the degree of

Master of Science

In

Bioengineering

TUFTS UNIVERSITY

May 2016

ADVISER:

Dr. David L. Kaplan

# ABSTRACT

Of all of the infectious diseases known in modern times {e.g. Tuberculosis, Cholera, Ebola, Severe Acute Respiratory Syndrome (SARS), Meningitis, Middle Eastern Respiratory Syndrome (MERS)} none has had greater impact on global health as malaria. About 1.2 billion people live in areas endemic with this disease with nearly half a million fatalities every year. Chemotherapeutic applications since the 1820s have been formulated as preventative measures and for the treatment of malaria infections. Unfortunately, since its inception, multiple issues with patient compliance and drug formulations have led to increasing resistance from the malaria causing parasite *Plasmodium*. This project focuses on using oral film technology (OFT) with the novel application of dissolvable silk films for drug delivery to the oral mucosa. The antimalarial prophylactic, mefloquine hydrochloride was studied and found to be suitable for this application. This approach has potential to be instrumental as a type of application for other antimalarial therapeutics that are unable to be orally administered and also to increase patient compliance in areas endemic with the disease.

# ACKNOWLEDGEMENTS

I will first thank God because without His grace, mercy, and blessing I would not be here today sharing this milestone with the people I love. I would like to thank my Dad, Mr. Raphael Ajayi, because without all you have sacrificed I wouldn't be here today. Thank you to my brothers and sisters: Michael, Ayo, Kunle, Taiwo, Kehinde, and Idowu for their support. To my husband, James Carrier, thank you for your patience, resilience, and sacrifice through this journey. Rest of my family, Mr. Ed Carrier, Mrs. Joan Carrier, Heidi, Jim, and Evan thank you for support. Thank you to Pastor Orlando Harris and New Life Christian Ministries for their spiritual guidance. Thank you to my close friends outside of Tufts (Iyabo, Patricia, Tara, Olivia, Brian, Angie, and my sorority sisters in my O EZ chapter of Zeta Phi Beta Sorority, Incorporated) and at Tufts (Elise, Judith, Jess, and Dr. Gittens). To my thesis committee - Professor Qiaobing Xu - thank you for your patience and continuing support during this journey. To Professor Hyunmin Yi - thank you for your interest in my research and teaching one of the best lab courses I've taken while at Tufts. To Professor David Kaplan, words fail to express how grateful I am to have you as an adviser, fellow Giants fan, and fellow Syracuse alum. Go 'CUSE! Dr. Jeannine Coburn thank you for all your guidance, your wealth of knowledge, and being a prime example of being down to earth and driven. Dr. Ming Wang thank you for answering every single question I had while I was in Xu's lab.

Lastly, I would like to dedicate this to my Mom, Ms. Anne Adeyinka Omolola, who I hope to share this amazing accomplishment with in the near future.

## TABLE OF CONTENTS

ABSTRACT .....	ii
ACKNOWLEDGEMENTS .....	iii
TABLE OF CONTENTS .....	v
LIST OF TABLES .....	ix
LIST OF FIGURES .....	xi
ABBREVIATIONS .....	xviii
CHAPTER 1: Introduction .....	1
1.1 Malaria - Clinical Relevance and Need.....	1
1.1.1. Rate of Infection, Reported Deaths, and Rate of Decline .....	1
1.1.2. Financial Burden.....	4
1.1.3. Method of Infection .....	6
1.1.4. Current Drug-targeting Approaches and Treatments for Malaria: Progress and Issues .....	10
1.2 Oral Disintegrating Films.....	16
1.2.1. Various Routes of Administration.....	16
1.2.2. Oral Film Technology (OFT) .....	27
1.2.3. Structure and Environment of the Oral Mucosa with Focus on Drug Delivery .....	38
1.2.4. Permeability Barriers and Absorption Mechanism of the Oral Mucosa .....	43
1.2.5. Different Types of OFTs and Formulation Characteristics .....	45
1.2.6. Oral Disintegrating Films (ODFs) - Potential Use/Benefits.....	51

1.3 Silk Fibroin Protein .....	52
1.3.1. The Wonderful World of Silk and Its Biomedical Applications .....	52
1.3.2. Silk Films.....	59
1.4. Research Objectives/Aims .....	60
1.4.1. Aim#1 - Determining drug loading of dissolvable silk fibroin films with mefloquine hydrochloride. ....	61
1.4.2. Aim#2 – Determining the rate of disintegration for dissolvable silk films as well as characterizing the rate of drug release of mefloquine hydrochloride from these films.....	62
1.4.3. Aim#3 – Establishing the robustness of dissolvable silk films for packaging and handling. ....	63
1.4.4. Aim#4 - Ensuring that Mefloquine Encapsulated Silk Films Do Not Illicit Immunogenic Effects .....	63
CHAPTER 2: Methods and Materials .....	64
2.1. Silk Fibroin Extraction: .....	64
2.2. Fabrication and Drug Loading into Silk Films.....	65
2.2.1. Fabrication of Silk Films .....	65
2.2.2. Drug Loading of Mefloquine Hydrochloride and Doping of Food Dye to Silk Films.....	65
2.2.3. Measuring Drug Loading Efficiency of Dissolvable Silk Films .....	68
2.3. Mechanical Properties .....	69

2.3.1. Mechanical Testing for Ultimate Tensile Strength, Elastic Modulus, & Strain to Failure (%) .....	69
2.3.2. Film Thickness .....	70
2.4. Disintegration Testing of Dissolvable Silk Films .....	70
2.5. <i>In Vitro</i> Dissolution Studies of Dissolvable Silk Films .....	71
2.6 Scanning Electron Microscope (SEM).....	72
2.7. Fourier Transform Infrared Spectroscopy (FTIR) .....	72
2.8. Cytotoxicity Testing of Dissolvable Silk Films with Mefloquine Hydrochloride.....	73
2.9 Statistical Analysis .....	75
CHAPTER 3: Results .....	76
3.1. Morphology .....	76
3.1.1. Silk Films Preparation, Appearance, and Weight.....	76
3.1.2. Scanning Electron Microscopy (SEM) of Dissolvable Silk Films .....	79
3.1.3. Fourier Transform Infrared Analysis (FTIR) .....	82
3.2. Disintegration Testing of Silk Films Doped with Blue Food Dye.....	84
3.3. Drug Loading of Mefloquine Hydrochloride with Dissolvable Silk Films	89
3.4. <i>In vitro</i> Dissolution Testing of Dissolvable Silk Films with Mefloquine Hydrochloride.....	91
3.5. Mechanical Testing of Dissolvable Silk Films .....	93
3.6. <i>In vitro</i> Cytotoxicity Testing of Silk Films .....	97
CHAPTER 4: Discussion and Future Directions.....	102

4.1. Discussion .....	102
4.1.1. Determining Drug Loading Efficiency of Dissolvable Silk Films ...	102
4.1.2. Determining Rate of Disintegration & Dissolution of Dissolvable Silk Films Doped with Mefloquine Hydrochloride .....	103
4.1.3. Establishing Robustness of Dissolvable Silk Films for Packaging and Handling .....	105
4.1.4. Cytotoxicity Study of Dissolvable Silk Films with Mefloquine .....	107
4.2. Future Directions.....	109
4.2.1. Stability Testing of Dissolvable Silk Films .....	109
4.2.2. Effects of Degumming Time and Fabrication of Silk Films .....	111
4.2.3. Perfusion Studies of Silk Films with Oral Mucosa Models .....	111
BIBLIOGRAPHY .....	114



# LIST OF TABLES

Table 1: Current antimalarial treatments, their cellular targets, advantages and disadvantages, clinical indications, and drug-susceptibility to Plasmodium species (Santos-Magalhaes, 2010).....	13
Table 2: Pros and cons of different routes of drug administration ( <a href="http://www.doctors.net.uk/_datastore/ecme/mod1227/Drug_dosage_Table1.pdf">http://www.doctors.net.uk/_datastore/ecme/mod1227/Drug_dosage_Table1.pdf</a> ). .....	17
Table 3: Market and Share of Pharmaceuticals by Route of Administration ( <a href="https://www.boomer.org/c/p4/c07/c07.pdf">https://www.boomer.org/c/p4/c07/c07.pdf</a> ). ....	18
Table 4: Marketed products - mostly over the counter oral films (Nagaraju et al., 2013). ....	30
Table 5: OFT platforms, their owners or developers, related patents and associated marketed prescription products (Borges et al., 2015).....	33
Table 6: Regional Variation in Epithelial Thickness and Permeability Pattern within Oral Mucosa. ++ means “very suitable”; -- means “least suitable”; NK means “Non-Keratinized”; K means “Keratinized” (Campisi et al., 2010).....	41
Table 7: Formulation and evaluation of polymers for oral disintegrating films (Nagaraju et al., 2013). ....	50
Table 8: Biomedical applications of silk scaffolds (Rockwood et al., 2011). ....	57
Table 9: Examples of the various routes of administration that have been established with silk (Seib et al., 2013). ....	58
Table 10: Table highlighting overview of aims for current thesis research. ....	60

Table 11: Comparison of the disintegration times amongst the different concentration of silk films in media (PBS/DiH <sub>2</sub> O). (N = 3); p≤ (0.01).....	87
Table 12: Conditions for stability testing according to ICH. *It is up to the applicant to decide whether long term stability studies are performed at 25 ± 2°/40% RH or 30°C ± 2°C/35% RH ±5% RH. **If 30°C ± 2°C/35% RH ±5% RH is the long-term condition, there is no intermediate condition. ....	110
Table 13: Drugs studied with porcine models for oral transmucosal drug delivery (Sattar et al., 2014).....	113

# LIST OF FIGURES

Figure 1: Countries with ongoing transmission of malaria, 2013 (World Health Organization 2014) .....	3
Figure 2: Malaria deaths per 100,000 populations in 2013 (World Health Organization 2014) .....	3
Figure 3: Percentage of population living on under US\$2 per day, 1995 – 2013 (World Health Organisation, 2014). .....	5
Figure 4: Anticipated funding if a) domestic and international investments increase in line with total government expenditure growth estimated by the International Monetary Fund for 2014-2020, and b) funders prioritize further investments in malaria control (World Health Organization, 2014).....	5
Figure 5: The life cycle of the Plasmodium parasite from the Anopheles vector to human host (Greenwood et al., 2008). .....	7
Figure 6: Diagram displaying drug targets of cellular components in a red blood cell invaded by merozoites (Greenwood et al., 2008). .....	12
Figure 7: Typical plot of Plasma concentration versus time after oral administration of fast (blue) and slow (green) dosage forms (www.boomer.org/c/p4/c07/c07.html).....	18
Figure 8: Typical plot of plasma concentration versus time after inhalation administration (www.boomer.org/c/p4/c07/c07.html). .....	20
Figure 9: Typical plot of plasma concentration versus time after rectal administration (https://www.boomer.org/c/p4/c07/c07.html). .....	20

Figure 10: Typical plot of plasma concentration versus time after topical administration ( <a href="https://www.boomer.org/c/p4/c07/c07.html">https://www.boomer.org/c/p4/c07/c07.html</a> ) .....	24
Figure 11: Illustration detailing the site of intramuscular (IM) injection, intravenous (IV) administration, and subcutaneous (SC) injection ( <a href="http://www.boomer.org/c/p4/c07.html">www.boomer.org/c/p4/c07.html</a> ). ....	24
Figure 12: Typical plot of plasma concentration versus time after subcutaneous administration ( <a href="http://www.boomer.org/c/p4/c07/c07.html">www.boomer.org/c/p4/c07/c07.html</a> ). ....	25
Figure 13: Typical plot of plasma concentration versus time after intramuscular administration ( <a href="http://www.boomer.org/c/p4/c07/c07.html">www.boomer.org/c/p4/c07/c07.html</a> ). ....	25
Figure 14: Typical plot of plasma concentration versus time after intravenous infusion administration ( <a href="http://www.boomer.org/c/p4/c07/c07.html">www.boomer.org/c/p4/c07/c07.html</a> ). ....	26
Figure 15: Typical plot of plasma concentration versus time after intravenous bolus administration ( <a href="http://www.boomer.org/c/p4/c07/c07.html">www.boomer.org/c/p4/c07/c07.html</a> ). ....	26
Figure 16: Different local application sites of the oral films. Depending on the type of films the site of application may vary (Borges et al., 2015). ....	39
Figure 17: Photography of three oral films and their corresponding dimensions (Castro et al., 2015). ....	39
Figure 18: Bioadhesive interactions. Simplified oral mucosa representation: sub-mucosa with nerves and blood vessels, lamina propria, essentially with connective tissue and with some blood vessels, basement membrane usually a single cell layer lying in the interface of the epithelium and lamina propria; a simplified oral epithelium only for representative purposes; and a mucus layer with mucin and glycoproteins. The mucoadhesiveness of the polymers to the oral mucosa may be	

explained by the non-covalent and covalent bonds, depending on the polymers' functional groups (Borges et al.,2015).....	41
Figure 19: Ultra-structural features of oral buccal epithelium. MCGs become evident microscopically in the prickle cell layer, approximately at the midpoint of the epithelium (Campisi et al., 2010).....	42
Figure 20: Routes of drug transport across oral epithelium (Campisi et al., 2010). .....	42
Figure 21: Schematic representation of different type of mucosal drug delivery system (Patel et al., 2011). .....	47
Figure 22(a-d): Schematic representation of some adhesive buccal drug delivery systems (Borges et al., 2015). .....	47
Figure 23: Simplified scheme with the different technologies (Borges et al., 2015). .....	50
Figure 24: Schematic of material forms fabricated from silk fibroin protein using both organic solvents and aqueous-based processing approaches (Rockwood et al., 2011). .....	56
Figure 25: Diagram of silk sources & various drug delivery systems. Numbers in parentheses refer to the approximate sizes of these materials; diameters or thickness in the case of particles & films/coatings, respectively (Seib et al., 2013). .....	56
Figure 26: Schematic of the silk fibroin extraction procedure. Starting from the raw material (cocoons) to the final aqueous solution takes 4 days (Rockwood et al., 2011). .....	64

Figure 27: Schematic of silk film fabrication for mechanical testing, disintegration testing, SEM imaging, FTIR characterization. ....	66
Figure 28: Schematic of silk film fabrication for disintegration testing. ....	66
Figure 29: Schematic of silk film fabrication and drug loading for drug loading, dissolution, and cytotoxicity testing. ....	67
Figure 30: Photo showing dried silk film sample (6% w/v) doped with mefloquine hydrochloride (dimensions: 33mm x 23mm). ....	77
Figure 31: Fabrication of 1% Silk Films Doped with Blue Food Dye (Dimensions of the films 33mm x 23mm; Dimensions of PDMS Molds = 33m x 23mm). ....	77
Figure 32: Graph displaying the relationship of silk concentration versus average mass of DSF. Error bars represent standard deviation of the samples (N=4); p (0.000005) $\leq$ (.05). ....	78
Figure 33: : SEM Image of Cross-section of 4% Silk Films without Mefloquine (scale = 20 $\mu$ m). ....	80
Figure 34: SEM Image of Cross-section of 5% Silk Films Doped with Mefloquine (scale = 20 $\mu$ m). ....	80
Figure 35: SEM Image of Cross-section of 2% Silk Films Doped with Mefloquine (scale = 20 $\mu$ m). ....	81
Figure 36: SEM image of the surface of 2% “as-casted” dissolvable silk film (scale = 20 $\mu$ m). ....	81
Figure 37: FTIR spectrum of dissolvable silk films (1-6%) without mefloquine hydrochloride. ....	83

Figure 38: FTIR spectrum of dissolvable silk films (1-6%) with mefloquine hydrochloride. ....	83
Figure 39: Disintegration Testing of 2% Silk Films Dissolving in Distilled Water (pH = 7).....	86
Figure 40: Disintegration Testing of 4% Silk Films Dissolving in PBS (pH=7). ....	86
Figure 41: Graph displays the relationship of silk concentration versus percentage of film disintegration in PBS (pH = 7). Error bars represent standard deviation of samples (N=3); $p \leq (0.01)$ . ....	87
Figure 42: Graph displays the relationship of silk concentration versus percentage of film disintegration in DiH <sub>2</sub> O (pH=7). Error bars represent standard deviation of the samples (N = 3); $p \leq (0.01)$ . ....	88
Figure 43: Total mass of mefloquine hydrochloride loaded into dissolvable silk films (1-6%). Error bars represent standard deviation of the samples (N = 3); $p (0.124) > (0.05)$ . ....	90
Figure 44: Percentage of mefloquine hydrochloride loaded into dissolvable silk films (1-6%). Error bars represent standard deviation of the samples (N = 3); $p (0.124) \geq (0.05)$ . ....	90
Figure 45: Rate of cumulative mass release of mefloquine from dissolvable silk films. Error bars represent standard deviation of the samples; $p \leq 0.01$ . ....	92
Figure 46: Cumulative rate release (%) of mefloquine from dissolvable silk films. Error bars represent standard deviation of the samples; $p \leq 0.01$ . ....	92
Figure 47: Flow chart of different characterizations of films based on mechanical properties (Kundu et al., 2008). ....	94

Figure 48: Comparison of concentration of silk films versus thickness. Error bars represent standard deviation of the samples (N = 4) $p(0.002) \leq 0.01$ .....	94
Figure 49: Relationship of silk concentration versus strain to failure of silk films. Error bars represent standard deviation of samples (N=4); $p(0.01) \leq (0.01)$ .....	95
Figure 50: Relationship of silk concentration versus elastic modulus (MPa) of silk films. Error bars represent standard deviation of samples (N=4); $p(0.008) \leq (0.01)$ .....	95
Figure 51: Relationship of silk concentration versus UTS (MPa) of silk films. Error bars represent standard deviation of samples (N=4); $p(0.006) \leq (0.01)$ .....	96
Figure 52: Microscopic images of attachment and proliferation of fibroblasts after exposure to serial dilutions of stock solution of mefloquine hydrochloride (500ug/mL). (Scale bar = 10X magnification). ....	99
Figure 53: Quantitative assessment of the cell viability from exposure to serial dilutions of mefloquine hydrochloride on fibroblasts (Error bars represent standard deviation of the samples; N=3). ....	99
Figure 54: Microscopic images of attachment and proliferation of fibroblasts after exposure to dissolvable silk films (1 – 6%) doped with mefloquine hydrochloride in fibroblasts. (Scale bar = 10X Magnification). ....	100
Figure 55: Quantitative assessment of the cell viability from exposure to dissolvable silk films doped with mefloquine hydrochloride on fibroblasts (Error bars represent standard deviation of the samples; N=3). ....	100



Figure 56: Microscopic images of attachment and proliferation of fibroblasts after exposure to dissolvable silk films (1 – 6%) in fibroblasts. (Scale bar = 10X Magnification).....	101
Figure 57: Quantitative assessment of cell viability from exposure of dissolvable silk films on fibroblasts (Error bars represent standard deviation of the samples; N=3). .....	101

# ABBREVIATIONS

ACTs – Artemisinin-based Combination Therapies

API – Active Pharmaceutical Ingredient

ART – Artemisinin

$C_0$  = Concentration of Donor Chamber Maintained at Sink Conditions

$C_i$  = Initial concentration of compound solution (mg/mL)

$C_s$  = Equilibrium drug concentration of the solution

CMC – Carboxymethylcellulose

D = Diffusion Coefficient ( $\text{cm}^2/\text{s}$ )

DSF – Dissolvable Silk Films

E – Eudragite

EMEM – Eagle's Minimum Essential Medium

FSD – Fourier self-deconvolution

FTIR – Fourier Transform Infrared Analysis

H = Hydrated film thickness

HPMC – Hydroxypropyl methylcellulose

HPC – Hydroxypropyl Cellulose

HS – Horse Serum

ISO – International Organization for Standardization

J = Net flux ( $\text{mg cm}^{-2} \text{s}^{-1}$ )

$K_d$  = Partition coefficient

LS – Least Squared

MCC – Microcrystalline Cellulose

MCGs – Membrane Coating Granules

MF – Mefloquine Hydrochloride

OFT – Oral Film Technology

P = Permeability Coefficient

RH – Relative Humidity

Pen-Strep - Penicillin - Streptomycin

PBS – Phosphate Buffered Saline

PDMS – Polydimethylsiloxane

PEG – Polyethylene Glycol

PEO – Polyethylene Oxide (PEO)

PVA – Polyvinyl Alcohol

PVP – Polyvinyl Pyrrolidone

SEM – Scanning Electron Microscopy

SF – Silk Films

UTS – Ultimate Tensile Strength

$V_f$  = Volume of the Solvent Equilibrated Silk Films ( $\text{cm}^3$ )

$V_s$  = Volume of the Compound Solution (mL)

WHO – World Health Organization

# CHAPTER 1: Introduction

## 1.1 Malaria - Clinical Relevance and Need

Paul F. Russel, in 1931, perfectly states the importance of malaria's historical implications, "Man ploughs the sea like a leviathan, he soars through the air like an eagle; his voice circles the world in a moment, his eyes pierce the heavens; he moves mountains, he makes the desert to bloom; he has planted his flag at the north pole and the south; yet millions of men each year are destroyed because they fail to outwit a mosquito" (Shah, 2010). Of all of the infectious diseases known in modern times {e.g. Tuberculosis, Cholera, Ebola, Severe Acute Respiratory Syndrome (SARS), Meningitis, Middle Eastern Respiratory Syndrome (MERS)} none has had greater impact on global health as Malaria.

### 1.1.1. Rate of Infection, Reported Deaths, and Rate of Decline

The World Health Organization (WHO) estimates that every year approximately 3.3 billion people spanning over 90 countries are at risk of infection due to malaria. Of this population, at least 1.2 billion are at high risk of infection. Malaria's most prominent effect occurs in areas that lack government funding, standard of living, infrastructure, and adequate health care necessary to eradicate the disease. **Figures 1 & 2** displays regions in the world that are currently dealing with ongoing malaria transmission and mortality rates per country around the world. In the WHO African region alone, an estimated 128

million people from 18 countries (sub-Saharan Africa) were reported to have been infected with malaria by one of the species of the parasite *Plasmodium* - *P.*

*falciparum*. Countries located in sub-Saharan Africa deaths amongst children < 5 years old (95% ~ 3.92 million). make up 90% of the infections in the WHO Africa region. Of the 198 million reported cases from all WHO regions, 584,000 deaths were reported to the WHO of which 90% of the deaths occurred in the WHO African region alone. The World Health Organization approximated that 453,000 deaths occurred in children under the age of 5. An estimated 96% of those reported deaths amongst children occurred in the WHO African region.

There are signs that malaria may be losing its stronghold on the global population. Since tracking cases began in 2000, WHO estimated that the percentage of the population at risk for malaria has decreased by a rate of 25% globally (227 million to 198 million) and by 43% in the WHO African Region. From 2000 - 2013, the rate of reported cases has decreased by a rate of 30% globally and 34% in the WHO African Region. Focusing on mortality rates, WHO reported a decline of 47% globally and 54% in the WHO African Region. In children under the age of 5, WHO reports a reduction in malaria mortalities by the rate of 53% globally and 58% in the WHO African Region. If the pace of reduction in risk of infection, reported cases, and mortalities continues to decline at this rate annually WHO projects a decrease in reported cases by 35% globally and 40% in the WHO African Region. WHO also projects a drop in deaths by 55% globally and 62% in the WHO African Region. This includes a dent in

deaths in children < 5 years old by 61% globally and 67% in the WHO African Region by 2015.

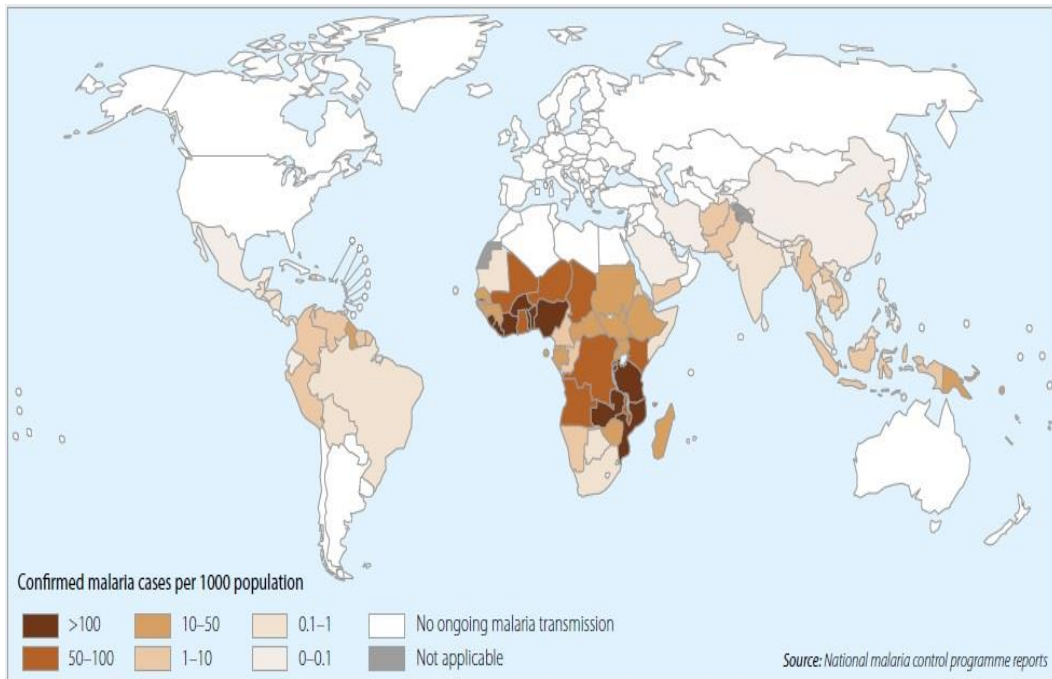


Figure 1: Countries with ongoing transmission of malaria, 2013 (World Health Organization 2014)

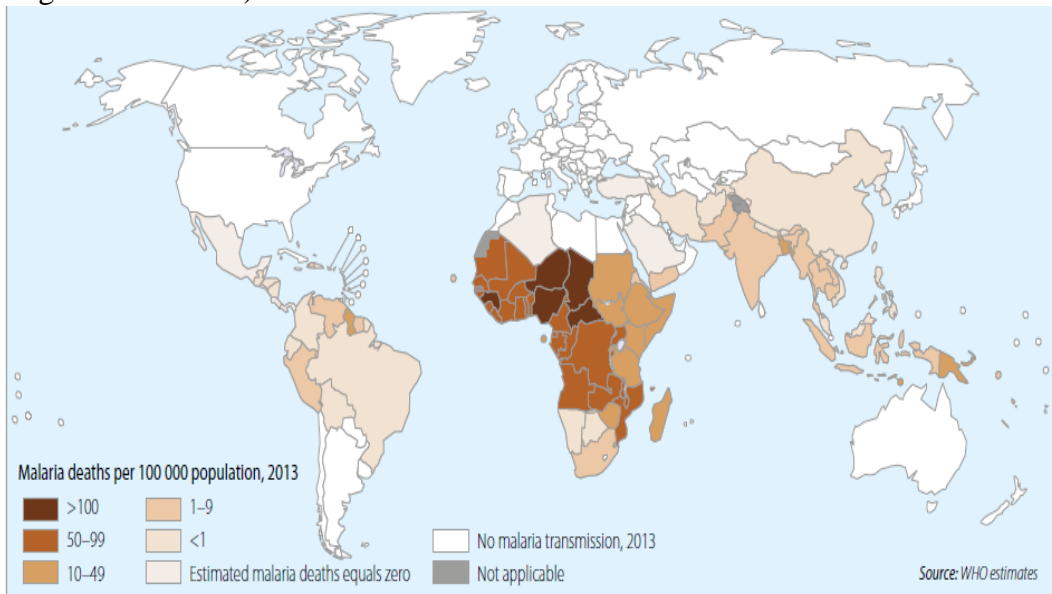


Figure 2: Malaria deaths per 100,000 populations in 2013 (World Health Organization 2014)

The WHO reports that 58 countries are projected to achieve a reduction rate in malaria mortality of >75% by 2015 globally. WHO also reports that between 2000 -2013, there was an estimated 670 million fewer cases and 4.3 million fewer deaths were prevented worldwide. Of the estimated 4.3 million deaths averted 3.9 million were among children under the age of 5 years old in sub-Saharan Africa. A high number of averted cases occurred in regions endemic with malaria. The WHO African Region had the highest rate of aversion for reported cases (66% ~ 444 million), overall deaths (92% ~ 3.93 million), and deaths amongst children < 5 years old (95% ~ 3.92 million).

#### **1.1.2. Financial Burden**

Financing for these global malaria programs have been an important factor in staying on target for the eradication of this disease. These initiatives are directed towards areas that lack government funding, have poor standard of living, and unequal infrastructure necessary to eradicate this disease. **Figures 3 & 4** highlights the cost of living in areas endemic with the disease and the global financing in eradicating this disease. The World Health Organization reported that global funding for malarial control and elimination has increased from over US\$900 million in 2005 to nearly US\$2.7 billion in 2013. 82% of total malaria funding (US\$2.18 billion) in 2013 were from global investments alone. Domestic investments also grew during the same time period at a rate of 4% in the WHO African Region compared to 2% in all other WHO Regions. In 2013 alone, the WHO African Region accounted for 72% of total funding (91% global funding

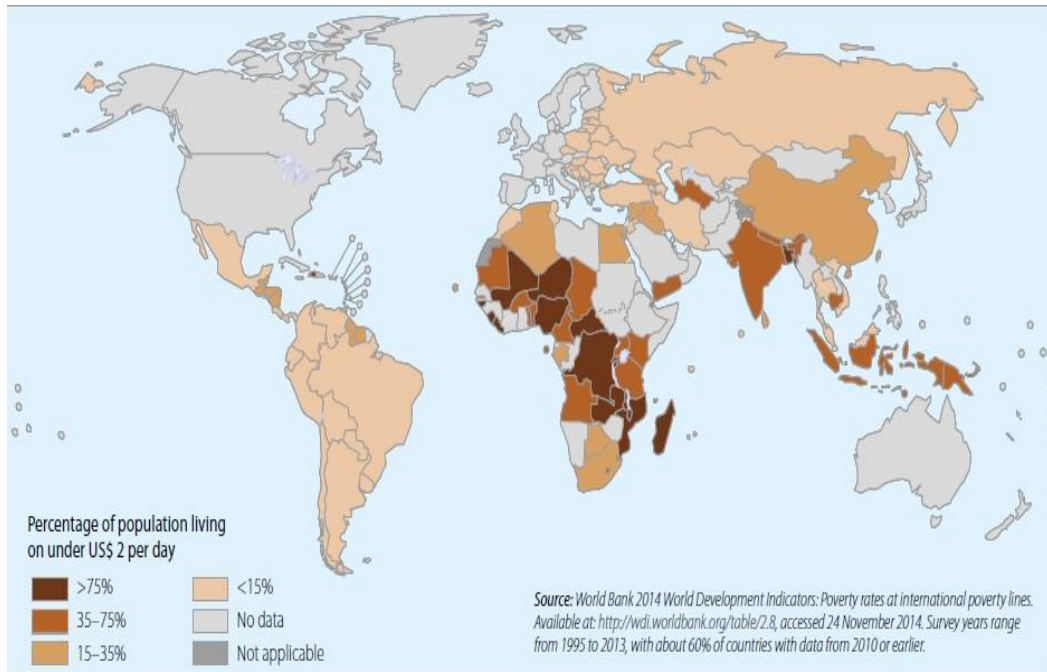


Figure 3: Percentage of population living on under US\$2 per day, 1995 – 2013 (World Health Organisation, 2014).

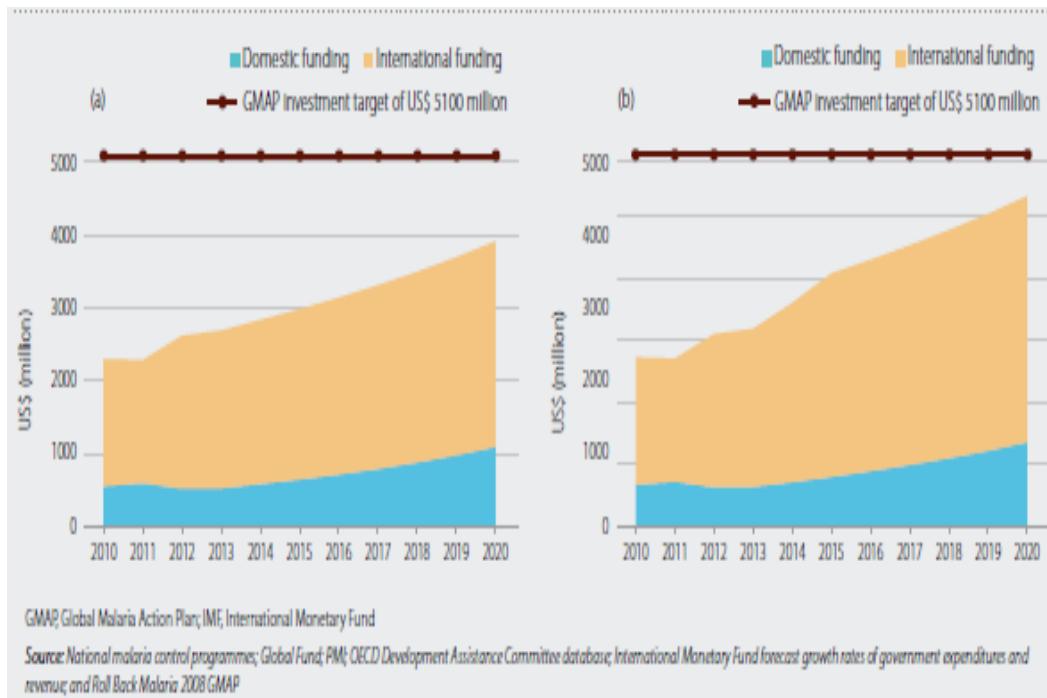


Figure 4: Anticipated funding if a) domestic and international investments increase in line with total government expenditure growth estimated by the International Monetary Fund for 2014-2020, and b) funders prioritize further investments in malaria control (World Health Organization, 2014).



compared to 41% in other WHO Regions) compared to 50% in 2005. The World Health Organization projects a significant increase in malaria funding as long as global investments are in line with domestic funding. This will come down to domestic and international funders establishing malaria control as a top priority in future investments.

### **1.1.3. Method of Infection**

As mentioned earlier, the genus of parasite that has been identified and associated with the cause of malaria infections is the parasitic Protozoan *Plasmodium*. This parasite consists of 5 species: *Plasmodium falciparum*, *Plasmodium vivax*, *Plasmodium malariae*, *Plasmodium ovale*, and *Plasmodium knowlesi*. The first four species are transmitted to humans by the female mosquito of the genus *Anopheles*. Although, there are over 400 different species of the *Anopheles* mosquitoes in existence, only 30 of these act as vectors for transmitting this disease. *P. falciparum* is the deadliest of the species due to its high mortality rate. It is also known to cause the complicated (severe) form of malaria that can be fatal if the patient does not receive adequate treatment immediately. This is due to its capability to bind to the epithelium during the blood stage (erythrocytic stage) and isolates itself in organs including the brain (severe malaria) (MacPherson et al., 1985; Krettli and Miller, 2001). The second deadliest species, *P. vivax* parasite, has the ability to develop in the *Anopheles* mosquitoes at lower temperatures and survive higher altitudes. This allows the parasite to acclimate well at cooler climates which translates it to a much broader

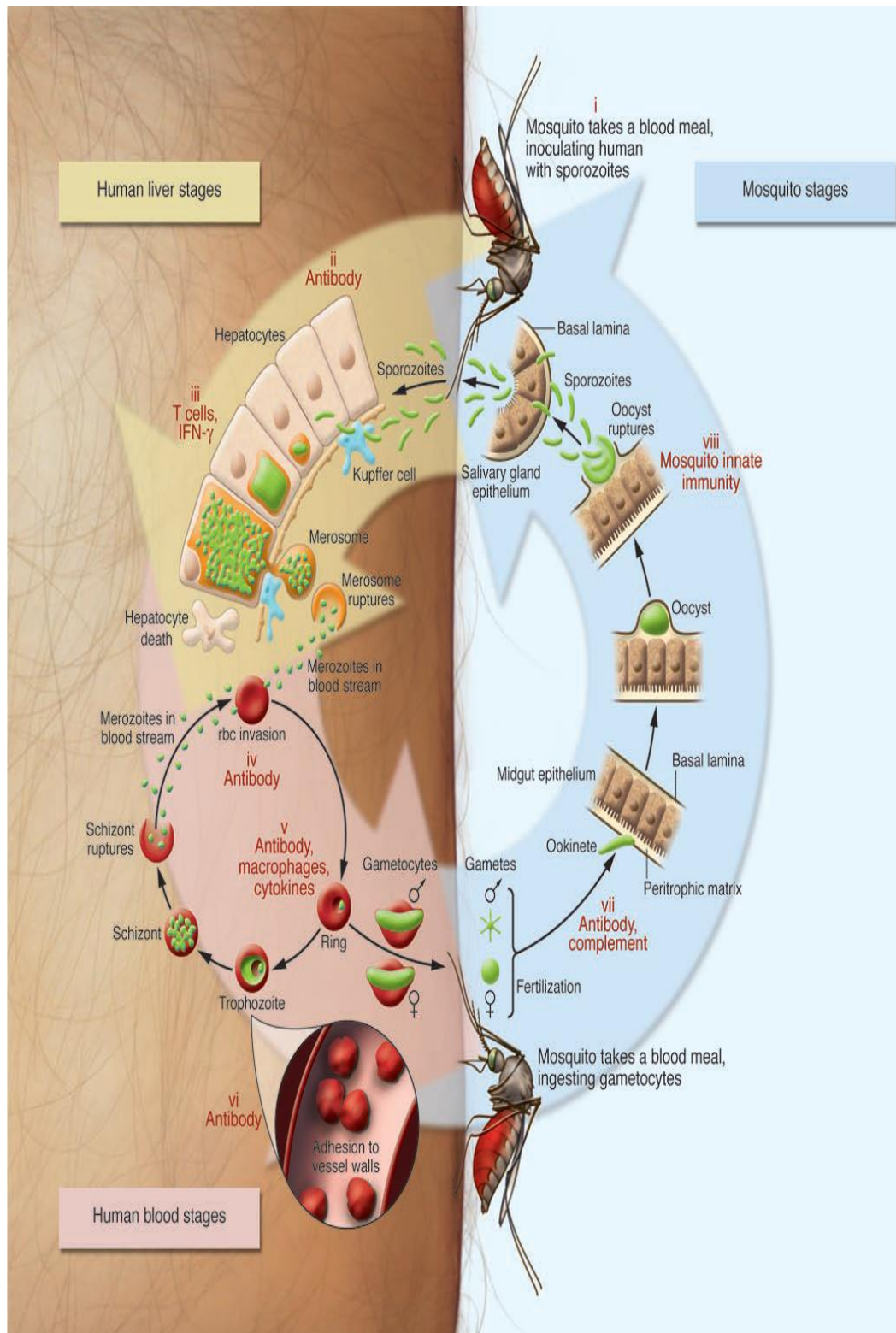


Figure 5: The life cycle of the *Plasmodium* parasite from the *Anopheles* vector to human host (Greenwood et al., 2008).

geographic impact compared to *P. falciparum*. Its life cycle also gives it the ability to live dormant in an infected individual for long periods of time causing relapses in infected patients. In India, Indonesia, and Pakistan, *P. vivax* infections account for 80% of the estimated infectious cases. In contrast, the *P. vivax* parasite has the least impact in the WHO African Region due to the absence of the Duffy gene from the African population (Shah, 2010).

The life cycle of the *Plasmodium* parasite begins in the vector - *Anopheles* mosquito. **Figure 5** illustrates the journey of the Plasmodium parasite from vector to host. Following ingestion during from the mosquito's blood meal from an infected human host, the gametocytes of the parasite finds its way to the vectors midgut lumen (Ghosh et al., 2000). Once in the basal lumen, the gametocytes rapidly differentiate into gametes, commencing the process of exflagellation which allows the formation of ookinetes, the invasive form of the parasite (Sinden and Hartley, 1985; Ghosh et al., 2000; Weber, 1988) . The ookinetes will now cross through the peritrophic matrix and invades the midgut epithelium (Torii et al., 1992; Syafruddin et al., 1991.; Ghosh et al., 2000). It will then traverse to the apical side of the epithelium and attaches itself to the epithelium differentiating to an oocyst. After approximately 10 - 24 days the oocyst ruptures introducing thousands of sporozoites into the hemolymph which then invades the distal lateral and medial salivary gland lobes (Ghosh et al., 2000). This cycle occurs in 25 days. Once the female *Anopheles* embarks on its next blood meal, the infectious sporozoites is inoculated in its second human host. There are varying theories describing the journey of sporozoites after inoculation

but there is a consensus that the parasite eventually makes its way to the host's liver where they invade hepatocytes. During this invasion the sporozoites evolve to hypnozoites.

This asymptomatic stage in the liver is known as the exo-erythrocytic stage. Hypnozoites are capable of lying dormant in the liver for months and is the main cause of relapses in infective individuals even up to two years post inoculation (Santos-Magalhães and Mosqueira, 2010). During this invasion (period of 6 days) each single hypnozoite is generating tens of thousands of merozoites (30,000 for *P falciparum* or 10,000 - *P vivax*) which will eventually rupture the invaded hepatocytes (Greenwood et al., 2008; Santos-Magalhães and Mosqueira, 2010). The newly formed merozoite commences the second stage of the parasitic cycle in the human host, the erythrocytic stage. During this stage, asexual forms of the parasite undergo repeated cycles of propagation. This includes gametocytes that will participate in the recursion cycle when it's ingested during another blood meal. After entering the bloodstream, the merozoites invades the red blood cells and lay dormant for a period of 10-15hrs (the ring stage). The parasite will then undergo a rapid stage of growth for the next 25hrs. This is characterized as the trophozoite stage. This will cause the parasite to expand more than 50% of the original size of the invaded cell. During the final cycle of this stage, the schizonts phase, the parasite divides several times within the infected red blood cell. 48 hours post cell invasion, the schizonts lyses the red blood cells and releases newly formed merozoites which will continue the recursion cycle. It is during this event that clinical malarial symptoms are noticed

such as headaches, recurrent high fevers, and anemia to name a few (Santos-Magalhães and Mosqueira, 2010). Since these symptoms closely resembles the flu, patients may fail to seek adequate treatment resulting in the development of the fatal form known as cerebral malaria. At this phase, symptoms would have evolved to neurological complications can have a lasting effect on survivors but can still be fatal in young children. This is due to the parasite's ability to inhibit blood flow in small vessels of the brain causing cerebral oedema and increased intra-cranial hypertension which can be fatal (Santos-Magalhães and Mosqueira, 2010).

#### **1.1.4. Current Drug-targeting Approaches and Treatments for Malaria:**

##### **Progress and Issues**

Malaria chemotherapy has been in existence since the 1820s when the pure chemical compound quinine was first isolated from cinchona bark. Around the same period methylene blue, developed by German scientist Paul Ehrlich, became the first synthetic chemical compound to treat malaria in humans (Rosenthal, 2001). Unfortunately, just as long as the manufacturing of malarial treatments have been in existence so has the evolution of *Plasmodium*'s potential resistance to antimalarial chemotherapeutics. Since the 1940s, the race to generate synthetic antimalarials has been the primary focus in the goal of eradicating malaria. One strategy of generating antimalarials has been the sequencing of the parasite's genome and use of functional genomics (Greenwood et al., 2008). Benefits of this research has elucidated drug targets of intervention

for several process during the parasite's life cycle (hepatocytes and erythrocytes). This includes hemoglobin degradation and heme detoxification, folate biosynthesis, and protein synthesis, in the apicoplast. **Figure 6** displays antimalarial drug targets in an infective cell. **Table 1** lists all of the current antimalarial treatments, their cellular targets, and the benefits and dangers associated for each treatment.

General characteristics for the ideal antimalarial candidate includes: fast acting, highly potent against sporozoites and merozoites (infectious forms of the parasite), minimal toxicity, and reasonably affordable individuals living in endemic areas (Greenwood et al., 2008). One primary issue when it comes to development and use of antimalarial drugs is *Plasmodium*'s invariant ability to evolve and become resistant against a plethora of these antimalarials.

Chloroquine, a synthetic derivative of the antimalarial quinine, was developed during World War II and was once considered as a powerful agent in treating malaria. It was the antimalarial product of choice by the WHO Global Eradication Program during the 1950s and 1960s. In the 1950s, signs of chloroquine resistance from *Plasmodium falciparum* began to emerge. Shortly after chloroquine-resistance disseminated world-wide (Rosenthal, 2001). As of today, the once promising antimalarial treatment from World War II now serves as cautionary tale of the struggles of generating therapeutics that are incapable of succumbing to resistance from the parasite. Another concern regarding the use of antimalarial drugs is patient compliance. Mefloquine Hydrochloride is a primary example of this issue.

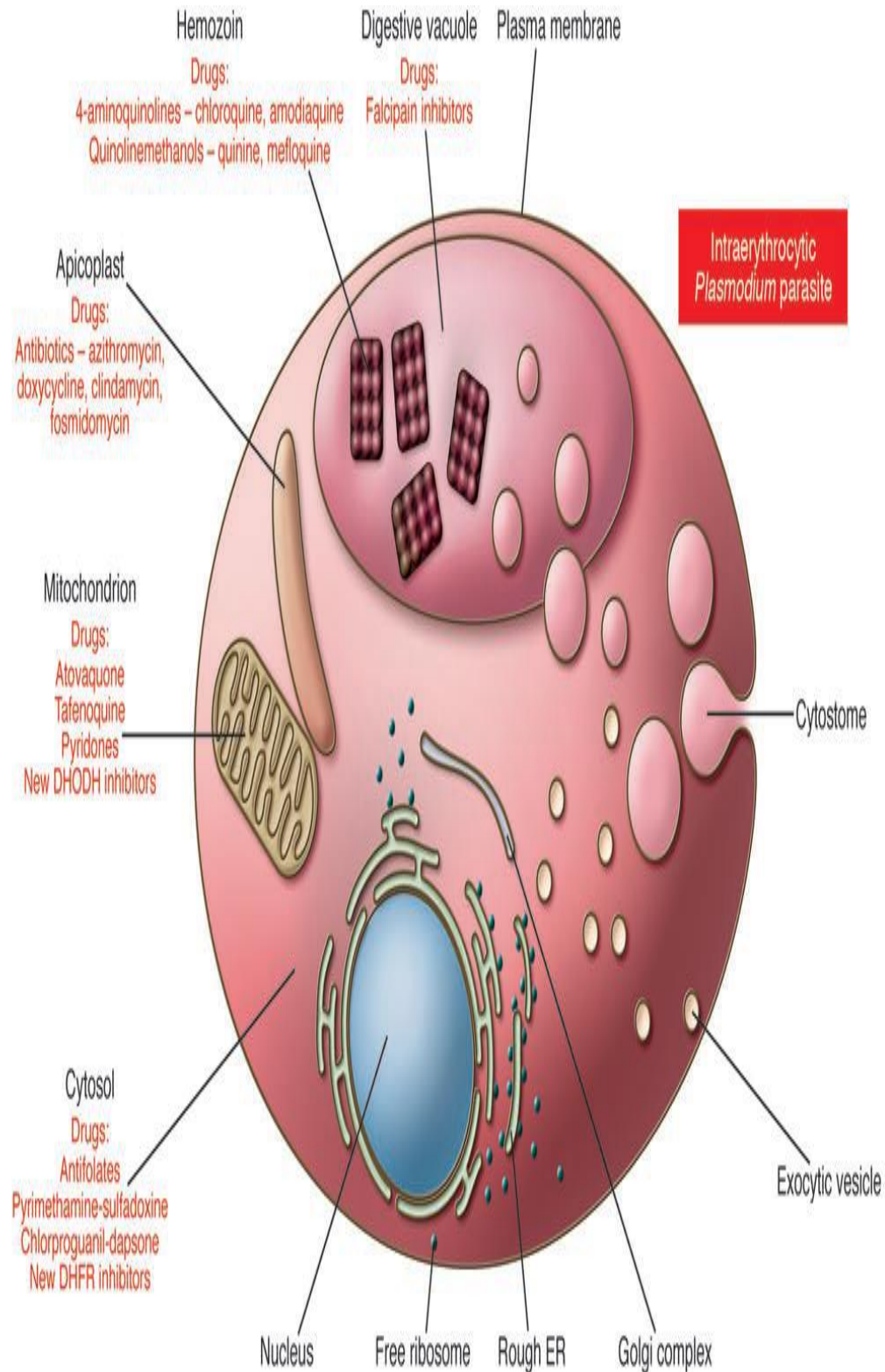


Figure 6: Diagram displaying drug targets of cellular components in a red blood cell invaded by *merozoites* (Greenwood et al., 2008).





Mefloquine is a FDA approved antimalarial most commonly used as a prophylactic for travelers and military personnel journeying to areas with high risk of the infectious disease. Travelers and military personnel select Mefloquine if they're unable or unwilling to take doxycycline or Malarone (combination of Proguanil and Atovaquone) (Dow et al., 2003). Important characteristics of Mefloquine is its long half-life (~2-4weeks) and its slow clearance. Mefloquine's poor solubility in aqueous solutions makes it extremely difficult to develop formulations for parental administration. However, its high permeability allows for it to be orally administered orally in tablet form. Typical single dosage of 250mg usually lasts from ~6.5 days to 22.7 days, which varies amongst ethnicities (Karbwang and White, 1990). Even though Mefloquine's mode of action hasn't been fully elucidated it is theorized that it prevents detoxification of hemoglobin digestion by merozoites during the erythrocytic cycle (**Figure 6**) (Skórska et al., 2006). David Saunders et al recently published a study in 2015 examining the safety, tolerability, and compliance of antimalarial drugs (Doxycycline, Mefloquine, and Atovaquone - Proguanil) distributed to US soldiers deployed in Afghanistan for a period of 12 months. Of the 2,206 military personnel that participated in the survey, 596 were prescribed Mefloquine during their deployment. Even though patient compliance was higher than individuals who took doxycycline, only 80% of participants were regularly taking the weekly dosage of 250mg (tablet). Criteria of compliance involved soldiers taking their medication with food, drinking a full glass of water, and waiting 30 minutes before lying down after taking the medication (Saunders et al., 2015).

Landers et al conducted a study published in 2006 examining compliance amongst travelers journeying to sub-Saharan regions endemic with malaria using a pill monitoring system. Of the 81 travelers that participated in this study only 32.1% of them took all of the required doses and was consistent in the dosing schedule. The remaining travelers were inconsistent with their compliance varying from missing their last dosage to failing to be consistent all together increasing their risk of contracting malaria. Another issue regarding the current use of antimalarials is in regards to the formulation of important antimalarials that have not been able to be administered orally. One prime example is the antimalarial drug artemisinin.

Artemisinin (*qinghaosu*) is a naturally occurring small molecule extracted from the Chinese plant *Artemisia annua* L. Its effectiveness as an antimalarial treatment is that it's fast acting and potent against the erythrocytic stage of *Plasmodium*'s cycle and eliminates gametocytocidal effects (**Table 1**) (Santos-Magalhães and Mosqueira, 2010). Since 2002, the World Health Organization recommended artemisinin as the first-line of treatment of uncomplicated but only in combination with other antimalarials (Shretta and Yadav, 2012).

Unfortunately, oral formulations for artemisinin are inefficient due to its very short elimination half-life, poor water solubility, and very poor (Santos-Magalhães and Mosqueira, 2010). Studies conducted by Ashton et al (1998) and Titulaer et al (1990) shows that despite its rapid on-set absorption, the bioavailability of artemisinin was <33% compared to other routes of administration such as intravenous and rectal administrations. This highlights

how much of a limiting factor the hepatic first pass clearance for certain small molecules like artemisinin.

The common denominator for the lack of compliance and bioavailability is the current commercially available formulation of drugs being used. What if a way to improve these issues involves a simpler form of administering the drug? One formulation that may resolve these complications involves a new technology that has been on the rise in the last 10 years - Oral Film Technology, specifically Oral Disintegrating Films.

## **1.2 Oral Disintegrating Films**

### **1.2.1. Various Routes of Administration**

In pharmacology there are various routes of administration for the drug delivery of small molecules and proteins. On the FDA's website<sup>1</sup> lists over 100 different routes of administration listed (systemic and localized) that have been approved by the organization. Only six of these are regularly studied during the preliminary phase of drug development: oral, rectal, subcutaneous/intramuscular, intravenous, topical, and inhaled. **Table 2** lists all of the advantages and disadvantages associated with administering small molecule/protein of choice. **Table 3** lists the market value and share of pharmaceuticals products based on the

---

<sup>1</sup>(<http://www.fda.gov/Drugs/DevelopmentApprovalProcess/FormsSubmissionRequirements/ElectronicSubmissions/DataStandardsManualmonographs/ucm071667.htm>)

Route	Advantages	Disadvantages
<b>Oral</b>	<ul style="list-style-type: none"> <li>• Easy</li> <li>• Preferred by patients</li> <li>• "Slow-release" preparations may be available to extend duration of action</li> <li>• Drugs can be formulated in such a way as to protect them from digestive enzymes, acid, etc.</li> </ul>	<ul style="list-style-type: none"> <li>• Unsuitable in patients who are uncooperative, strictly "nill by mouth", are vomiting profusely or have ileus</li> <li>• Most orally administered drugs are absorbed slowly</li> <li>• Unpredictable absorption due to degradation by stomach acid and enzymes</li> </ul>
<b>Rectal</b>	<ul style="list-style-type: none"> <li>• Good absorption – the haemorrhoidal veins drain directly into the inferior vena cava, avoiding hepatic first pass metabolism</li> </ul>	<ul style="list-style-type: none"> <li>• May not be suitable after rectal or anal surgery</li> <li>• Some patients dislike suppositories</li> </ul>
<b>Subcutaneous or intramuscular</b>	<ul style="list-style-type: none"> <li>• Good absorption, especially for drugs with a low oral bioavailability</li> <li>• Onset is more rapid than the above routes</li> <li>• Depending on formulation can have very long duration of action, e.g. depot antipsychotics and contraceptives</li> </ul>	<ul style="list-style-type: none"> <li>• Absorption may still be unpredictable if peripheries are poorly perfused</li> <li>• Injections hurt, cause bruises and frighten children and needle phobics</li> </ul>
<b>Intravenous</b>	<ul style="list-style-type: none"> <li>• Dependable and reproducible effects</li> <li>• Entire administered dose reaches the systemic circulation immediately - the dose can be accurately titrated against response</li> </ul>	<ul style="list-style-type: none"> <li>• Requires a functioning cannula</li> <li>• More expensive and labour intensive than other routes.</li> <li>• Cannulation is distressing to some patients, especially children</li> <li>• Cannulae are prone to infection</li> <li>• IV injection of drugs may cause local reactions</li> </ul>
<b>Topical</b>	<ul style="list-style-type: none"> <li>• Easy</li> <li>• Non-invasive</li> <li>• High levels of patient satisfaction</li> </ul>	<ul style="list-style-type: none"> <li>• Most drugs have a high molecular weight and are poorly lipid soluble, so are not absorbed via skin or mucous membranes</li> <li>• Very slow absorption</li> </ul>
<b>Inhaled</b>	<ul style="list-style-type: none"> <li>• Very rapid absorption due to the huge surface area of the respiratory endothelium</li> <li>• Bronchodilators and inhaled steroids can be targeted to lungs with low levels of systemic absorption</li> </ul>	<ul style="list-style-type: none"> <li>• Bioavailability depends on patient's inhaler technique and the size of drug particles generated by the delivery technique</li> </ul>

Table 2: Pros and cons of different routes of drug administration  
[http://www.doctors.net.uk/datastore/ecme/mod1227/Drug\\_dosage\\_Table1.pdf](http://www.doctors.net.uk/datastore/ecme/mod1227/Drug_dosage_Table1.pdf).

ROA	Market Value	Market Share
Oral	\$24.1B	32 %
Pulmonary	\$20.0B	27 %
Nasal	\$8.2B	11 %
Injection/Implants	\$6.6B	9 %
Transdermal/Dermal	\$5.7B	8 %
Transmucousal	\$0.4B	0 %
Other ROA or Devices	\$10.0B	13 %

Table 3: Market and Share of Pharmaceuticals by Route of Administration (<https://www.boomer.org/c/p4/c07/c07.pdf>).

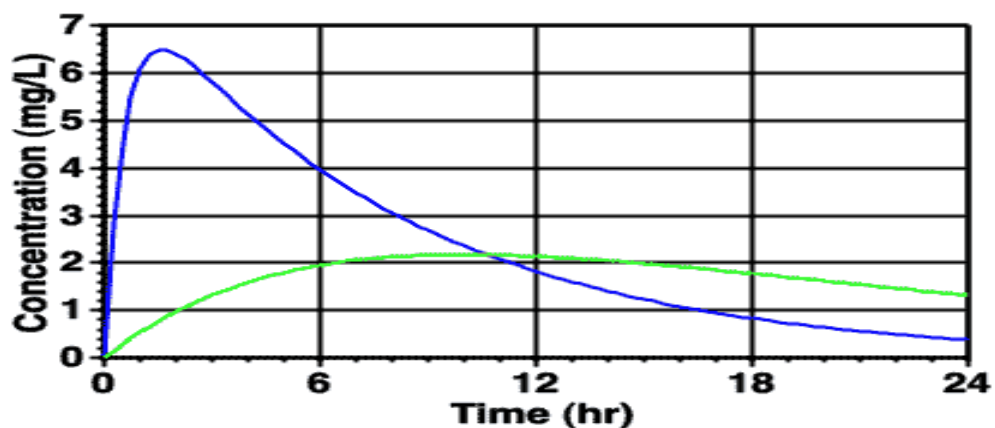


Figure 7: Typical plot of Plasma concentration versus time after oral administration of fast (blue) and slow (green) dosage forms ([www.boomer.org/c/p4/c07/c07.html](http://www.boomer.org/c/p4/c07/c07.html)).

route of administration. It should be no surprise that there is a direct correlation between patients driving the market value of oral administered therapeutics and their treatment of choice. So why is oral administration the favored route of administration for patients? Well it's important to know exactly how oral administration compares to other forms of administration.

Oral administration (also known as enteral) is when drugs administered are absorbed directly through the stomach or gastrointestinal tract (GI) which they later find its way into the bloodstream (**Figure 7**). The presence of food in the system can have an impact on the rate of absorption. It is the most convenient and most commonly prescribed form of dosage. Formulations that apply to this route of administration are tablets, liquids, and capsules. There are some disadvantages to the use of oral administration:

- cannot be administered to unconscious patients or patients who are vomiting.
- Inactivity due to low acidic pH in the stomach and enzymes
- First-pass effect - after the drug is absorbed from the GI tract from the stomach, it must pass through the liver before entering the bloodstream. This process may have a tremendous effect on the drugs bioavailability (concentration of drug present in the circulatory system). In some cases, reduces the drugs bioavailability (artemisinin is a great example with a bioavailability of ~30% when administered orally).

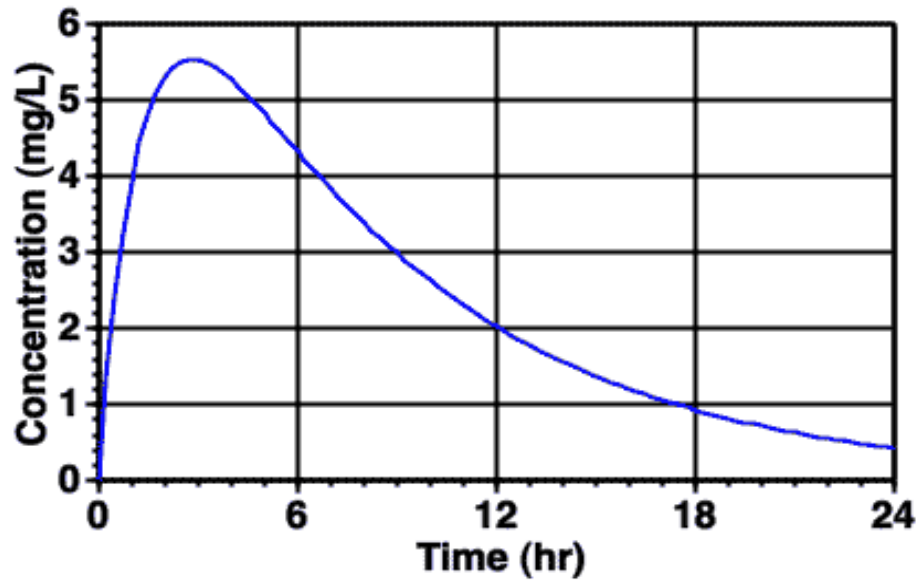


Figure 8: Typical plot of plasma concentration versus time after inhalation administration ([www.boomer.org/c/p4/c07/c07.html](http://www.boomer.org/c/p4/c07/c07.html)).

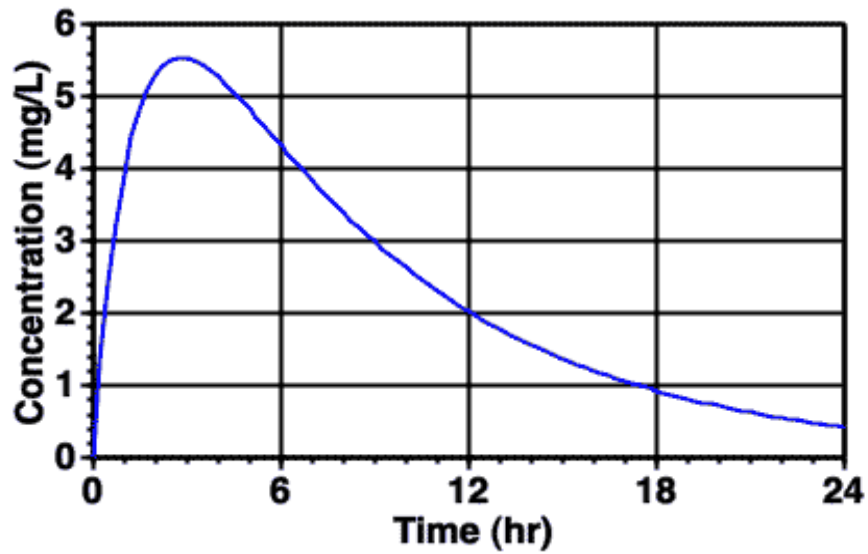


Figure 9: Typical plot of plasma concentration versus time after rectal administration (<https://www.boomer.org/c/p4/c07/c07.html>).

- Incompatibility with some foods which may cause severe side effects or insoluble complexes (Turley, 2009).

Nasal/Inhalation administration (**Figure 8**) is the ability to target drug delivery into the nasal cavity. A common example is the use of nasal sprays to treat allergies (Nasonex). This form of administration allows for rapid absorption due to readily available capillaries in the nose. This also benefits the administration of anesthetics (e.g. Propofol), treating patients suffering from certain breathing conditions (e.g. asthma, COPD, etc), and rare disease afflicting the lungs (cystic fibrosis, etc.). However, disadvantages of this form of administration includes:

- Solid and liquid forms of the drug have to be  $0.5\text{microns} < (\text{particle size}) < 20\text{microns}$
- Drug will have to be highly potent (absorption is only 10% of drug administered) (Turley, 2009)

Rectal administration (**Figure 9**) is most commonly formulated as suppositories or enemas for patients who are unable to ingest their medication due to nausea and vomiting. It is also used for localized treatment of ailments such as hemorrhoids. Disadvantages of this ROA are:

- Incomplete and erratic absorption from suppositories
- Patient discomfort

Topical administration (**Figure 10**) is the ability of the drug to be delivered directly to the surface of the skin, eyes, ears, nose, mouth, throat, rectum, and vagina. Purpose of this application is therapeutic treatment for



localized pain/discomfort (Feucht and Patel, 2011). Disadvantages associated with topical treatment include:

- Skin irritation at the site of application
- The drug being administered should have a low molecular weight
- Drug must be lipophilic
- Skin condition of the patient may affect how the drug is absorbed

Intramuscular (IM) and subcutaneous (SC) route of administration allows drug solutions to be administered under the skin and become readily absorbed into the blood circulation of the body (**Figure 11**). Subcutaneous delivery (**Figure 12**) is commonly used by diabetics for insulin injections which allows them to self-administer their medications. Intramuscular injections (**Figure 13**) allow for the ability of certain treatments to be formulated for sustained release (depot). Disadvantages associated with IM and SC delivery include:

- skin irritation/tissue damage
- localized pain at the site of the injection (especially in the case of SM where they will be repeated injections) - Site of injection has influence on the rate of absorption of drug administered
- Erratic absorption

An intravenous route of administration allows for the delivery of compounds into the peripheral vein within 1 to 2 minutes for bolus injection (**Figure 15**) or longer in a form of infusion (**Figure 14**). This form of rapid injection is beneficial for the treatment of epileptic seizures, acute asthma, and

cardiac arrhythmias<sup>2</sup>. It also permits 100% bioavailability of the drug being delivered since it bypasses the liver in large doses over an extended period of time (fusion). Disadvantages associated IV administration include:

- Toxicity due to rapid absorption which requires administration by infusion and close monitoring from trained personnel

The main driving force for oral formulations as a preferred route of administration is its relatively ease to take and painless without the risk of toxicity. Unfortunately, there are a number of obstacles that certain drugs (e.g. insulin) cannot bypass that make oral delivery nearly impossible. However, there is a form of oral drug delivery that may circumvent these roadblocks. Allowing for improved viability and access for some compounds. This is where oral mucosa delivery by way of Oral Film Technology addresses these concerns.

---

<sup>2</sup> ([www.boomer.org/c/p4/c07/c07.html](http://www.boomer.org/c/p4/c07/c07.html)).

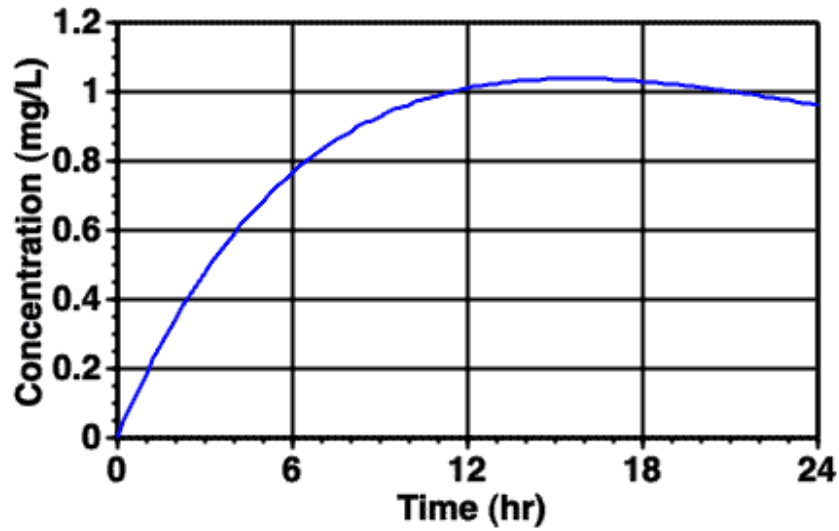


Figure 10: Typical plot of plasma concentration versus time after topical administration (<https://www.boomer.org/c/p4/c07/c07.html>)

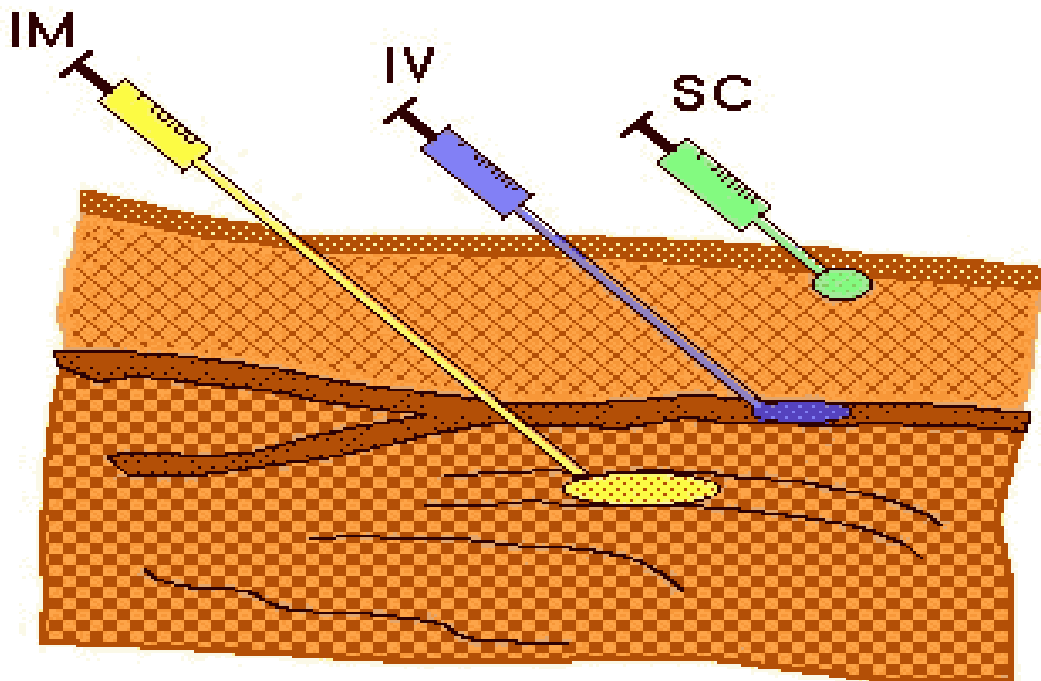


Figure 11: Illustration detailing the site of intramuscular (IM) injection, intravenous (IV) administration, and subcutaneous (SC) injection ([www.boomer.org/c/p4/c07/c07.html](http://www.boomer.org/c/p4/c07/c07.html)).

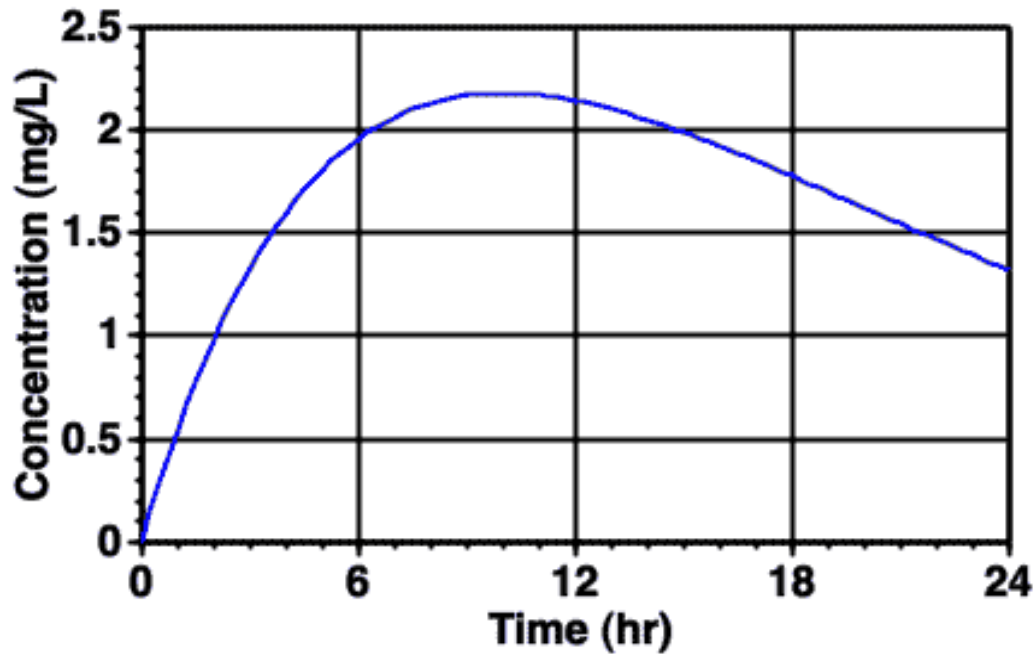


Figure 12: Typical plot of plasma concentration versus time after subcutaneous administration ([www.boomer.org/c/p4/c07/c07.html](http://www.boomer.org/c/p4/c07/c07.html)).

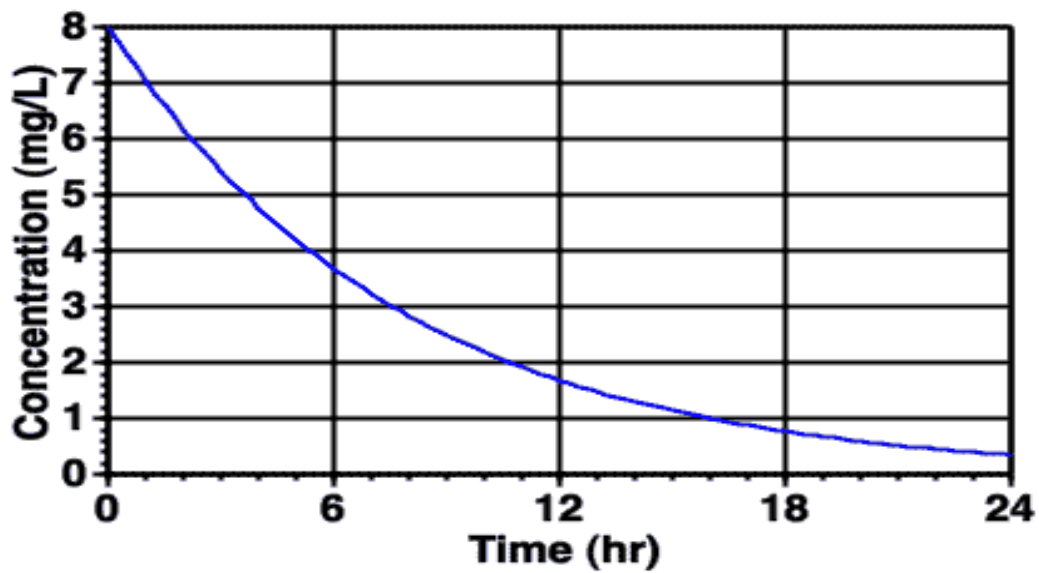


Figure 13: Typical plot of plasma concentration versus time after intramuscular administration ([www.boomer.org/c/p4/c07/c07.html](http://www.boomer.org/c/p4/c07/c07.html)).

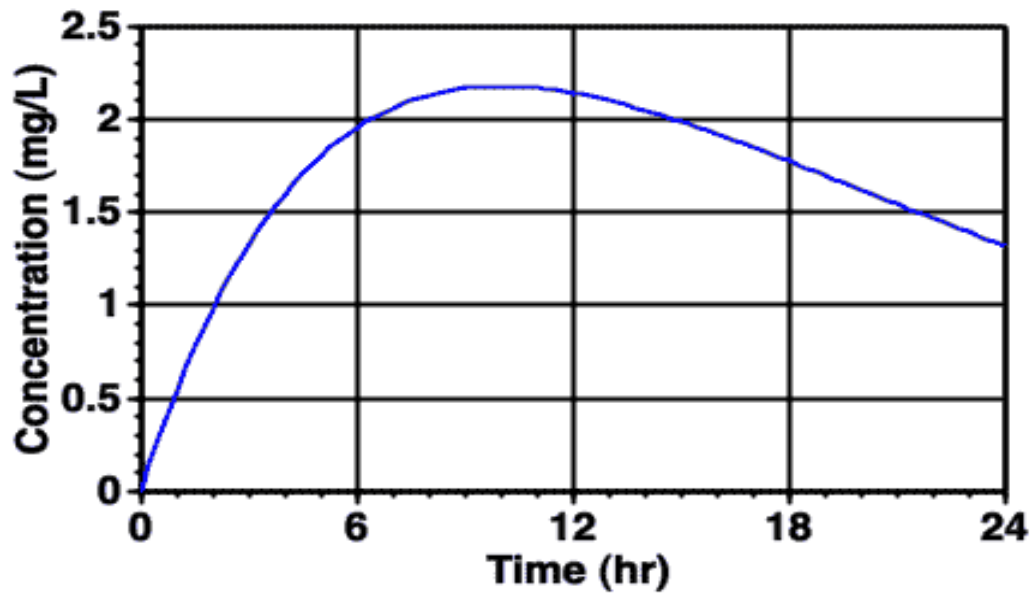


Figure 14: Typical plot of plasma concentration versus time after intravenous infusion administration ([www.boomer.org/c/p4/c07/c07.html](http://www.boomer.org/c/p4/c07/c07.html)).

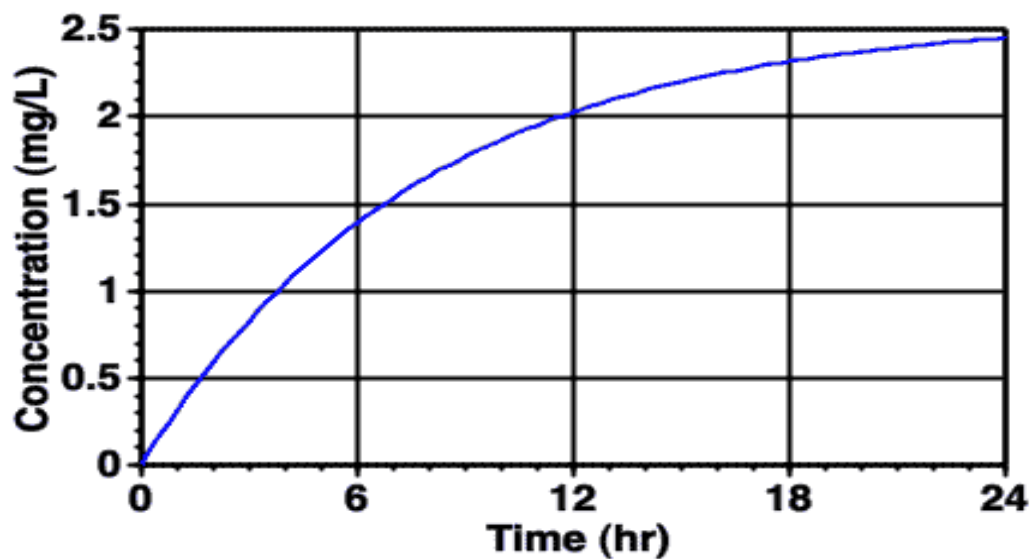


Figure 15: Typical plot of plasma concentration versus time after intravenous bolus administration ([www.boomer.org/c/p4/c07/c07.html](http://www.boomer.org/c/p4/c07/c07.html)).

### **1.2.2. Oral Film Technology (OFT)**

OFT is a form of oral drug delivery that was developed in the late 1970s as fast dissolving tablets. Later on this form of technology evolved to thin strip films. Due to the inabilities of certain patient populations (geriatric and pediatric groups) to ingest tablets, there has been a recent spike in interest (past 10 -15 years) from pharmaceutical companies (Borges, 2015). The first blockbuster product from the OFT market was the Listerine Pocketpaks® produced as a breath freshener by Pfizer in 2001. Since the commercial release of the Listerine pocket strips, OFTs have expanded as a form of drug delivery for vitamins and pain relievers to treating impotence, smoking cessation, some psychiatric disorders, and opioid dependence (Nagaraju et al., 2013; Borges et al., 2015).

Since 2001, the OFT market has seen a steady rise in the pharmaceutical industry thanks not only to the industry targeting the pediatric and generic populations but overall acceptance from consumers who have opened up to the novelty of OFTs. The launch of the Listerine Pocket Packs brought in <175 million dollars that year. The market for OFTs brought in 500 million dollars in 2006 and reached 2 billion dollars in 2010 in the US alone. Another prime initiative is the drive for companies to stave off competition from generics by extending patent due new formulations based on OFTs (Borges et al., 2015). A recent look at FDA approvals revealed reformulations or combinations of certain products were the majority of approved compared to only 25% of new drug applications (Borges et al., 2015). In 2010, the OFT market saw the launching of the very first prescription oral films from MonoSol Rx LLC (Pharmafilm -

Suboxone) and Labtec GmbH/Applied Pharma Research (APR) (RapidFilm - Odanestron). US sales of Suboxone were \$513 million in 2011 and exceeded \$1.5 billion in 2012 (Borges et al., 2015). **Tables 4&5** lists current commercial products (OTCs and RxS) on the market and the companies producing these films. As the industry continue the drive to reformulate OTC, prescription products, and expand to untapped markets such as veterinarian products and vaccine formulations the role of OFTs will continue to grow.

Compared to liquid, tablet, and capsule formulations, OFTs has the ability of bypassing seven main issues associated with typical oral delivery of small molecules and proteins:

- 1.) The mucosa is highly vascularized and allows direct access to the systemic circulation through the capillaries and venous drainage (Feucht and Patel, 2011). This form of drug delivery averts the first pass hepatic metabolism commonly characteristic for traditional oral delivery (Sattar et al., 2014).
- 2.) Provides an environment that is conducive to the stability and efficacy of the drug being administered. This is due to the relatively neutral pH of the saliva in the mouth (pH ~ 6.8-7 vs pH ~1-2 in the stomach) and the continuous secretion of the saliva. This would be highly favorable to small molecules and proteins which would be inactive by way of the traditional oral route (Feucht and Patel, 2011).
- 3.) Compared to the GI tract, enzymatic activity in the oral mucosa is relatively low thanks to the friendly and consistent physiological conditions in the saliva which contains much less mucin, limited enzymatic activity, and relatively no

proteases (Feucht and Patel, 2011). This environment would also be conducive to small molecules and proteins which would be hindered in the GI tract.

4.) Accessibility to a large surface area of the oral cavity leads to rapid disintegration and dissolution of films.

5.) Most orodispersible tablets are fragile and brittle which would require special packaging and handling.

6.) Compared to liquid oral formulations, precision of dosing is not required for administration.

7.) Ease of swallowing and no need for water due to wettability of films in contact with saliva in the oral cavity (Dixit and Puthli, 2009).

These seven characteristics are essential to examining drug delivery of therapeutics because it allows for the drug to sustain a high bioavailability once the small molecule/protein reaches the bloodstream through the oral mucosa<sup>3</sup>.

---

<sup>3</sup> ([www.boomer.org/c/p4/c07/c07.html](http://www.boomer.org/c/p4/c07/c07.html))



Product Category	Ingredient /s	Indication / Applications
<b>1. Bio film</b>		
Energy boosters	Caffeine, green tea extract and guarana	The product maintains the energy levels
Detoxification strip	Green tea extract which is high in polyphenols and rich in anti-oxidants, spearmint flavor	Green tea has been used as a traditional medicine to help everything from wound healing, regulating body temperature, blood sugar and promoting a healthy digestion
Male vitality strip	Macaroot extract and saberian ginseng extract, herbs which enhance libido, cinnamon flavor	It acts as an aphrodisiac and improves the libido in males
Female vitality strip	Botanical ingredients like damiana and passion flower	It is used to improve general wellbeing, increase energy and enhance mood
Appetite suppressant	Fucus vesiculosus, guarana extract and garcinia cambogia	These are top selling natural ingredients associated with weight loss, cambogia helps to reduce the food intake by suppressing appetite
Vitamins and food Supplements	Various vitamins, minerals and supplements	It is useful for the people who don't like to pop up the tablets or soluble supplements
Breath freshener strip (anti-bacterial strip)	Contain mint flavor and anti-bacterial agent, cetyl pyridinium chloride	It is used as mouth freshener and to stop bad breath
Saliva promoting strip	Fruit acid extracts, orange flavor	It is used in the dry mouth as a side effect of the other medications
<b>2. Labtec GmbH</b>		
Ondansetron rapid film	Ondansetron 4mg and 8mg	It is used in the prevention of chemotherapy and radiation induced nausea and vomiting and prevention of post-operative nausea and vomiting
Donepezil rapid film	Donepezil Hcl 5mg and 10mg	Treatment of mild to moderately severe dementia of the alzheimer's type
<b>3. Paladin Labs (bioenvelop)</b>		
Smoking cessation	Nicotine	To reduce the smoking habit

Table 4: Marketed products - mostly over the counter oral films (Nagaraju et al., 2013).

Product Category	Ingredient /s	Indication / Applications
Multi vitamin for kids and Adults	B6, B12, C, D3 for kids, D3 for adults	Multi vitamin supplement
Teeth whitening	—	Life style improvement product
Food supplements	Benzocaine, caffeine, melatonin, menthol, vilpocetina	Nutraceuticals
Minerals	Chromium	Mineral supplements
Natural products	Ginseng and guarana	Aphrodisiac, appetite reducer
<b>4. Innozen Inc</b>		
Chloraseptic Relief Strips	Benzocaine 3 mg, BHT, corn starch, erythritol, FD&C Red 40, hydroxypropyl methylcellulose, malic acid, menthol, monoammonium glycyrrhizinate, cherry flavors, polyethylene oxide, sucralose	Occasional minor irritation, pain, sore throat and sore mouth
Chloraseptic Kids sore throat Relief strips	Benzocaine 2 mg & menthol, grape flavor, BHT, corn starch, erythritol, FD & C Blue 1, FD & C Red 40, hydroxypropyl methylcellulose, malic acid, menthol, monoammonium glycyrrhizinate, polyethylene oxide, sucralose	Occasional minor irritation, pain, sore throat and sore mouth
Suppress cough strip with Dextromethorphan	Dextromethorphan hydrobromide 2.5 mg, Asulfame potassium, FD&C Blue 1, glycerin, menthol, natural and artificial flavors, pectin, peppermint oil, sucralose, sugar, water	Temporarily suppresses coughs due to minor throat and bronchial irritation associated with cold or inhaled irritants.
Suppress cough strip with Menthhol	Artificial Flavors, ascorbic acid, aspartame, asulfame potassium, carageenan, diglycerides, fatty acid ester, FD&C yellow 5 (tartrazine), glycerin, menthol, mono glycerides, pectin, sodium alginate, sorbitan monoaurate, sorbitol, spices, starch, water	Temporarily suppresses coughs due to minor throat and bronchial irritation associated with cold or inhaled irritants.
<b>5. Hughes Medical Corporation</b>		
Methylcobalamine	1mg	Peripheral neuropathy, Diabetic neuropathy
Dextromethorphan	2.5mg-5.5mg-15mg	Anti-tussive agent used to prevent cough
Folic Acid	1mg-5mg	Required for formation of healthy red blood cells and used in anemia.
Loratidine	10mg-15mg	Allergy
Caffeine	2.5mg	CNS stimulant
Diphenhydramine Hcl	2.5mg-5mg	Antihistaminic
<b>6. Novartis Pharmaceuticals</b>		
Night Time Triaminic Thin Strips® Cold & Cough	Diphenhydramine HCl 12.5 mg, Phenylephrine HCl 5 mg, acetone, FD&C blue #1, FD&C red #40, Flavors, hyprolose, maltodextrin, mannitol, polyethylene glycol, polypropylene glycol, purified water, sodium polystyrene sulfonate, sucralose, titanium dioxide.	Antihistamine/cough suppressant.Nasal decongestant. It temporarily relieves cough due to minor throat and bronchial irritation as may occur with a cold.
Triaminic Thin Strips® Long Acting Cough	Dextromethorphan 5.5 mg (equivalent to 7.5 mg Dextromethorphan HBr), acetone, alcohol, dibasic sodium phosphate, FD&C red #40, Flavors, hydroxypropyl cellulose, hypromellose, isopropyl alcohol, maltodextrin, microcrystalline cellulose, polacrillin, polyethylene glycol, pregelatinizedstarch, propylene glycol, purified water, sodium phosphate, sorbitol, sucralose, titanium dioxide.	It temporarily relieves cough due to minor throat and bronchial irritation as may occur with a cold.

Table 4 cont’d

<b>Product Category</b>	<b>Ingredient /s</b>	<b>Indication / Applications</b>
Tianninic Thin Strips® Cough & Runny Nose	Diphenhydramine HCl 12.5 mg, acetone, alcohol, FD&C blue #1, FD&C red #40, flavors, hydroxypropyl cellulose, hypromellose, isopropyl alcohol, maltodextrin, microcrystalline cellulose, polyethylene glycol, pregelatinized starch, propylene glycol, purified water, sodium polystyrene sulfonate, sorbitol, sucralose, titanium dioxide	It reduces cough due to minor throat and bronchial irritation as may occur with a cold. It relieves itchy, watery eyes due to hay fever.
Day Time Tianninic Thin Strips® Cold & Cough	Dextromethorphan 3.67 mg (equivalent to 5 mg Dextromethorphan HBr), Phenylephrine HCl 2.5 mg, acetone, alcohol, FD&C blue #1, FD&C red #40, flavors, hypromellose, isopropyl alcohol, microcrystalline cellulose, polacrifin, polyethylene glycol, propylene glycol, purified water, sodium polystyrene sulfonate, sucralose, titanium dioxide	It is used as nasal decongestant.
Tianninic Thin Strips® Cold with Stuffy Nose	Phenylephrine HCl 2.5 mg, acetone, alcohol, FD&C blue #1, FD&C red #40, flavors, hypromellose, isopropyl alcohol, maltodextrin, microcrystalline cellulose, polyethylene glycol, propylene glycol, purified water, sodium polystyrene sulfonate, sucralose and titanium dioxide	It temporarily relieves nasal and sinus congestion as may occur with a cold.
Theraflu® Daytime Thin Strips	Dextromethorphan 14.8 mg (equivalent to 20 mg Dextromethorphan HBr), Phenylephrine HCl 10 mg, acetone, alcohol, FD&C red #40, flavors, Hypromellose, mannitol, polyethylene glycol, polystyrene sulfonate, polacrifin and sucralose	It reduces cough due to minor throat and bronchial irritation as may occur with a cold.
Theraflu® Nighttime Thin Strips	Diphenhydramine HCl 2.5 mg, Phenylephrine HCl 10 mg, acetone, alcohol, FD&C blue #1, flavors, Hypromellose, mannitol, polyethylene glycol, polystyrene sulfonate, polacrifin and sucralose	It is used for nasal congestion, runny nose, sneezing, itchy nose and throat etc.
Theraflu® Thin Strips®—Multi Symptom	Diphenhydramine HCl 2.5 mg, acetone, alcohol, FD&C red #40, flavors, Hypromellose, hydroxypropyl cellulose, maltodextrin, microcrystalline cellulose, polyethylene glycol, pregelatinized starch, polystyrene sulfonate, sorbitol and sucralose, Titanium dioxide.	It temporarily relieves nasal and sinus congestion as may occur with a cold.
<b>7. Pfizer Inc</b>		
Listerine® pocketpaks®	Available in cool mint®, Fresh Citrus, Cinnamon, and fresh burst®, Povidone is used as a film forming polymer.	These strips dissolve instantly and kill 99 percent of bad breath germs.
<b>8. Prestige Brands</b>		
Little cold sore throat Strip	Ascorbic acid, pectin	Cold/allergy
Chloraseptic relief strip	Benzocaine, menthol	Sore throat
<b>9. Bio Delivery Sciences International</b>		
Onsolis™	Fentanyl buccal soluble film	Pain in opioid-tolerant patients
BEMAX™ Buprenorphine	Buprenorphine	Therapeutic alternative for patients with incomplete pain relief or those unable to tolerate

Table 4 cont'd

Brand name/designation	Owner/originator company	Patent (s)	Active companies/partner/distributor	Commercial products	Drug substance (if any)		Oral film type	Polymer	Ref
					Drug substance (if any)	Phase/status			
Buccal wafer	LTS Lohmann	US-07407669 B2	Pfizer	Ustinex® Pocket Packs® Suddled PEM Bendryl® Niquitin Strips 2.5 mg oral film	Phenylephrine Diphenhydramine hcl Nicotine Rizatriptan film Tadafil film	Launched Discontinued Discontinued Launched Approved by the FDA Phase 2 clinical pilot study planned for Q1 2014	Dispersible		[70,71]
Versafilm™	Intelligence Technology Corp.	US-20110136815	RedHill Biopharma		INT0020 Isosmia INT-0022; ant-psychotic agent INT-0023 – allergy INT-0025 – prostate hyperplasia INT0031 Benign prostatic hyperplasia INT0030 – Animal health Versafilm INT0036 – CNS	Phase 2 clinical Phase 2 clinical Phase 1 clinical Phase 1 clinical Phase 1 clinical Pilot study Pilot study Pilot study Discovery	Dispersible Dispersible Dispersible Dispersible Dispersible Dispersible Dispersible Dispersible		[31,32,72]
Thinsoft™	Paladin Labs Bioenvelops™	WO-2009055923							[20,55–57,73]
Brand name/designation	Owner/originator company	Patent(s)	Active companies/partner/distributor	Products	Drug substance (if any)		Oral film type	Polymer	Ref
					Drug substance (if any)	Phase/status			
Pharmfilm®	MonoSol Rx LLC	U.S. patent No. 7,824,588 WO-2011017483	C.B. Fleet Company Reckitt Benckiser Pharmaceuticals	Pedia Lax® Quick Dissolve Strips Suboxone® Sublingual Film	Sermosides Buprenorphine Hydrochloride + Naloxone Hydrochloride Benzocaine (Pectin) + Ascorbic acid Methylphenidate prodrug + ligand Mometasone sodium Diphenhydramine hydrochloride Escalopram Rizatriptan Epinephrine Testosterone	Discontinued Launched Discontinued Discontinued Discovery Clinical No development reported Discovery No development reported Discovery	Dispersible Dispersible Dispersible Dispersible Dispersible Dispersible Dispersible Dispersible Dispersible	Polyethylene oxide and HPAC	[14,20–25,70,74–82]
		WO-2013019187 WO-2008098151 WO-2012040262	KentPharm's MonoSol Rx LLC MonoSol Rx LLC MonoSol Rx LLC	Prestige brands Chloraseptic® Little cnd sore throat strip					
		WO-2013028002	MonoSol Rx LLC						

Table 5: OFT platforms, their owners or developers, related patents and associated marketed prescription products (Borges et al., 2015).

Brand name/designation	Owner/originator company	Patent (s)	Active companies/partner/distributor	Commercial products		Oral film type	Polymer	Ref
				Drug substance (if any)	Phase/status			
Rapid Dissolving Film	Kyulkyu Pharmaceutical Co Ltd	WO-2012177326	Midatech Midazolam Therapeutics					
		WO-2004065986	BiondVax					
		WO-2006031209	Monosol Rx LLC; Vestiq Pharmaceuticals Inc.	Zuplenz®	Insulin nanoparticles (Midaforn insulin) Multimeric-001 Ondansetron hydrochloride	Phase 1 clinical	Buccal	
		WO-03030881						
		WO-2012040262	Monosol/Midatech					
		WO-2011124570	APR Applied Pharma; Monosol Rx LLC; Tesa Labtec GmbH	Ambodipine OD film	Discovery	Buccal		[83]
		WO-2005117803	Kyulkyu Pharmaceutical Co Ltd; BIOMEDIX CO LTD		Launched	Dispersible		[33,34,84-88]
		WO-2011108643						
		WO-09917753	MOCHIDA PHARMACEUTICAL CO., LTD.	Voglibose OD film	Launched	Dispersible		
		WO-2010023674	Kyulkyu Pharmaceutical Co Ltd					
Adhesive and dissolving film (ADF) Dissolvable film technology	ABRx	US 20040126330	Kyulkyu Pharmaceutical Co Ltd; Marinho Co. Ltd.	Olopatadine Hydrochloride OD Film	Launched	Dispersible		
		AT WO-03028654	Kyulkyu Pharmaceutical Co Ltd	Donepezil Hydrochloride OD film	Launched	Dispersible		
		WO-2013121663	Elmed Fesal co. Ltd	Donepezil Hydrochloride	Launched	Dispersible		
			Mochida Pharmaceutical Co Ltd	Zolpidem Tartrate OD Film	Launched	Dispersible		
			Mochida Pharmaceutical Co Ltd	Lorazepam OD Film	Launched	Dispersible		
			Teva Pharma Japan Inc.	Waripon	Launched	Dispersible		
			Kyulkyu Pharmaceutical Co Ltd		Discovery	Buccal		[89]
			Novartis Consumer Health	Case-X®				
				Therfluo®/Thin Strips®	Launched	Dispersible	PVA	[70]
				Triamcinolone Acetonide	Discontinued	Dispersible	Starch	
RapidFilm®	Labtec GmbH/APR Applied Pharma Research	WO-2008040634	Norgine (Europe and Middle East, Africa and Australasia)/SciClone Pharmaceuticals, Inc. (China and Vietnam) /Takeda Canada (Canada) /Monosol Rx §	Donepezil Hydrochloride	Launched	Dispersible	Medium MwPEG	[20,75,90-93]
		WO-2009043588	APR Applied Pharma Research SA; Monosol Rx LLC; Tesa Labtec GmbH	Zolmitriptan OD Film	Launched	Dispersible		[94,95]
		WO-2011124570	APR Applied Pharma Research SA; Monosol Rx LLC; Tesa Labtec GmbH	RapidFilm®	Launched	Dispersible		
				Antipirazole ODF	No development reported	Dispersible		
		WO-2012110222	APR Applied Pharma Research SA; Tesa Labtec GmbH	Olanzapine ODF	Registered	Dispersible		[96]
		WO-2009043588	APR Applied Pharma Research SA; Ferrer International SA; Tesa Labtec GmbH	Donepezil ODF	Registered	Dispersible		[97]
		EP-02213278						
		WO-2007002901						
		WO-2007002900						
		WO-2010115724						
Schmelzfilm	Hexal Pharmaceuticals		Hexal/Sandoz					
				Olanzapine HEXAL® SF	Launched	Oral dispersible	Ethylcellulose	
				Schmelzfilm	*	Oral dispersible	HPMC	
				Antipirazole HEXAL® SF	Launched	Oral dispersible		
				Antipirazole HEXAL® SF	Launched	Oral dispersible		
				Schmelzfilm	Launched	Oral dispersible		
				Risperidon HEXAL® SF	Launched	Oral dispersible		[98]
				Risperidon HEXAL® SF	Launched	Oral dispersible		
				Donepezil HCl Hexal®SF	Launched	Oral dispersible		
				Donepezil	Launched	Oral dispersible		

Table 5 cont'd

BEMA™	Biodelivery Sciences International (BDSI)	WO-2012055947 WO-03086345 WO-2008011194; WO-2007070632	KumWha Pharmaceutical Co Ltd; Meida AB; TTY Biopharm Co Ltd	SlideHEXAL SF (Tornetts) Onsolis®	Sildenafil Fentanyl	Launched Launched	orodispersible Buccal	Backing layer – HPC, HEC Active layer – polycaprolin and NaCMC	[99–101]
Fast dissolving film Pharmform technology	Hughes Medical Corp Auxilium Pharmaceuticals	WO-2010002418		Rotavac™	Rotavirus Testosterone Oxybutynin Fentanyl Nicotine	Phase II clinical trials (May 2013) Discontinued No development reported No development reported No development reported	Buccal Buccal Buccal Buccal Buccal		[20] [50,51,103,104]
	Bioprogress	WO-2009151574 WO-2006114604 (A3)	Mel dex International		Nicotine	No development reported	Buccal	Cellulose derivative	[20,54] [46,105]
	NAL Pharma	WO-2010062688			Seligline Rizatriptan Benzoate Nicotine Levocetirizine Zolmitriptan Sumatriptan Sildenafil citrate Tadalafil Montelukast Fentanyl Ceftriaxone HCl Donepezil Zolmitriptan Sildenafil citrate SPD-1202 Attention deficit hyperactivity disorder SPD-1201 Depression SPD-1113 Schizophrenia SPD-1108 Asthma SPD-1112 - Dementia Montelukast	Discovery Phase 1 clinical Discovery Discovery Discovery Discovery Phase 1 Clinical Discovery Discovery Discovery Discovery Discovery Discovery Launched Discovery	Dispersible	[35,36,38]	
SmartFilm®	Seoul Pharma Co Ltd	WO-2013129889	Pfizer Inc	Valtis®		Discovery	Dispersible		[35,36,38]
Quideol®	SK Chemicals Co Ltd	WO-2013100664 WO-2013085276	SK Chemicals Co Ltd			Launched (Korea) initiated EU development Launched	Dispersible Dispersible		[47,106,107]
Orally rapid disintegration	AstraZeneca plc			Anastrozole ODF	Mifepridone hydrochloride Anastrozole	Phase 1 clinical completed	Dispersible		[108,109]

Table 5 cont'd:



Brand name/designation	Owner/originator company	Patent (s)	Active companies/partner/distributor	Commercial products	Drug substance (if any)		Oral film type	Polymer	Ref
						Phase/status			
Film									
Thin film	Neurohealing Pharmaceuticals Inc	WO-2006078998			Tropicamide	Phase 2 Clinical	Buccal	Pullulan	[58,59,110]
Eluting Bandage Platform	Pharmedica	WO/2012/104834			Insulin	No development reported	Buccal		[111,52]
					Cannabimimids	No development reported	Buccal		
Fast-onset sublingual bilayer film	Cynapsus Therapeutics	WO-2012083269; WO-2010144817	Cynapsus Therapeutics	APL-130277	Apoprotein	Phase 1 clinical	Dispersible bi-layer sublingual	Cellulose (HEC7) and/or modified starch (MDX)	[49,112,113]
Transmucosal matrix patch	ESohly Laboratories, Inc Aoxing Pharmaceutical				Dronabinol	Discovery	Buccal		[114]
					Mildazolam maleate	No development reported	Dispersible		[115]
					Naloxone	No development reported	Sublingual		[116]
					Montelukast sodium	Pre-registration	Dispersible		[117]
					Clonidine	Pre-registration	Dispersible		[118]
					Donepezil	Clinical	Dispersible		[119]
					Sildenafil	Launched	Dispersible		[120-122]
Oral thin film	CTC Bio Inc	WO-2012108738	CTC Bio Inc.; Dong Kook Pharmaceutical Co Ltd.; Huons Co Ltd.; Jell Pharmaceutical Co Ltd.; Jin Yang Pharm Co Ltd.; Kun Wha Pharmaceutical Co Ltd						
Oral thin film	CURE Pharmaceutical Inc	WO-2010151020 WO-2012121461 WO-201402506 WO-2013002578	CURE Pharmaceutical Inc.	PediasUNATE™	Artisanate and amniol aqueine	Discovery			[123]
Trans-mucosal drug delivery	PFT medical	WO-2007073846			Adrenaline	Pre-clinical pending/under negotiation		Film-forming agent comprising an alginate salt of monovalent cation	[11,69,124]
					Cancer pain	Out-licensed			
					Erectile dysfunction	Out-licensed			
					Migaine	Out-licensed			
					Parkinson's disease	Under development			
					NK1/Nicotine	Out-licensed			[125]
					Tadalafil	Launched			[126]
					Ondansetron Hcl	Launched			
					Simethicone	Launched			
					Dextromethorphan Hbr	Launched			
					phenylephrine Hcl 2.5 mg strips (cough & cold)				
					Vitamin B12	Launched			
					Vitamin D3	Launched			
					Vitamin B12 + Vitamin C + Sodium	Launched			
					+ Potassium				
					Caffeine + Vitamin B12 + Vitamin E + Vitamin B6 + Biotin	Launched			
Oral dispersible film	Avishkar	WO-2013143891							

Table 5 cont'd

Table 5 cont'd

Melatonin strips	+ Vitamin B5	
Teeth whitening strips	Melatonin	Launched
Breath freshening strips	6% hydrogen peroxide	Launched
		Launched
	AMSH-01 (AIDS)	Discovery
	AMSH-02 (Vaginal infections)	R&D completed



### 1.2.3. Structure and Environment of the Oral Mucosa with Focus on Drug Delivery

The oral mucosa comprises of 3 main structures in the mouth: the buccal mucosa, sublingual mucosa, and the gingival and palatal tissues. Other components of the mucosa, such as saliva and mucus play significant roles in the application of OFs. The composition of the oral mucosa mirrors the lining mucous membranes of the vagina and the esophagus (Campisi et al., 2010). The total surface area of the mucosa averages around 200 cm<sup>2</sup> which consists of two layers. The first is the lamina propria - slightly vascularized of mesodermal origin. The second is the squamous avascular epithelium - thick and stratified which is directly connected to the basal lamina which is consisted of a proteinaceous fibrous extracellular matrix of 1-2 um in thickness (Campisi et al., 2010). **Figure 18** highlights the oral structure of the multiple sites of application sites for oral film drug delivery. Figure illustrates the histological structure of the oral mucosa with **Table 6** listing the thickness and permeability of certain regions in the oral mucosa.

The buccal mucosa is a non-keratinized stratified squamous which composes of the lining of the cheek as well as the area between the gums and upper and lower lips. It has an average surface area of 100cm<sup>2</sup>. It serves as a barrier to protect the underlying tissues from any chemical damage, mechanical stresses, or invasion from foreign substances (Sattar et al., 2014). The structural composition consists of the outer epithelium and basal laminar (basement

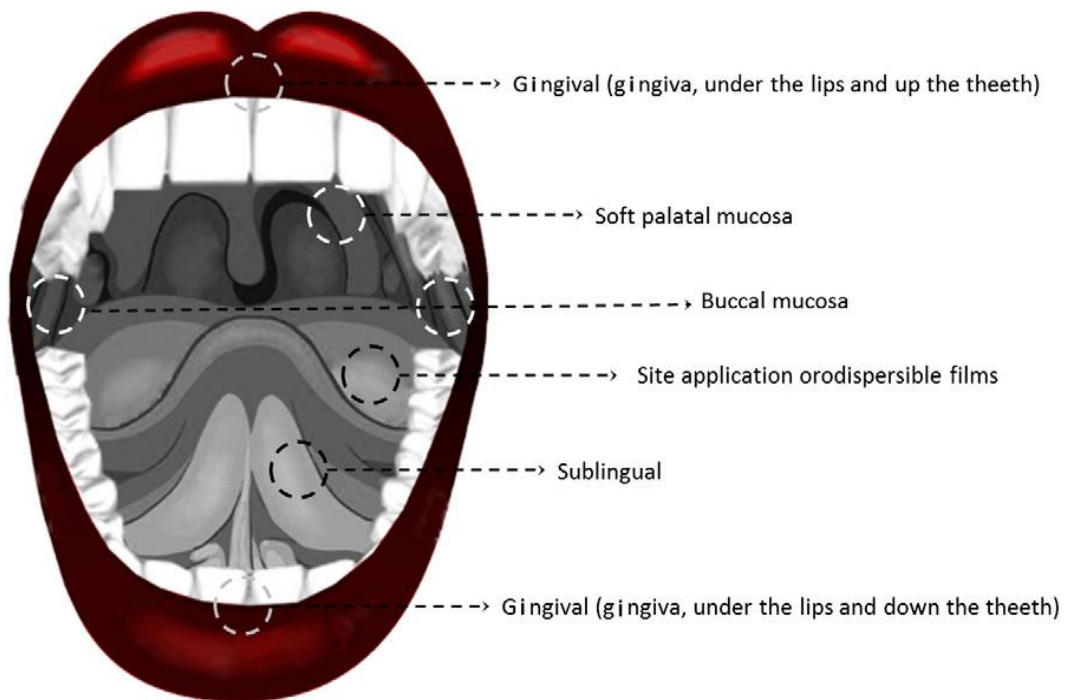


Figure 16: Different local application sites of the oral films. Depending on the type of films the site of application may vary (Borges et al., 2015).

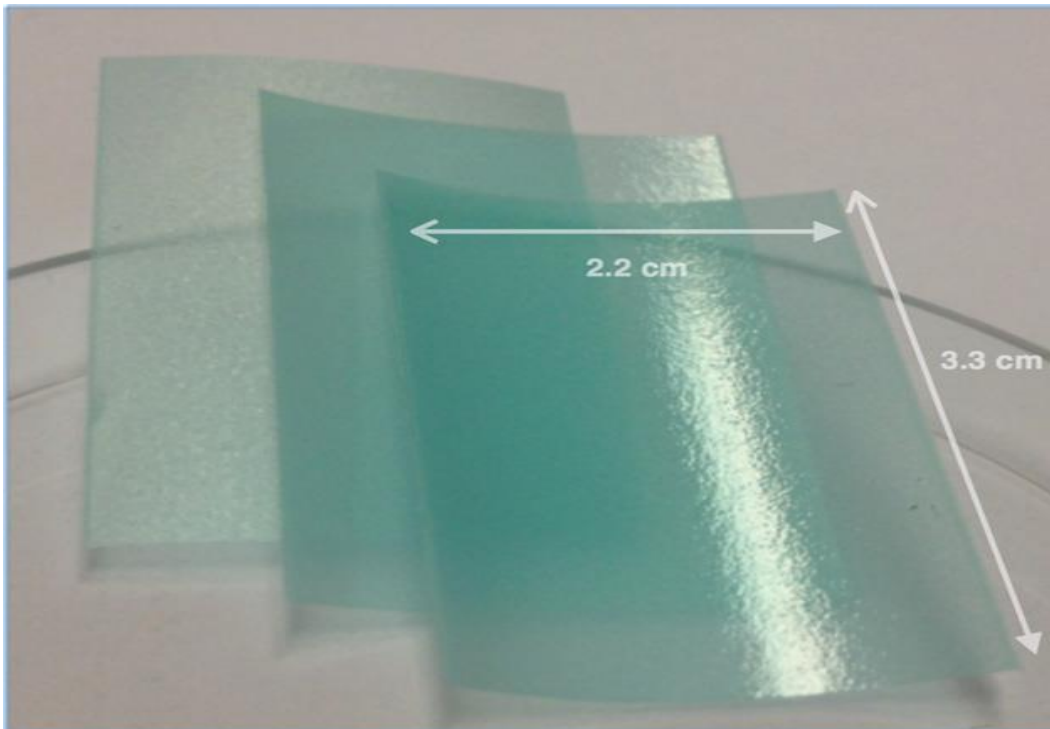


Figure 17: Photography of three oral films and their corresponding dimensions (Castro et al., 2015).

membrane). Connective tissue that consist of the lamina propria and the submucosa supports the basal lamina. This regional area has a turnover every 5 - 7 days.

This region is connected to the salivary glands and capillaries with blood flow to the buccal at the rate of 2.4 ml per min  $\text{cm}^2$  (Sattar et al., 2014). It is substantially less permeable than the sublingual mucosa which doesn't allow access to rapid absorption or great bioavailability for products (Rogers et al., 1992).

The sublingual mucosa is comprised of thinner, non-keratinized epithelium cells that are more permeable to drug absorption compared to the buccal mucosa. The sublingual mucosa consists of the ventral surface of the tongue and the floor of the mouth. Blood flow to this region at a much slower rate compared to the buccal mucosa at rate of 1.9 mL per min  $\text{cm}^2$  (Sattar et al., 2014). This area is the most widely studied area for drug delivery of compounds due to its permeability allowing access to rapid absorption and satisfactory bioavailability for many drugs. The sublingual and buccal mucosa constitutes 60% of the oral mucosa's surface area which makes it a primary target of drug delivery (Madhav et al., 2009).

The gingival and palatal tissues are keratinized cells that have very limited permeability compared to the buccal and sublingual mucosa. This region of the mucosa is usually subjected to mechanical stresses (Rogers et al., 1992).

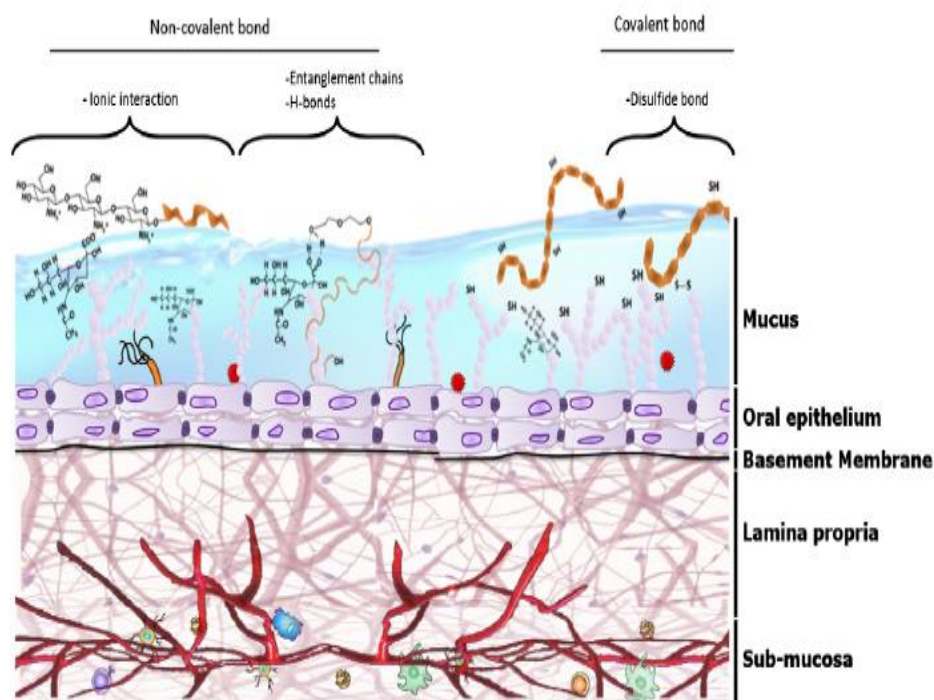


Figure 18: Bioadhesive interactions. Simplified oralmucosa representation: sub-mucosa with nerves and blood vessels, lamina propria, essentially with connective tissue and with some blood vessels, basement membrane usually a single cell layer lying in the interface of the epithelium and lamina propria; a simplified oral epithelium only for representative purposes; and a mucus layer with mucin and glycoproteins. The mucoadhesiveness of the polymers to the oral mucosa may be explained by the non-covalent and covalent bonds, depending on the polymers' functional groups (Borges et al.,2015).

Tissue	Structure	Epithelial thickness ( $\mu\text{m}$ )	Permeability
Buccal	NK	500-600	+
Sublingual	NK	100-200	++
Gingival	K	200	--
Palatal	K	250	--

Table 6: Regional Variation in Epithelial Thickness and Permeability Pattern within Oral Mucosa. ++ means “very suitable”; -- means “least suitable”; NK means “Non-Keratinized”; K means “Keratinized” (Campisi et al., 2010).

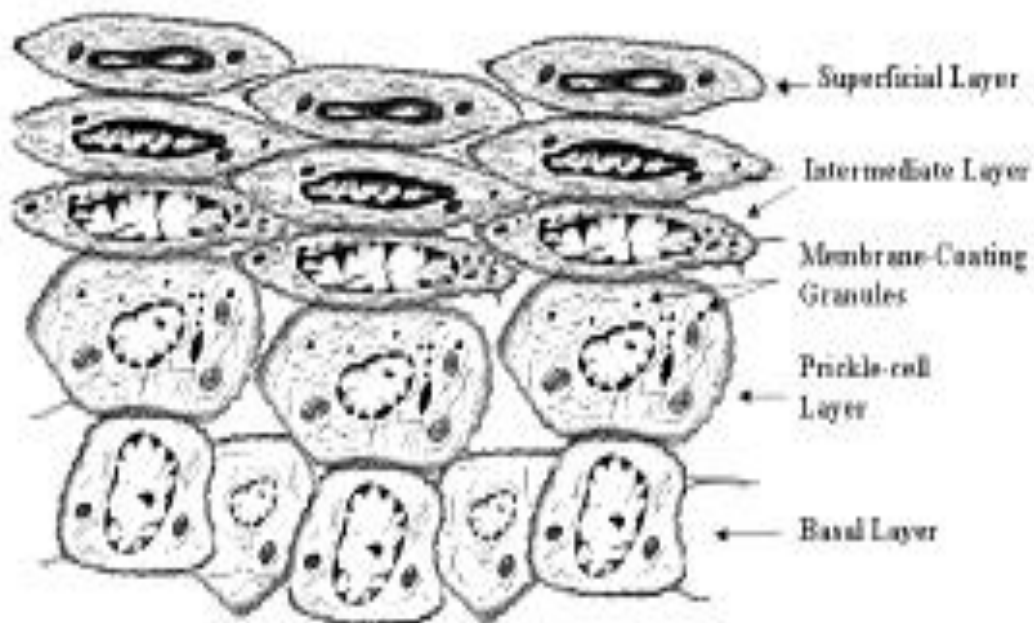


Figure 19: Ultra-structural features of oral buccal epithelium. MCGs become evident microscopically in the prickle cell layer, approximately at the midpoint of the epithelium (Campisi et al., 2010).

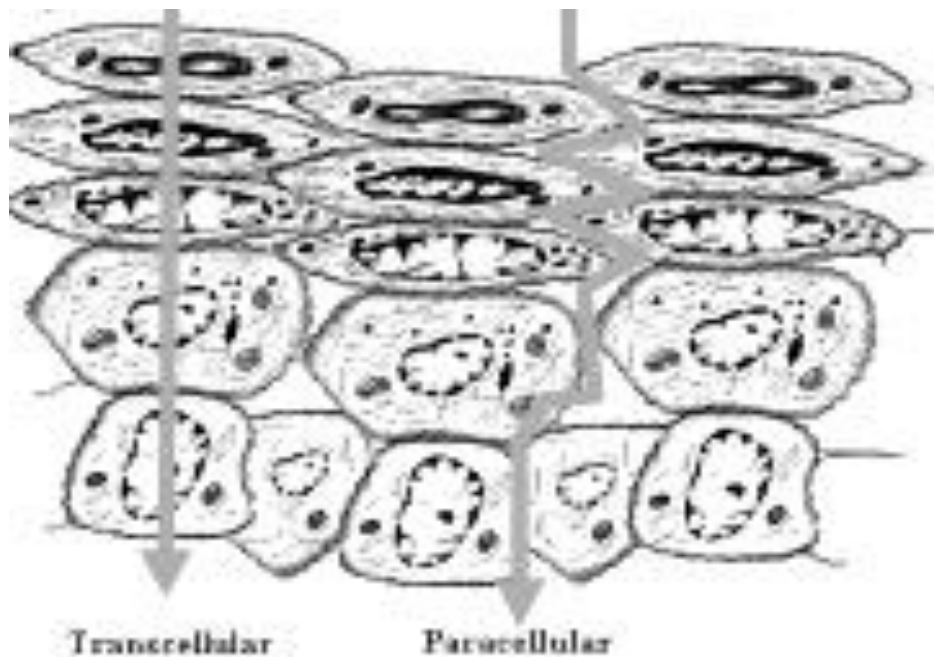


Figure 20: Routes of drug transport across oral epithelium (Campisi et al., 2010).

Saliva is an aqueous fluid excreted in the submucosa that has multiple functions that shapes the physiological environment of the oral cavity including lubricant, assisting in food mastication, preventing teeth demineralization, carbohydrate metabolism, and modulating growth of the oral flora (Patel et al., 2011; Sattar et al., 2014). The saliva mainly consists of mucus, proteins, mineral salts, and enzymes. The pH environment is weakly acidic to neutral (pH 5.5 - 7) varying based on what is being consumed (smell, taste, type of food). Normal flow rate is ~ 0.5mL/min with a secretion between 0.5 - 2L per day (Sattar et al., 2014). As mentioned earlier, the mucus is a component of salivary fluids that is an intercellular ground material that mainly composed of glycoproteins known as mucins (MW 0.5 - 20MDa). The negative charge on the mucins at physiological pH allows for binding to epithelium cells which results in forming a gelatinous layer. This serve as a physical barrier that limits drug diffusion by inhibiting specific and non-specific binding of compounds to the mucus layer (Sattar et al., 2014).

#### **1.2.4. Permeability Barriers and Absorption Mechanism of the Oral Mucosa**

The permeability characteristics of the oral mucosa falls within the range of the intestinal epithelium and the skin (Rogers et al., 1992; Campisi et al., 2010). Due to structural variations of the different regions in the oral mucosa the rate of permeability is generalized as sublingual > buccal > palatal (Rogers et al., 1992). Unlike the intestinal epithelium, the buccal mucosa is deficient of tight junctions and instead are incorporated with gap junctions, desmosomes and

emidesmosomes that are loose intercellular links which makes the mucosa have a higher permeability than skin (Campisi et al., 2010).

Studies examining the permeability coefficient values with water and horseradish shows that it is 3-5 times higher and 2-7 times higher respectively than skin.

There two sites that may serve as barriers in the oral epithelium: the basal complex and the intercellular spaces of the superficial epithelial layers. Even though the basal lamina may play a role in limiting the permeability of the certain substances (immuno-complexes and polar charged substances) it's structure is still allows absorption of other compounds such as non-polar compounds (Campisi et al., 2010). The actual barrier of the oral mucosa is shown to be caused by the membrane coating granules (MCGs) located in the intermediate layers of both keratinized and non-keratinized epithelium (Campisi et al., 2010). MCGs are spherical cell organelles that are 100-300 nm in diameter with variations in size and function based on their location in the epithelium. MCGs located keratinized regions are ovoid in shape with the diameter of 0.1 - 0.3  $\mu\text{m}$ . In non-keratinized regions, the MCGs are spherical in shape and have a diameter of 0.2 $\mu\text{m}$ . However, they also contain an electron-dense amorphous core similar to what is seen of its keratinized counterpart (Campisi et al., 2010). **Figure 19** illustrates the ultrastructure of the oral epithelium highlighting the various structure of the MCGs. Even though the function of MCGs hasn't been elucidated it's believe that their function is essential to membrane thickness, cell adhesion, production of cell surface coat, cell desquamation, and permeability

barrier (Patel et al., 2011). As the content of MCGs increases, the permeability of the oral mucosa decreases (non-keratinized > keratinized).

The absorption mechanism in the oral mucosa is theorized to occur by way of passive diffusion across lipid membranes either due to paracellular transport or transcellular transport. However, some compounds have the ability to diffuse through membrane by both mechanisms simultaneously as this would depend on the physiochemical properties of the compound. **Figure 20** illustrates these two various pathways within the ultrastructure of the oral epithelium. Hydrophilic drugs would favor paracellular transport due to the hydrophilic nature of the paracellular spaces hence acting as a barrier to lipophilic compounds. The rate of absorption being directly correlates to the molecular weight (MW) of the compound. As the MW of the compound increases the permeability of the membrane decreases. Conversely, transcellular transport would be highly favorable to lipophilic drugs while behaving as a barrier to hydrophilic compounds (Rogers et al., 1992; Patel et al., 2011). Parameters that need to be taken into account in understanding the oral mucosa's absorption and permeability properties were previously discussed in this section. They are the diffusion coefficient, partition coefficient, and the thickness of the tissue.

#### **1.2.5. Different Types of OFTs and Formulation Characteristics**

Drug delivery through the oral mucosa has been designed to occur by one of three ways, i) fast onset drug release in the oral cavity, ii) pulsatile release with rapid absorbency in the bloodstream followed by maintenance of consistent drug



concentration over time, iii) controlled release of compound over an extended period of time (Patel et al., 2011). These criteria are governed by either the application will be delivered through the sublingual mucosa, buccal mucosa, or local delivery in the oral cavity. **Figure 21** illustrates profiles of plasma concentration for each form of OFT delivery system designed for oral mucosa delivery. **Figure 22** illustrates the various formulations of films based on the approaches of delivery in the cavity.

As mentioned in the previous section, selection of delivery for particular compounds are determined on the condition the drug is treating. For application of a drug for rapid onset treatment of acute disorders, sublingual delivery would be the preferred choice. This is also known as orodispersible/orodisintegrating delivery. The flow of saliva limits the residence time of the drug based on this application and would require the use of high concentration of a potent small molecule. For treatment of chronic illnesses, sustained delivery of “systemically-acting” compounds would be the preferred route of administration through the buccal due to its structure. It allows for the attachment of a system to its expansively smooth and immobile surface that will permit sustained release. Local delivery of compounds is usually applied to direct treatments in the oral cavity such as toothaches, bacterial and fungal infections, ulcers, and periodontal diseases. Prime examples of this application are conventional mouthwashes, lozenges, and ointments (Campisi et al., 2010; Rogers et al., 1992). Mucoadhesion of oral films particularly with relation to the formulation to surfaces in the oral

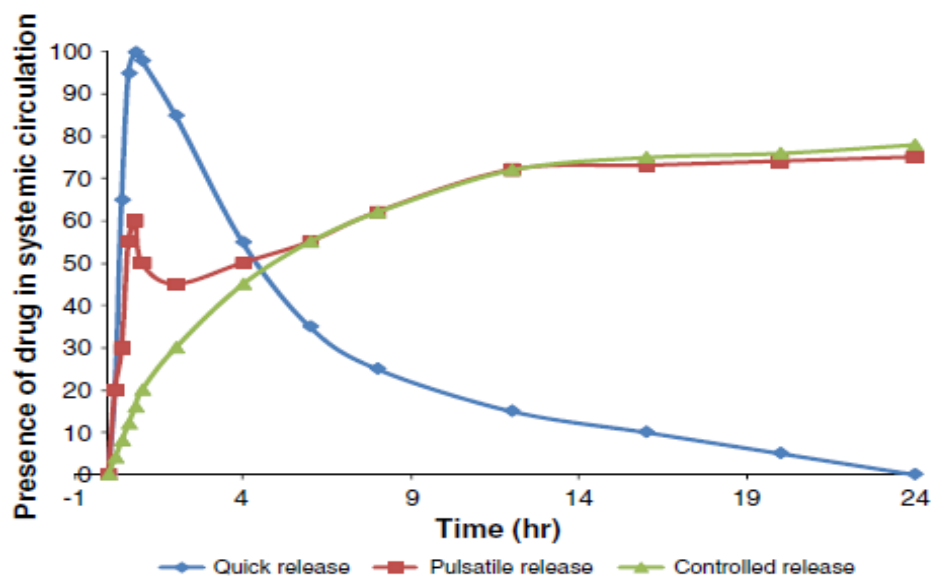


Figure 21: Schematic representation of different type of mucosal drug delivery system (Patel et al., 2011).

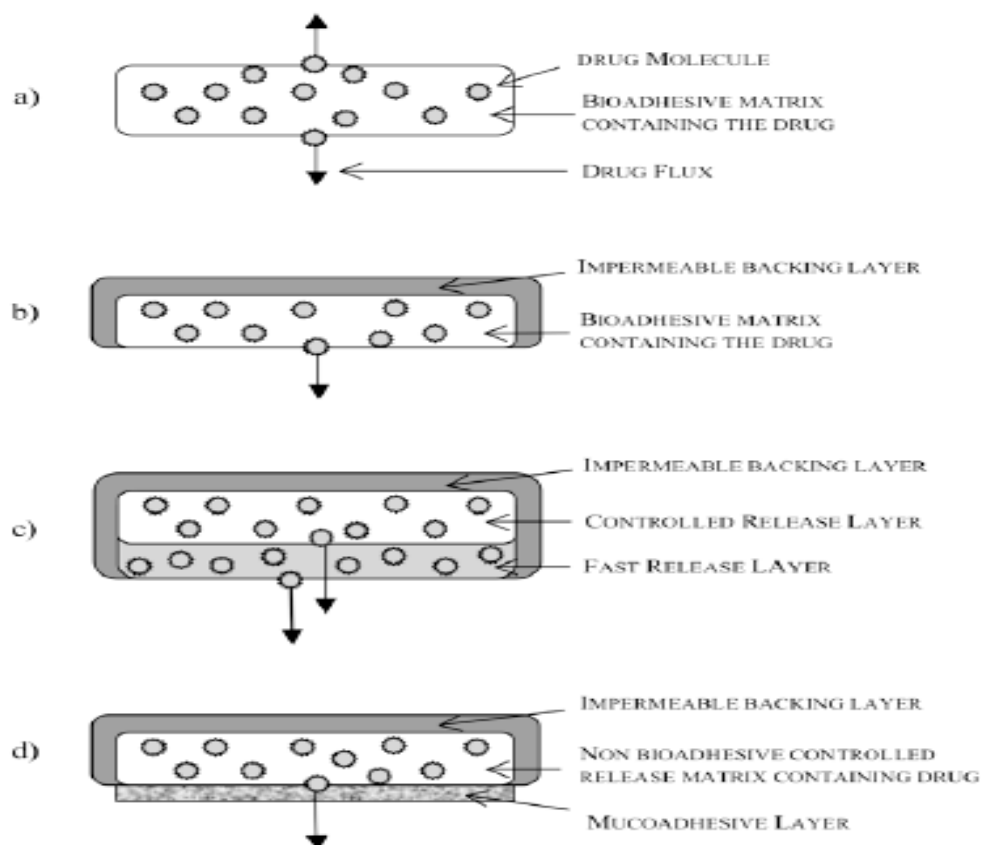


Figure 22(a-d): Schematic representation of some adhesive buccal drug delivery systems (Borges et al., 2015).

cavity is a principle of oral mucosa delivery that deserves to be highlighted as it plays an important role in buccal film delivery. There are various theories that have been postulated to characterize this mechanism, however, there are few that need to be mentioned. One of the most widely used is the wettability theory. This theory measures the “spreadability” of the delivery system across the biological substrate of interest. Primarily, the focus on surface tension of two adherent phases subtracted from their apparent interfacial tensions. Another hypothesis is the electronic theory which describes adhesion by means of electron transfer between the mucus. This results in the formation of a double layer of electrical charges at the mucus and mucoadhesive interface which is the formation of attraction forces within the double layer (**Figure 20**). The fracture theory explains the adhesive forces between these systems as it relates to the force needed to separate both surfaces from one each other. This highlights the force required for “polymer detachment” from the mucus in comparison to the strength of its adhesive bond. The adhesion theory defines this property as the result of various surface interactions between the adhesive polymer and the mucus substrate. The diffusion-interlocking theory focuses on the time-dependent diffusion of mucoadhesive polymer chains into glycoproteins of the mucus layer. This two-way diffusion process allows for the penetration rate to be dependent upon the diffusion coefficients of both interacting polymers. Depending on the depth of contact between the substrate and the polymer adhesive chains, semi-permanent bonds may form. The polymer’s MW and cross-linking density may influence the diffusion coefficient (Patel et al., 2011; Borges et al., 2015).

There are several criteria that applies to oral film formulations such as taste masking, fast dissolving, physical appearance, and mouth-feel (Dixit and Puthli, 2009). Selectivity of polymers is an essential component for formulation consideration. When choosing the appropriate polymer incorporate several crucial characteristics such as mucoadhesiveness, disintegration time, drug loading capacity, mechanical strength, elasticity, and handling properties. The polymers should be non-toxic, non-irritant, and barren of leachable impurities. It should have a long shelf-life and should not contribute to any secondary infections in the oral mucosa and dental regions. Regarding mechanical properties, the films should have sufficient peel, shear, and tensile strengths. Oral films are forged either by themselves or in combination with another polymer based on its use. The robustness of the films will rely on the polymers selected, its composition in the formulation along with other excipients, and the use of film (buccal or orodisintegrating). Dixit et al (2009) recommends that at least 45% (w/w) of the total dry weight of OFs should contain polymer of use. **Table 7** lists all of the commonly used polymers in oral films (orodisintegrating and buccal) for clinical and commercial use. The most commonly used polymers for fabricating OFs are pullulan, gelatin, and hypromellose (Dixit and Puthli, 2009). As mentioned earlier, polymers maybe used in combination when fabricating films in modulating certain characteristics such as the rate of disintegration of films especially in the case of buccal films. This research will highlight the benefits and use of oral disintegrating films (ODFs).

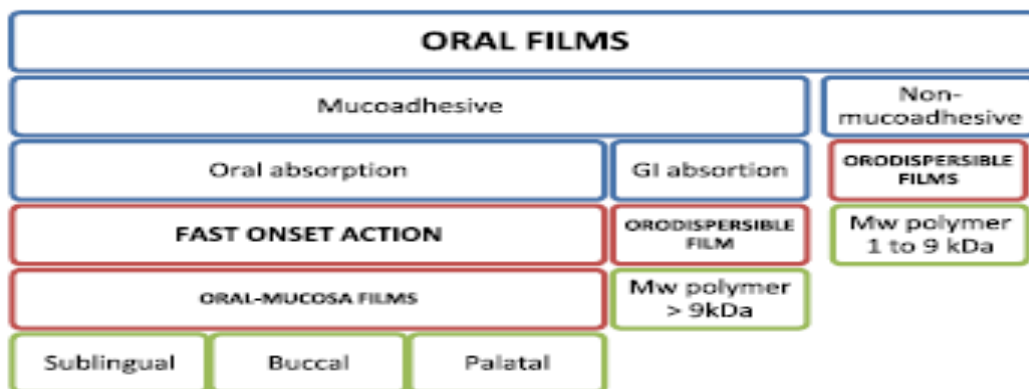


Figure 23: Simplified scheme with the different technologies (Borges et al., 2015).

S. No	Polymer Used	Film Forming Capacity	Appearance	Disintegration Time (sec)
1	HPMC E - 15 + PEG 400	GOOD	TRANSPARENT	120
2	HPMC E - 15 + GLYCERIN	GOOD	TRANSPARENT	92
3	HPMC KAM	VERY POOR	-----	-----
4	HPMC E - 5	AVERAGE	SEMI TRANSPARENT	127
5	PVA	AVERAGE	TRANSPARENT	52
6	PVP	VERY POOR	-----	-----
7	GELATIN	VERY POOR	-----	-----
8	EUDRAGITE RL - 100	VERY POOR	-----	-----
9	HPMC E - 15 + PULLULAN	POOR	-----	-----
10	PVA + PVP + GLYCERINE	AVERAGE	TRANSPARENT	64
11	PVA + PVP + PEG 400	AVERAGE	TRANSPARENT	52
12	HPMC E - 15 + PVA	AVERAGE	TRANSPARENT	78
13	HPMC E - 15 + PVP	AVERAGE	TRANSPARENT	67
14	HPMC E - 15 + PVA + MCC	POOR	-----	-----
15	PULLULAN + PVA	VERY POOR	-----	-----
16	HPMC E - 15 + MCC	BETTER	SEMI TRANSPARENT	42
17	PULLULAN + GUAR GUM + XANTHON GUM + CARRAGENON	BEST	TRANSPARENT	19

Table 7: Formulation and evaluation of polymers for oral disintegrating films (Nagaraju et al., 2013).

### **1.2.6. Oral Disintegrating Films (ODFs) - Potential Use/Benefits**

Oral disintegrating films (ODFs) (also known as orodispersible films) are thin films that readily dissolve in the oral cavity upon contact. Ghosh and Pfister defines ODFs as a films which is composed of water soluble and/or water swellable film forming polymers which permits the unit to dissolve instantaneously when its placed on the tongue in the oral cavity (Borges et al., 2015). ODFs can be single-layered or multi-layered depending on purpose of the formulation. They should be thin and flexible with the reproducibility in manufacturing and processing these films (Hoffmann et al., 2011). A major benefit of ODFs is the ability to increase the bioavailability of compounds that have been rendered inactive due to harsh conditions exposed during the traditional oral formulation. ODFs are extremely beneficial for a patient population, described earlier, who are unable/uncomfortable to swallowing conventional tablets, capsules, and liquids (Nagaraju et al., 2013). They're also beneficial for travelers and military personnel who have limited access to clean water. A typical ODF contains (Hoffmann et al., 2011):

- Active Pharmaceutical Ingredient - 30% (average maximum drug load is 25mg)
- Water-soluble film forming polymer(s) - 40-50%
- Plasticizers - 0-20%
- Fillers, colors, flavors, etc. - 0-40%

As mentioned earlier, selectivity is crucial for the effectiveness of ODFs as a form of drug delivery. Fast - dissolving films are composed of hydrophilic polymers with a very low molecular weight (MW) (~ 1,000 - 9,000 Daltons) are

usually not site-specific and dissolve in the cavity between 5 - 30 seconds. ODF polymers are hydrophilic such as pullulan, gelatin, and hypromellose (cellulose derivative). **Table 7** lists polymers that have been examined based on their appearance, disintegration time, and mixability if used in combination with another polymer.

One biomaterial that has had quite an impact in the application of drug delivery that will be discussed in the next section is silk fibroin protein.

### **1.3 Silk Fibroin Protein**

#### **1.3.1. The Wonderful World of Silk and Its Biomedical Applications**

Silk has been generally known for its wide use in the textile industry due to its radiance and mechanical characteristics. It is produced from spiders (over 30, 000 species) and several members of the Lepidoptera family such as mites, butterflies, and moths (Vepari and Kaplan, 2007). Silk fibers consists of repetitive protein sequences that are structural foundations in cocoon formation, nest building, traps, web formation, safety lines, and egg protection. The protein consists of sheet structures owing to the potency of hydrophobic domains that are comprised of short side amino acids that are tightly packed in the primary structure. Silk fibroin protein comprises of both large hydrophobic regions interspaced with small hydrophilic areas that are essential for the assembly of the polymer and the strength and resiliency of its fibers (Vepari and Kaplan, 2007). So how does silk transcend from a textile product to use in biomedical applications?

Biomaterial design has been an essential component in tissue engineering by incorporating physical, chemical, and biological cues in guiding cells into functional tissues via cell migration, adhesion, and differentiation. A biomaterial must degrade at a rate proportional to new tissue formation. This rate permits cells to deposit new extracellular matrices (ECM) and regenerate functional tissue. Biomaterials should also provide mechanical support equivalent to the level of functional tissue development. Central characteristic of a biomaterial is its ability of being biocompatible and non-immunogenic (Vepari and Kaplan, 2007).

Silk sutures from the domesticated silkworm *Bombyx mori* has been used for centuries as sutures. Silk protein produced from *B. mori* consists of two types of protein at a 1:1 ratio: light chain (~26 kDa) and heavy chain (~390 kDa). These chains are linked together by a single disulfide bond. These proteins are coated by a group of hydrophilic proteins located on the surface of the fibroin, silk filament core in the cocoon filament that illicit immunogenic reactions in humans, known as sericin (20 - 310 kDa). They are adhesive proteins that account for 25-30% of the total *B. mori* cocoon weight. Sericin is removed through the degumming process (Vepari and Kaplan, 2007; Rockwood et al., 2011). Silk fibroin protein produced from *B. mori* has an amino acid composition that primarily consists of glycine (43%), alanine (30%), and serine (12%) located in both heavy and light chain domains. The heavy chain regions comprise of 12 crystalline domains that incorporates Gly-X repeats (X being Alanine, Serine, Threonine, and Valine). This sequence results in a hydrophobic protein that



constructs materials that are strong and resilient (Vepari and Kaplan, 2007; Rockwood et al., 2011). These regions permits for the silk fibroin materials to exhibit its high mechanical strength and toughness that rivals materials such as Kevlar, collagen (0.9-7.4 MPa), and poly lactic acid (28-50 MPa) with a tensile strength of 740 MPa (Rockwood et al., 2011). Not only is silk fibroin protein durable but it also degradable. Its order of degradation can be amenable based on implantation site, mechanical environment, and processing impacting this characteristic *in vivo*. Mediated by proteases, it is inversely correlated to the overall Beta sheet content and degree of organization of the non-crystalline regions in the protein (Rockwood et al., 2011). This also depends on the state of structure in silk I (water soluble, non-crystallized) or silk II (water insoluble; crystallized -heat exposed) (Vepari and Kaplan, 2007). Silk fibroin protein has also been shown to exhibit lower inflammatory responses *in vitro* (in human and rat mesenchymal cells) and *in vitro* comparison to polymers such as PLA and collagen. These characteristics has been manipulated for innovative applications of other silk-based biomaterials such as sponges, tubes, films, particles, and fibers. **Figure 24** displays that various materials fabricated from silk fibroin protein. **Table 8** lists various applications of silk fibroin protein (Rockwood et al., 2011). In the past 10 years, the application of silk as a form of drug delivery have been examined in great detailed. **Figure 25** illustrates drug delivery systems that been established in recent years. Sill fibroin protein have been synthesized into tablets, films, scaffolds, hydrogels, fibers, microparticles, and nanoparticles as vehicles of drug delivery (Seib and Kaplan, 2013). Release characteristics of

these applications are controlled by either diffusion of the encapsulated compound or solubilization and/degradation of silk. These parameters can be adjusted by examining treatment conditions which can produce Beta sheet content ranging from 14% - 57% silk II structure. Rate of release of therapeutics are governed by the molecular weight (MW) of the drug. Release small MW drugs ( $<1,000$  g/mol) from silk are determined by the drug's physiochemical properties while release of larger MW compounds are based on Fickian diffusion model (Seib and Kaplan, 2013). Drugs are typically loaded together with silk fibroin solution (doped) or after formation of the delivery system of choice. Preferential interest that drug is loaded with silk solution as this improves uniform drug loading and entrapment efficiency (Seib and Kaplan, 2013).

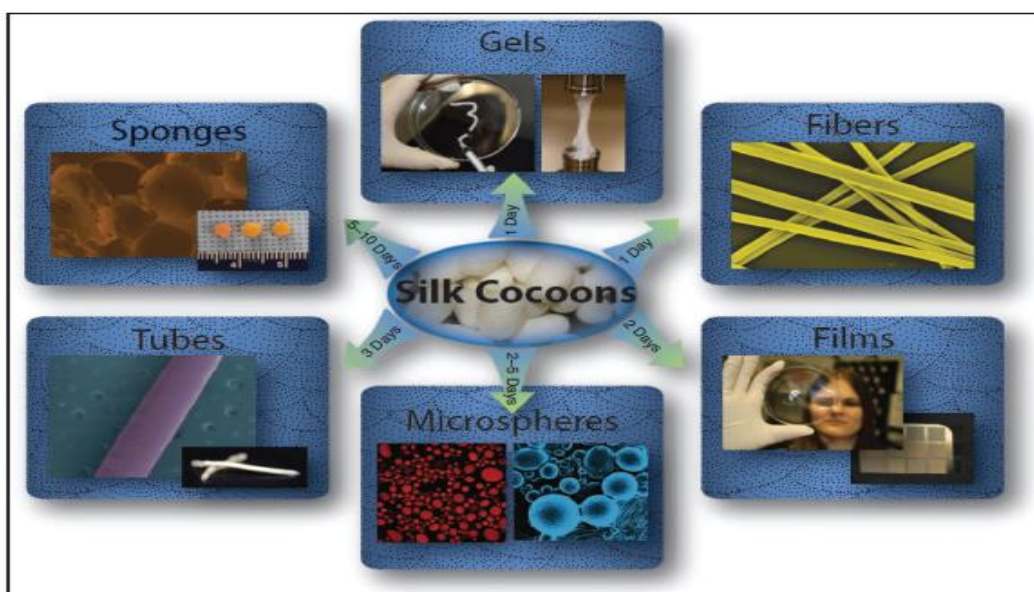


Figure 24: Schematic of material forms fabricated from silk fibroin protein using both organic solvents and aqueous-based processing approaches (Rockwood et al., 2011).

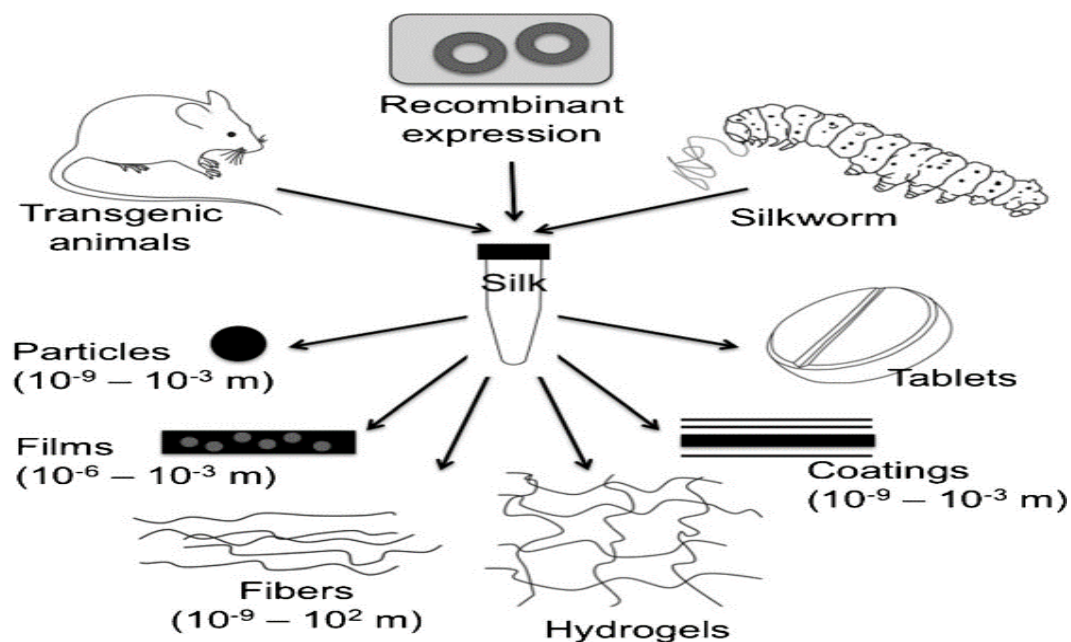


Figure 25: Diagram of silk sources & various drug delivery systems. Numbers in parentheses refer to the approximate sizes of these materials; diameters or thickness in the case of particles & films/coatings, respectively (Seib et al., 2013).

Application	Tissue type	Material format
Tissue engineering	Bone	HFIP sponges <sup>41,43,44</sup>
		Aqueous sponges <sup>43,45,46</sup>
		Electrospun fibers <sup>36</sup>
	Cartilage	HFIP sponges <sup>47</sup>
		Aqueous sponges <sup>48–50</sup>
		Electrospun fibers <sup>51</sup>
	Soft tissue	HFIP sponges <sup>52</sup>
		Aqueous sponges <sup>52</sup>
		Hydrogels <sup>15</sup>
	Corneal	Patterned silk films <sup>31,53</sup>
Disease models	Vascular tissues	Tubes <sup>22</sup>
		Electrospun fibers <sup>54–56</sup>
		Aqueous sponges <sup>57</sup>
	Cervical tissue	Aqueous sponges <sup>57</sup>
	Skin	Electrospun fibers <sup>58,59</sup>
	Breast cancer	HFIP sponges <sup>60</sup>
		Aqueous sponges <sup>61,62</sup>
		Aqueous sponges <sup>63</sup>
Implant devices	Autosomal dominant polycystic kidney disease	
	Anterior cruciate ligament	Fibers <sup>64,65</sup>
	Femur defects	HFIP sponges <sup>17</sup>
	Mandibular defects	Aqueous sponges <sup>66,67</sup>
Drug delivery		
	Drug delivery	Spheres <sup>34,68–70</sup>
	Growth factor delivery	Spheres <sup>71</sup>
	Small molecule	Spheres <sup>33</sup>

Table 8: Biomedical applications of silk scaffolds (Rockwood et al., 2011).

Route of administration	Study	Comment	Reference
Transdermal	Microneedles of various designs were able to penetrate the human stratum corneum and deliver model drugs.	First example of silk-based ex vivo transdermal delivery. The track record of silk in the skin setting (i.e., suture) bodes well for the future of such devices.	[51]
Inhalation	Occupational exposure of textile workers to silk fibers induced chronic obstructive pulmonary disease (COPD).	Inhalation of fibers is commonly associated with COPD. In the case of asbestos exposure, mesothelioma is typical.	[52]
Oral	Silk tablets containing theophylline were administered to healthy volunteers and compared to a commercial slow-release tablet.	Silk tablets showed a similar concentration-time curve to the commercial products. In the presence of food, complete release was observed, suggesting that digestive enzymes facilitated silk degradation.	[36]
Intravenous	Injection of recombinantly engineered silk polyplexes with a tumor-homing peptide into NOD/SCID mice.	A silk polylysine block copolymer with the F3 tumor-homing peptide was able to induce in vivo transfection. No data were presented on biodistribution or impact on cells.	[53]
Subcutaneous	Silk hydrogels were encased by a fibrous capsule that varied in thickness; no obvious signs of giant cells, but some cell infiltration.	One of the first studies that provided histological evidence for the in vivo response of silk hydrogels.	[48]
Intramuscular	Silk films generated from HFIP were implanted in rats, retrieved after six weeks and subjected to histology.	No evidence of silk degradation. Films were surrounded by a small fibrous capsule. The overall inflammatory response was less than for collagen or poly(L-lactide).	[49a]
Intraosseous	BMP-2-loaded scaffolds were implanted into critical-sized cranial defects in mice.	BMP-loaded scaffolds showed new bone development. No in-depth histology was performed to examine additional aspects of the tissue response to treatment.	[54]

Table 9: Examples of the various routes of administration that have been established with silk (Seib et al., 2013).

### 1.3.2. Silk Films

Water soluble silk films have release characteristics that align with the solubilization characteristics of the film in an aqueous environment. As previously mentioned, this is due the non-crystallized  $\beta$  - sheet structure (silk I) that allows for this mode of degradation. Silk I structures are completely water soluble allowing for release of drug within seconds. However, silk films can be modified into insoluble films (silk II) by applying additional applications of shearing, spinning, heating, salts, exposure to solvents (e.g., methanol, ethanol, pH, slow freezing, and water vapor annealing (Seib and Kaplan, 2013). Silk films have been demonstrated as delivery vehicle for doxorubicin (Seib et al., 2012; Chiu et al., 2014; Coburn et al., 2015; Seib et al., 2015) and enzymes (Lu et al., 2010; Lu et al., 2009). However, these studies mostly highlight the use of insoluble silk films. Kundu et al. (2008) did examine the characteristics of DSF for oral mucosa delivery; however, only mechanical and morphological characteristics of DSF blended with HPMC and PEG were examined (Kundu et al., 2008) .

This research will demonstrate the potential use of water soluble silk films for oral mucosa delivery using the antimalarial drug mefloquine as the active pharmaceutical ingredient (API) of choice.

#### 1.4. Research Objectives/Aims

The hypothesis presented is that silk can be fabricated into dissolvable films for the delivery of chemotherapeutics for prevention of malaria infection. The goal of this research is to introduce a novel mode of drug delivery for antimalarial drugs. Mefloquine hydrochloride was chosen as the drug of choice to test this delivery system since it is already formulated for oral delivery (tablets) and it is directly relevant for the treatment of malaria.

Table 10: Table highlighting overview of aims for current thesis research.

<b><u>Aims of Research</u></b>	<b><u>Current Commercial OFTs</u></b>	<b><u>Current Research Target</u></b>
<b>Aim#1 – Drug loading of silk fibroin films w/MF.</b>	Mean max drug load of API into commercial OFT products ~ 25mg (Hoffman et al., 2011)	Drug load of 1mg of mefloquine into silk films (1 – 6%).
<b>Aim#2 – Rate of disintegration and drug release for dissolvable silk – mefloquine films.</b>	Mean disintegration time and cumulative release of commercial OFT products 50 - 95% within 30 – 70 seconds (Nagaraju et al., 2013).	Disintegration Time & Drug Release: 95% cumulative release within 10 – 60 seconds <i>in vitro</i> .
<b>Aim#3 – Robustness of DSF for packaging and handling.</b>	Tensile Strength: 36.20 - 61 MPa Elongation at Break %: 4.37 – 16 Elastic modulus: 987.5 – 1656 MPa (Brindle & Krochta, 2008; Prasad et al., 2008)	TS, EB, and EM for DSF fall within range of commercial OFTs.
<b>Aim#4 – Toxicity of DSF.</b>	N/A	DSF with and without mefloquine hydrochloride do not illicit immunogenic effects.

#### **1.4.1. Aim#1 - Determining drug loading of dissolvable silk fibroin films with mefloquine hydrochloride.**

The goal of this aim is to fabricate DSF and determine the morphological characteristics and drug loading capabilities of these films. Design targets in this study for the creation of DSF are listed in **Table 10**. Silk films will be fabricated from various concentrations of silk fibroin solution (1% - 6% w/v) based on previous studies using water insoluble silk films as a vehicle of drug delivery of other small molecules and proteins (Seib et al., 2012; Seib et al., 2015). The average maximum drug load of API in commercial OFT products on the market is 25mg (**Table 10**). For this study, this research determined the drug loading efficiency of 1mg of mefloquine hydrochloride in DSF. Drug loading efficiency (Equation 1) was calculated as:

$$\text{Drug Loading (\%)} = \left( \frac{(\text{ML} - \text{MS})}{\text{ML}} \right) * 100 \quad (1)$$

where “ML” is the amount of mefloquine loaded into films and “MS” is the amount of mefloquine isolated in supernatant after films were dissolved. Drug loading will be determined analytically with the use of UV spectrophotometer by light absorbance (283nm). The absorbance values will be transformed to concentration by reference to a standard calibration curve obtained experimentally ( $R^2 = .9998$ ). SEM and FTIR were used to characterized the morphological features of the films.



**1.4.2. Aim#2 – Determining the rate of disintegration for dissolvable silk films as well as characterizing the rate of drug release of mefloquine hydrochloride from these films.**

The goals of this aim is to determine the rate of disintegration of DSF and characterize the rate of release for mefloquine from the films (1 – 6%) to show that they are within range with commercially available OFTs (**Table 10**). With the use of blue food coloring (McCormick and Company) the rate of disintegration (mass loss of film over time) was determined on how rapidly the films dissolved in media (Nagaraju et al., 2013; Preis et al., 2012). During disintegration testing, fabricated films were placed in a petri dish containing 5mL of media (PBS/distilled water) in ambient room temperature. The rate of disintegration of the films was determined both qualitatively (recording total time of the film dissolving in media) and quantitative (determining mass of loss of silk films over time until 95% of the films dissolve). The results of this this study will help assess whether these films are considered fast – dissolving or slow releasing films. Rate of dissolution will also be determined in PBS (pH7) with the collection of samples over various time intervals (1min, 3mins, 5mins, 10mins, 15mins, 30mins) (Mashru et al., 2008; Chiu et al., 2014). Samples used in the dissolution study will be performed in triplicates. Rate of drug released was determined analytically as mentioned in section 1.4.1.

#### **1.4.3. Aim#3 – Establishing the robustness of dissolvable silk films for packaging and handling.**

The goal of this aim is to characterize the mechanical properties of the DSF and to ensure that they are in line with commercially available OFTs (**Table 10**). Tensile testing was used to assess the robustness of the fabrication process and assess the mechanical characteristics of the water soluble silk films. It is important to state that there are no FDA approve guidelines outlining the basic criteria for OFTs at the moment. Mechanical features will be ascertained using an Instron universal testing instrument. Examination of the films will focus on its thickness (with use of a micrometer), ultimate tensile strength (UTS), elastic modulus, and elongation to break %.

#### **1.4.4. Aim#4 - Ensuring that Mefloquine Encapsulated Silk Films Do Not Illicit Immunogenic Effects**

This aim is to determine whether DSF doped with mefloquine hydrochloride are cytotoxic *in vitro*. The ultimate goal is to show that DSF doped with mefloquine hydrochloride do not produce any illicit effects especially with the highest concentration of drug theoretically loaded into films (~150ug/mL). Silk films fabricated will be examined to ensure safety for potential clinical use. Cytotoxicity testing based on the ISO 10993 (Biological Evaluation of Medical Devices, Part 5: Tests for Cytotoxicity: *In vitro* Methods) using L-292 mouse fibroblast cells that will help determine the safety of this formulation.

# CHAPTER 2: Methods and Materials

## 2.1. Silk Fibroin Extraction:

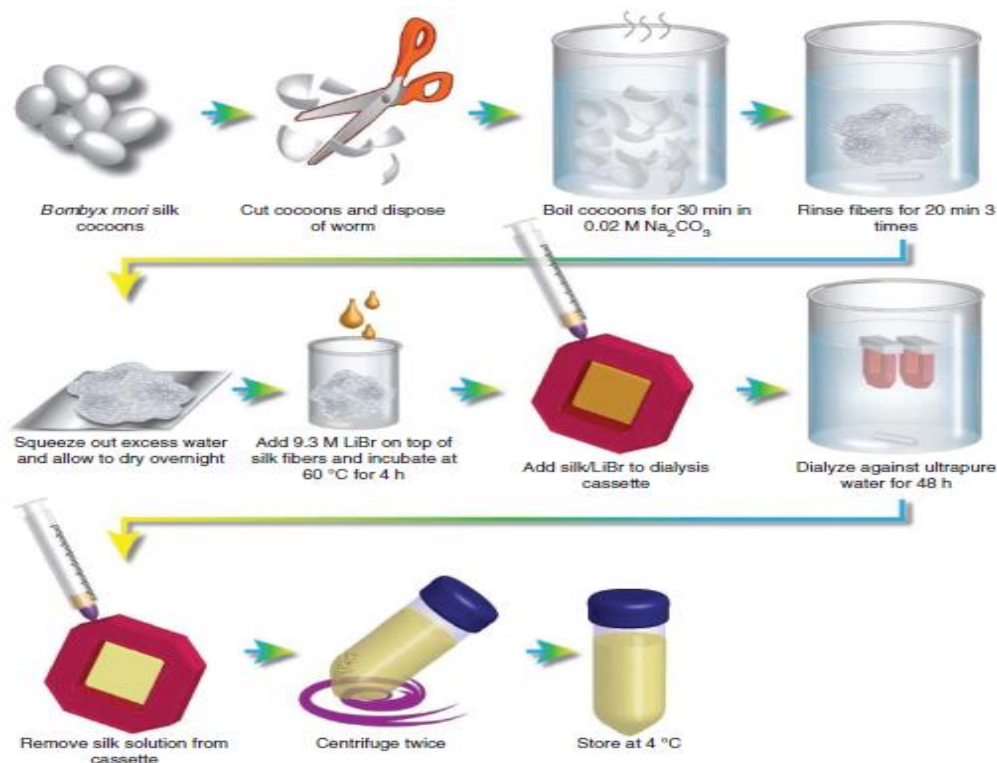


Figure 26: Schematic of the silk fibroin extraction procedure. Starting from the raw material (cocoons) to the final aqueous solution takes 4 days (Rockwood et al., 2011).

Silk fibroin solutions were prepared as a modification of a procedure described in Rockwood et al. (2011). Briefly, cocoons (~5g) were boiled for 30 minutes in an aqueous solution of 0.02M  $\text{Na}_2\text{CO}_3$ , then rinsed thoroughly with water to extract the sericin proteins from the degumming process. After drying for at least 24hrs, the extracted silk is then dissolved in 9.3M LiBr solution at room temperature. This yields a 20% (w/v) solution that is dialyzed in ultrapure water using a Slide-a-Lyzer dialysis cassette (Pierce, MWCO 3500) for a total of 48 hours. The final concentration of aqueous silk solution yielded, which is

determined by weighing 0.5mL of the remaining solid after drying, is ~8.0% (w/v). Silk solutions with concentration of <8% were prepared by diluting with ultra-pure water.

## **2.2. Fabrication and Drug Loading into Silk Films**

### **2.2.1. Fabrication of Silk Films**

Fabrication of silk films was modified from the procedure described in Seib and Kaplan (2012). Briefly, 2 mL of silk fibroin solution varying in concentration (w/v) (1% - 6% } were cast on 33mm x 23mm polydimethylsiloxane (PDMS) (Dow Corning Corporation Midland, USA) molds. The films were dried for at least 6hrs in a chemical under laminar conditions at room temperature (**Figure 27**). Once dried, the films were trimmed down to 27mm x 17mm. The resulting films generated are soluble in water. Films were collected and stored in petri dishes at room temperature until further use.

### **2.2.2. Drug Loading of Mefloquine Hydrochloride and Doping of Food Dye to Silk Films**

Stock solution of mefloquine hydrochloride (Sigma-Aldrich) was prepared by adding 50mg of mefloquine hydrochloride to a 50mL conical tube. 40mL of distilled DNase/RNAase free water (Invitrogen) was added, sonicated, and brought to a final volume of 50mL. This resulted in a final concentration of 1mg/mL of mefloquine hydrochloride. Fabrication of the films involved mixing a 1:1 volume ratio of silk solution (1-6%) with mefloquine hydrochloride stock

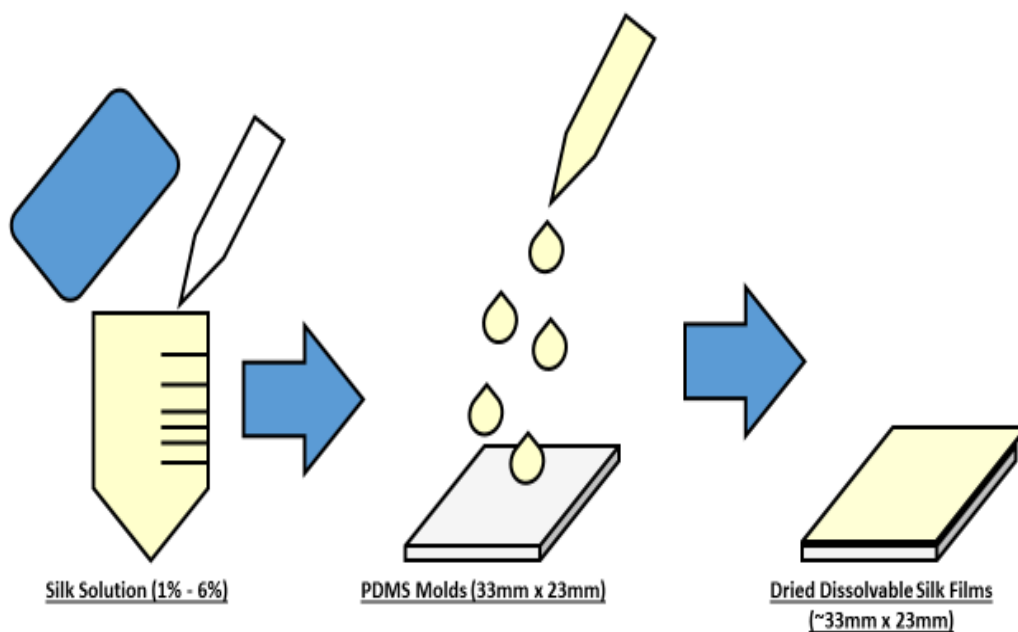


Figure 27: Schematic of silk film fabrication for mechanical testing, disintegration testing, SEM imaging, FTIR characterization.

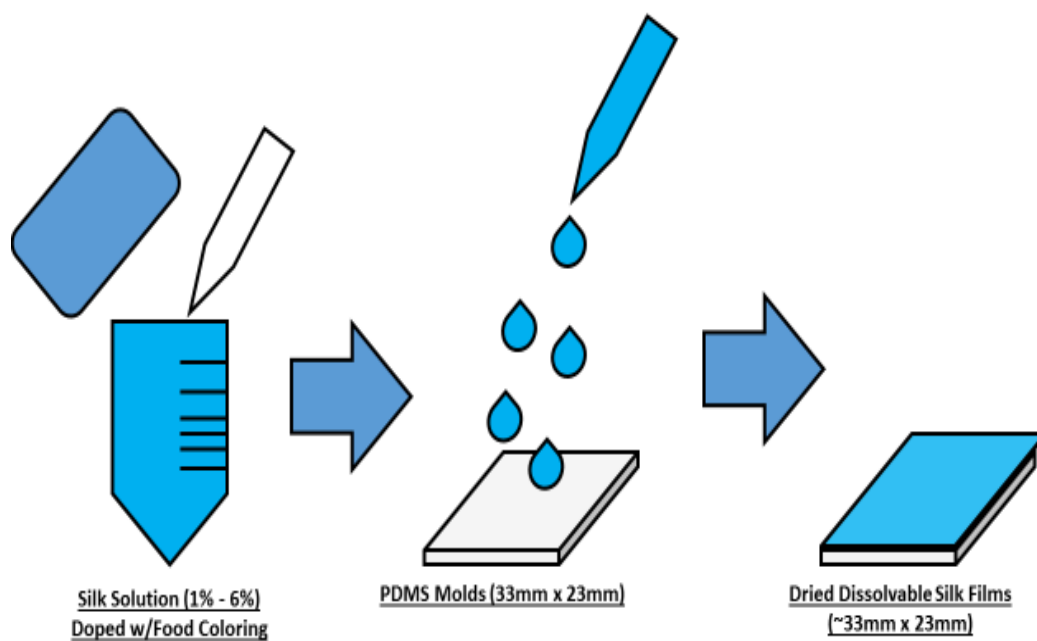


Figure 28: Schematic of silk film fabrication for disintegration testing.

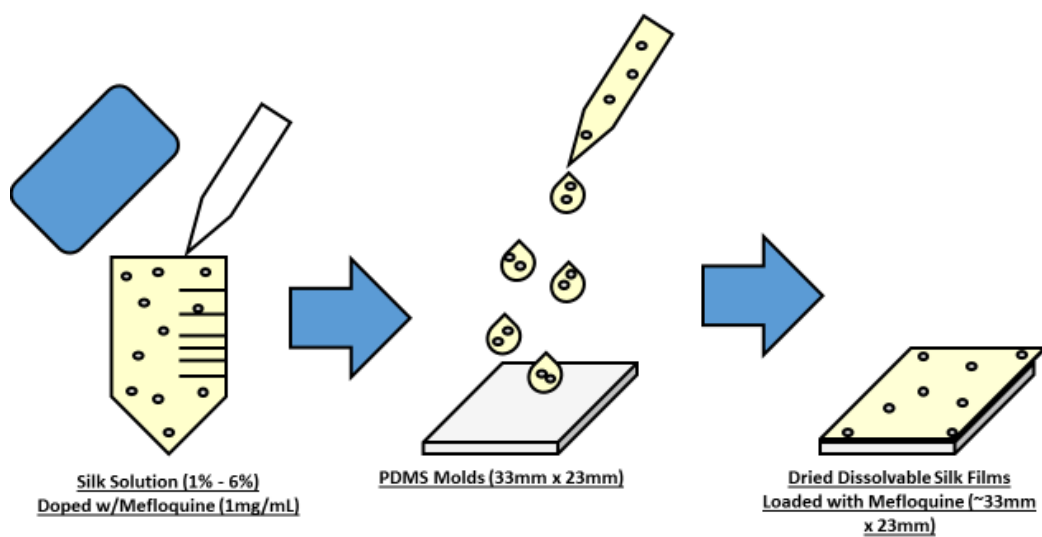


Figure 29: Schematic of silk film fabrication and drug loading for drug loading, dissolution, and cytotoxicity testing.

solution. 2mL of each solution were casted on PDMS molds with dimensions of 33mm x 23mm in a chemical hood under laminar conditions at room temperature (**Figure 29**) and were dried for at least 10hrs. Once dried, the films were trimmed to 27mm x 17mm. The resulting films generated are soluble in water. Films were collected and stored in 4°C until further use.

For fabrication of silk films doped with food coloring, 2.5uL of McCormick blue food dye was added to silk solution after they were casted on PDMS molds. The films were dried for at least 6hrs in a chemical under laminar flow conditions at room temperature and stored in 4°C until further use.

### **2.2.3. Measuring Drug Loading Efficiency of Dissolvable Silk Films**

As mentioned in section 1.4.1., drug loading of mefloquine hydrochloride into silk films was determined by completely dissolving silk films in 1mL of PBS (pH7) at room temperature. Mefloquine was then isolated by extracting the small molecule from silk protein using a 1:1 volume ratio of methanol and PBS (pH7), centrifuging, isolating the supernatant from the gelled silk debris, and airing out the remaining methanol solution in a chemical hood. The supernatant containing free drug was analyzed spectrophotometrically by light absorbance using a SpectraMax M2 spectrophotometer (Molecular Devices, Sunnyvale, CA, USA) for each corresponding supernatant: mefloquine - 283nm. For quantification of dissolution, films were dissolved in the corresponding media and absorbance

values were converted to concentrations via a standard curve made in the corresponding media. All samples analyzed were conducted as triplicates.

## **2.3. Mechanical Properties**

### **2.3.1. Mechanical Testing for Ultimate Tensile Strength, Elastic Modulus, & Strain to Failure (%)**

The protocol for measuring tensile strength, elastic modulus, and strain to failure of each silk film (1-6%) was modified from (Lu et al., 2010).

Briefly, DSF were assessed using an Instron Universal Testing Instrument (model 3366) equipped with a load cell of 10N with the Biopuls testing system that included submersible pneumatic clamps. For dry tests, the films (dimensions of 33mm x 17mm, dried and stored in a vacuum) were loaded onto the instrument and tested under ambient conditions (22C, 50% RH). The strain control rate of  $0.1\% \text{ s}^{-1}$  was used for testing. The original cross-sectional area was determined by measuring the thickness of the films (mentioned in the next section) and multiplying by the specimen gauge width (17mm). The nominal tensile stress and strain were graphed on the basis of the original cross-sectional area and length, respectively, and the stiffness, yield strength, strain to failure, and ultimate tensile strength (UTS) were determined.

UTS was determined as the highest stress value attained during the test. The stiffness (elastic modulus) was calculated by using a least-square (LS) fitting between the points corresponding to 30% & 60% of the UTS. This was deemed to be sufficient enough to capture the linear portion of the stress/strain curve



objectively for all samples tested. The yield strength was determined by offsetting the LS line by 0.2% strain and finding the data intercept. The strain to failure was determined as the last data point before any decrease in load (failure strain minus the strain corresponding to 30% UTS noted earlier). At least N=4 samples were used under every condition, ranging from 1%-6% (w/v) silk concentration.

### **2.3.2. Film Thickness**

Briefly, the films (in quadruplicates) were measured using a thickness micrometer (Mitutoyo 700-118-20) at five locations on the film (center and four corners). These measurements were calculated and the mean thickness was determined. Samples that contained air bubbles, nicks, or tears were omitted from testing.

### **2.4. Disintegration Testing of Dissolvable Silk Films**

A protocol for measuring disintegration of silk films was modified from (Nagaraju et al., 2013). Briefly, similar to orally disintegrating tablets the disintegration time limit of 30 seconds or less can be applied to fast dissolving oral strips. Any films dissolving in time points greater than 90 seconds would be considered slow releasing films. Silk films, doped with blue food coloring, were placed in 35mm x 10mm petri dishes 5mL of media (PBS and distilled water). Disintegration of the films was timed from the moment the films made contact with the media. The tests were recorded using a Samsung S6 Galaxy phone.

For measuring the mass loss/rate of disintegration of films three time points were selected based on the total disintegration time of 1 – 6% films samples were collected and placed in weight boat then put in a 60°C oven to dry overnight. Once dried, the total mass of the films was measured and percentage of film disintegration was calculated (Equation #2):

$$\% \text{ of Disintegration} = \left( \frac{M_t}{M_i} \right) * 100 \quad (2)$$

Where  $M_t$  is the mass of film measured at time =  $t$  and  $M_i$  is the initial mass of film prior to testing. The test was conducted in a triplicate.

## **2.5. *In Vitro* Dissolution Studies of Dissolvable Silk Films**

An *in vitro* dissolution protocol was modified from (Mashru et al., 2008; Chiu et al., 2014). Briefly, the dissolution studies were conducted in Phosphate Buffer Saline (PBS) solution (pH7). Each film was placed in a 1.5mL Eppendorf tube and 1mL of media was added to each tube and placed in a water bath at 37°C +/- 0.5C under static conditions. At each time interval (1min, 3mins, 5mins, 10mins, 15mins, and 30mins) 900uL was withdrawn and transferred to an empty, sterilized 1.5mL Eppendorf tube. Samples were stored in 4°C until further analysis. Then 900uL of fresh media was replaced and samples were returned to heat bath.

Since silk fibroin protein contains tyrosines that absorb near the same wavelength as mefloquine hydrochloride (Lu et al., 2010) (280nm), isolation of silk protein occurred as mentioned in section 2.2.3. The samples were then analyzed spectrophotometrically by light absorbance using a SpectraMax M2

spectrophotometer (Molecular Devices, Sunnyvale, CA, USA) for each corresponding supernatant: mefloquine - 283nm. For quantification of dissolution, films were dissolved in the corresponding media and absorbance values were converted to concentrations via a standard curve made in the corresponding media. All samples analyzed were conducted as triplicates.

## **2.6 Scanning Electron Microscope (SEM)**

SEM analysis was modified from Lu et al. (2010). Briefly, due the thinness of the films, only the cross-section of the silk films (1% - 6%) were imaged with a Zeiss Supra 55 VP SEM (Oberkochen, Germany). Each sample were cut into small squares with use of a razor blade and staged on the mount facing upwards, and sputter coated with gold for at least 60 seconds. The images were imaged with a Zeiss Supra 55 VP SEM.

## **2.7. Fourier Transform Infrared Spectroscopy (FTIR)**

FTIR analysis protocol was modified from Coburn et al. (2015).

Briefly, samples were examined with a Jasco FT/IR6200 spectrometer (JASCO, Tokyo, Japan) equipped with a MIRacle™ attenuated total reflection (ATR) Ge crystal cell in reflection mode. For each measurement, 32 scans of 4  $\text{cm}^{-1}$  resolution were co-added and Fourier transformed using a Blackman-Harris apodization function. The secondary structure of the silk films was characterized between 1585 and 1710  $\text{cm}^{-1}$  representing the amide I region. The amid I region was deconvoluted using Opus 5.0 software (Bruker, Billerica, MA). The spectra is normalized and baseline corrected between 1750 and 1150 $\text{cm}^{-1}$  followed by

Fourier self-deconvolution (FSD) between 1720 and 1585  $\text{cm}^{-1}$  using a bandwidth of 27.5  $\text{cm}^{-1}$  and curve-fitted to measure the relative areas of the Amide I region structures assuming the C = O stretch is the same for all secondary structures. Peak positions were first defined using the second derivative of the original spectra and a local least squared analysis performed. These peaks were then held constant and a Levenberg - Marquardt algorithm was used to optimize the peak width and height. This allowed for the resulting curve fit to closely resemble the initial FSD spectrum. Peak positions were defined as follows: 1615-1630 $\text{cm}^{-1}$  and 1695-1705  $\text{cm}^{-1}$  as  $\beta$ -sheet structure; 1631-1655  $\text{cm}^{-1}$  as random coil structure; 1650-1660  $\text{cm}^{-1}$  as  $\alpha$ -helical bands; and 1660-1695  $\text{cm}^{-1}$  as  $\beta$  turns.

## **2.8. Cytotoxicity Testing of Dissolvable Silk Films with Mefloquine Hydrochloride**

Cytotoxicity study was modified from the International Organization for Standardization 10993: Biological Evaluation of Medical Devices, Part 5: Tests for Cytotoxicity: *In vitro* Methods. Briefly, twelve experimental test groups were (six groups ranging from 1% - 6% silk films doped with mefloquine and six groups ranging from 1% - 6% silk films without any drug) were prepared by dissolving each sample in 1mL of EMEM (ATCC 30-2003) supplemented with 10% horse serum (Sigma H1138), and 1% penicillin - streptomycin (100x, ATCC 30-2300) after being sterilized under ultra-violet light for 30 mins (each side). A stock solution of 500 $\mu\text{g/mL}$  of mefloquine hydrochloride was created and used as a positive control while EMEM supplemented with HS and pen-strep served as a

negative control in the study. The experimental groups and controls were incubated for 24 hours in an incubator at 37°C with 5% CO<sub>2</sub> and approximately 95% RH. Study was conducted on L-292 mouse fibroblasts (ATCC CCL 1, NCTC Clone 929, of strain L).

On the first day, L-292 cells were seeded into 4 – 96 well plates, cell suspension for seeding 1x10<sup>5</sup> cells/mL, 0.1mL per well. Once seeded, well plates were maintained in an incubator to propagate the cells at 37°C and 5% CO<sub>2</sub> atmosphere. On day 2, sample preparation of experimental groups and controls occurred and were placed in incubator for 24hrs as previously mentioned. On day 3, 100uL of samples from test groups and controls were transferred to three 96 well plate cultured with near confluent L-292 cells (after removal of media) (well plate #1 100uL of stock solution of all samples – silk films with mefloquine and control which was silk films without mefloquine; well plate #2 – 100uL of 1/10 dilution of previous samples and controls used in plate #1; well plate #3 – 1/100 dilution of previous samples used in well plate #2; well plate #4 – serial dilutions (13) of mefloquine stock solution of 500 ug/mL). Samples were placed back in the incubator for a period of 2 days. On days 4&5, all samples were examined microscopically (10X) to evaluate cell morphology, presence, or absence of cell detachment and cell lysis using. Quantitative evaluation consisted of visually assessing changes in the general morphology, vacuolization, detachment, cell lysis, and membrane integrity of the cells with the use of a phase contrast light microscope (Zeiss, Jena, Germany). This was based on a number scale of 0 = no reactivity to 4 = severe reactivity. Qualitative evaluation consisted of measuring

cell death, inhibition of cell growth, cell proliferation or colony formation.

Alamar blue staining was used to quantitatively assess cell cytotoxicity. In order to determine cell attachment, 50  $\mu$ L was added to each sample and incubated for 3 hours after cell seeding of the experimental groups. The samples were then analyzed spectrophotometrically by using fluorescence (excitation = 560 nm, emission = 590nm) on a SpectraMax M2 spectrophotometer (Molecular Devices, Sunnyvale, CA, USA).

## **2.9 Statistical Analysis**

All experiments were performed with a minimum of  $N = 3$  for each set of data. Statistical analysis was performed using SPSS for Windows version 23 (IBM SPSS, Chicago, IL). Independent samples Kruskal-Wallis non-parametric test and Independent samples Mann – Whitney U test were used to determine significant differences among data obtained. Statistical differences were considered significant when  $p \leq 0.05$  and very significant when  $p \leq 0.01$ .

# CHAPTER 3: Results

## 3.1. Morphology

### 3.1.1. Silk Films Preparation, Appearance, and Weight

The fabrication of DSF was in accordance with protocols described in sections 2.2.1. and 2.2.2 that were derived from published work evaluating the rate of release of chemotherapeutics from water insoluble films (Coburn et al, 2015; Seib and Kaplan, 2012; Seib et al., 2015). Assessing the quality of the films, the appearance of the samples (1% - 6%) collected from the PDMS molds were transparent and clear for all concentrations of the films. The same composition was observed for films that were incorporated with either mefloquine hydrochloride or the blue food coloring (**Figures 30 & 31**). Each silk film's mass was measured, and statistical analysis was used to determine if there were any significant differences between dissolvable films doped with or without mefloquine. The only statistical difference observed was between the silk films' concentration and their mass ( $p \leq 0.01$ ). As the concentration of silk increased the weight of the films increased as well (**Figure 32**). There was no statistical difference observed when comparing the mass of the samples with or without mefloquine hydrochloride. A possible explanation for this is that the small amount of drug loaded onto the films was negligible and the amount added was consistent for each concentration of silk (w/v).

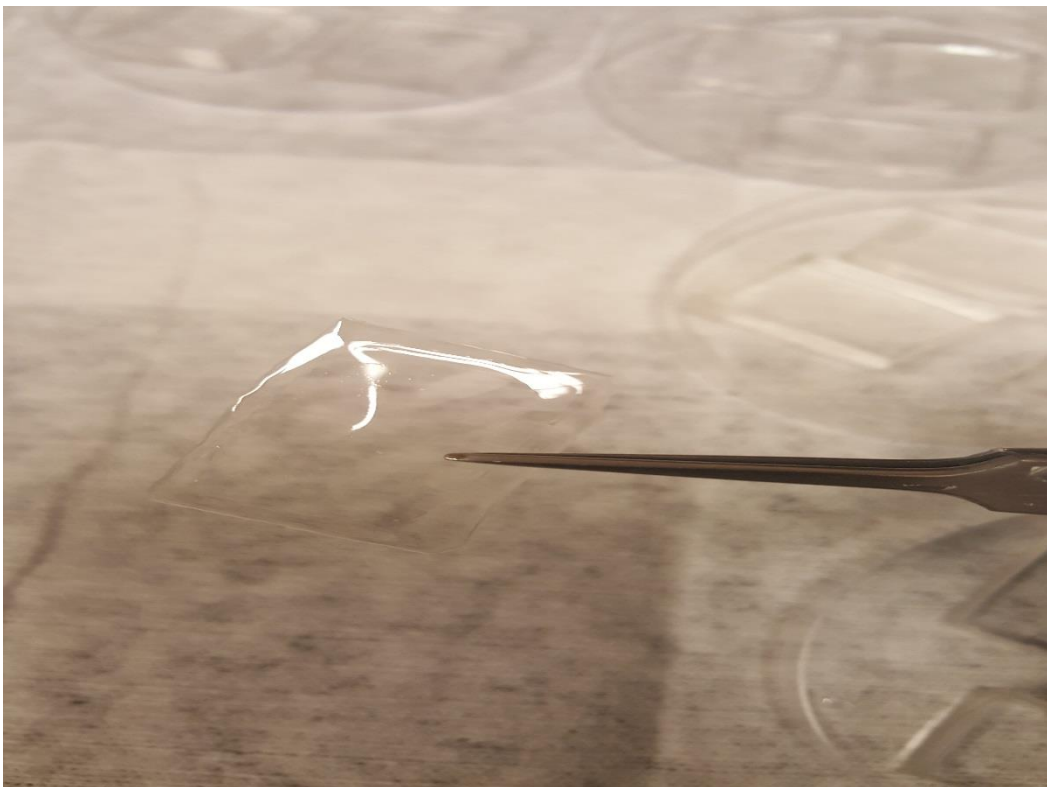


Figure 30: Photo showing dried silk film sample (6% w/v) doped with mefloquine hydrochloride (dimensions: 33mm x 23mm).

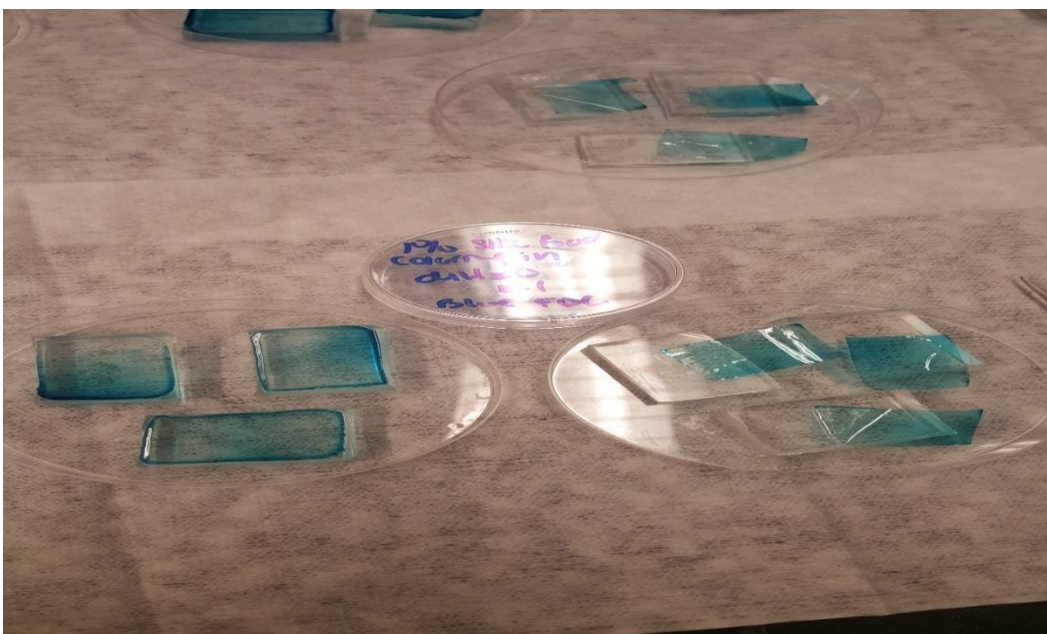


Figure 31: Fabrication of 1% Silk Films Doped with Blue Food Dye (Dimensions of the films 33mm x 23mm; Dimensions of PDMS Molds = 33m x 23mm).



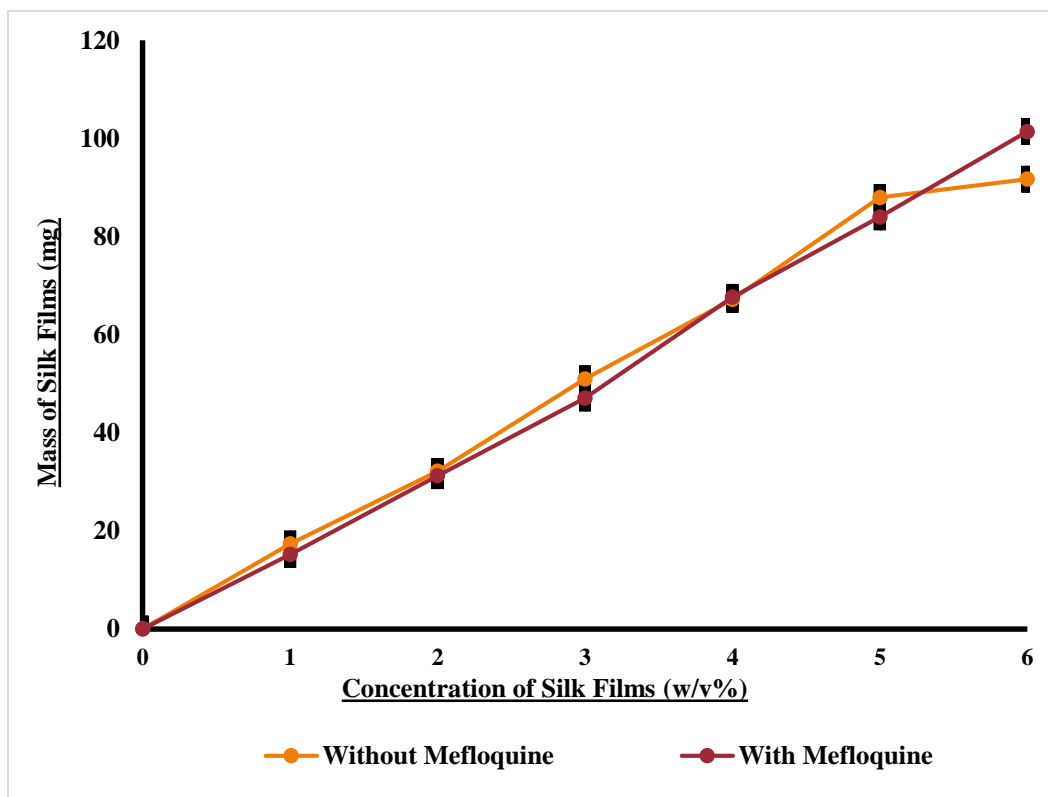


Figure 32: Graph displaying the relationship of silk concentration versus average mass of DSF. Error bars represent standard deviation of the samples (N=4);  $p(0.000005) \leq (.05)$ .

### 3.1.2. Scanning Electron Microscopy (SEM) of Dissolvable Silk Films

SEM is a vital tool to help visualize the surfaces and cross-sections of the dissolvable films and determine if any crystallinity or porosity are present within the samples. The images obtained for dissolvable silk film samples were used to determine the morphology of DSF “as – casted” or samples incorporating mefloquine. **Figures 33 – 35** display the cross-section of the samples while **Figure 36** displays the surface of a sample without mefloquine. Comparing dissolvable films with or without mefloquine demonstrated no distinct differences between the two types of samples regardless of silk concentration.

Based on the imaging there were no glaring morphological differences between the two types of films. Both types of films exhibited smooth morphologies for the cross-sectional area and surface of the samples. These results resemble morphologies reported for as-casted films that went through a slow drying process (Lu et al., 2011). What can be concluded is that, visually, DSF resemble an amorphous structure and lack of porosity since they lack crystallinity. This is further analyzed in the next section with FTIR analysis.

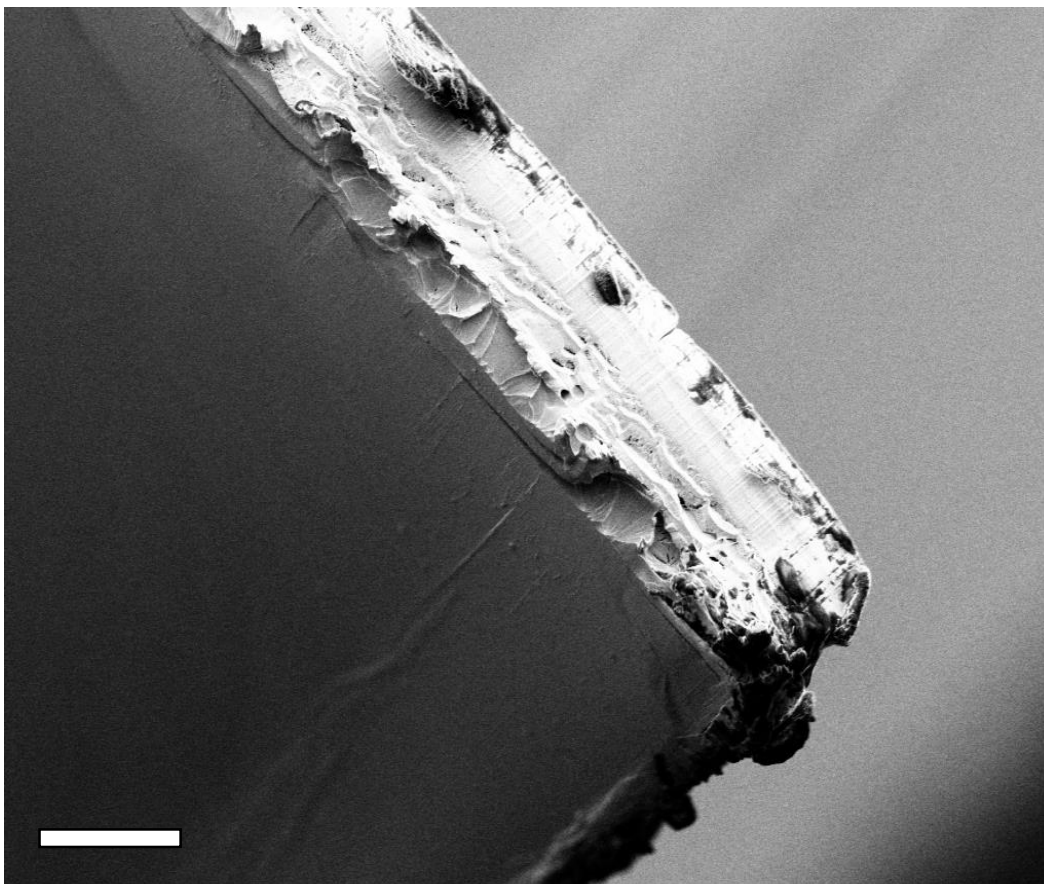


Figure 33: : SEM Image of Cross-section of 4% Silk Films without Mefloquine (scale = 20  $\mu\text{m}$ ).

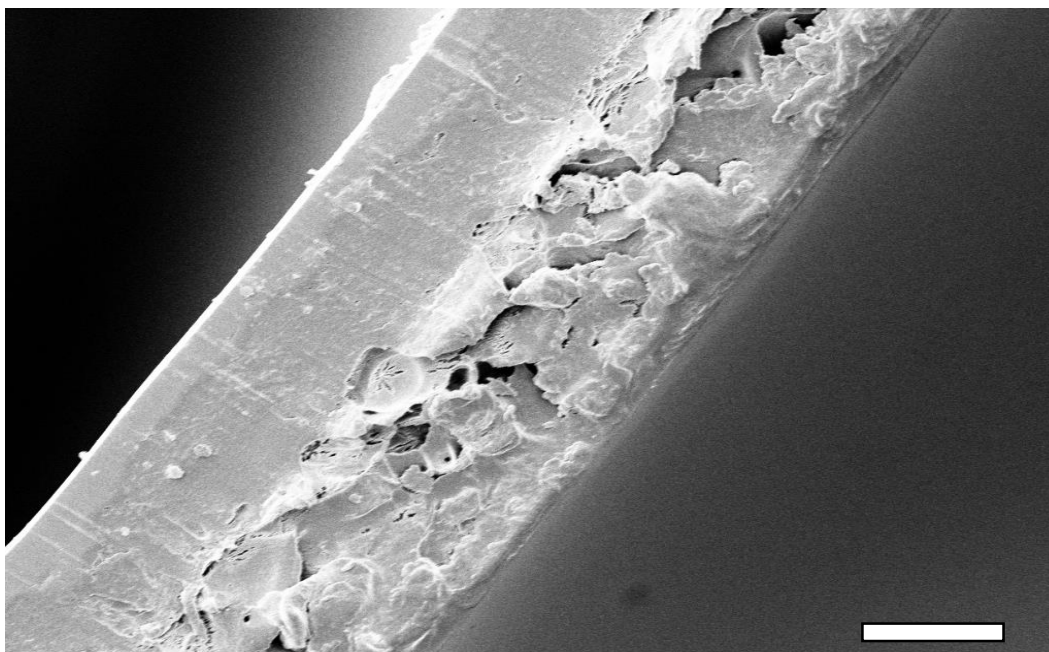


Figure 34: SEM Image of Cross-section of 5% Silk Films Doped with Mefloquine (scale = 20  $\mu\text{m}$ ).

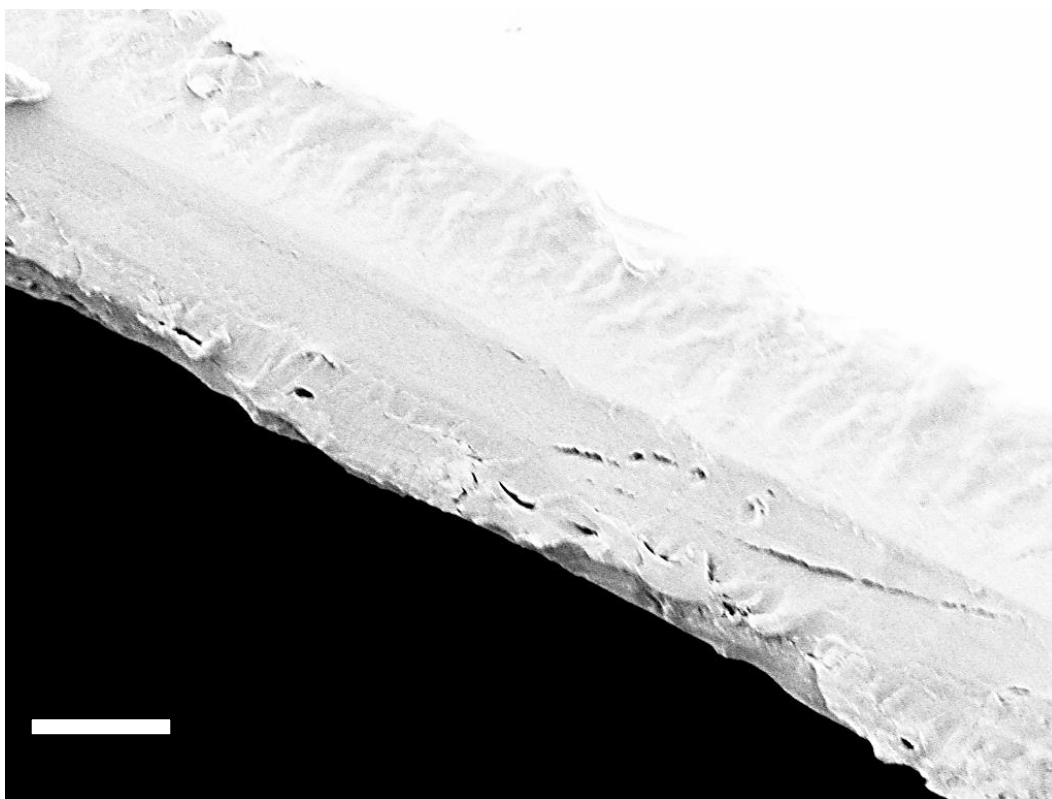


Figure 35: SEM Image of Cross-section of 2% Silk Films Doped with Mefloquine (scale = 20  $\mu\text{m}$ ).

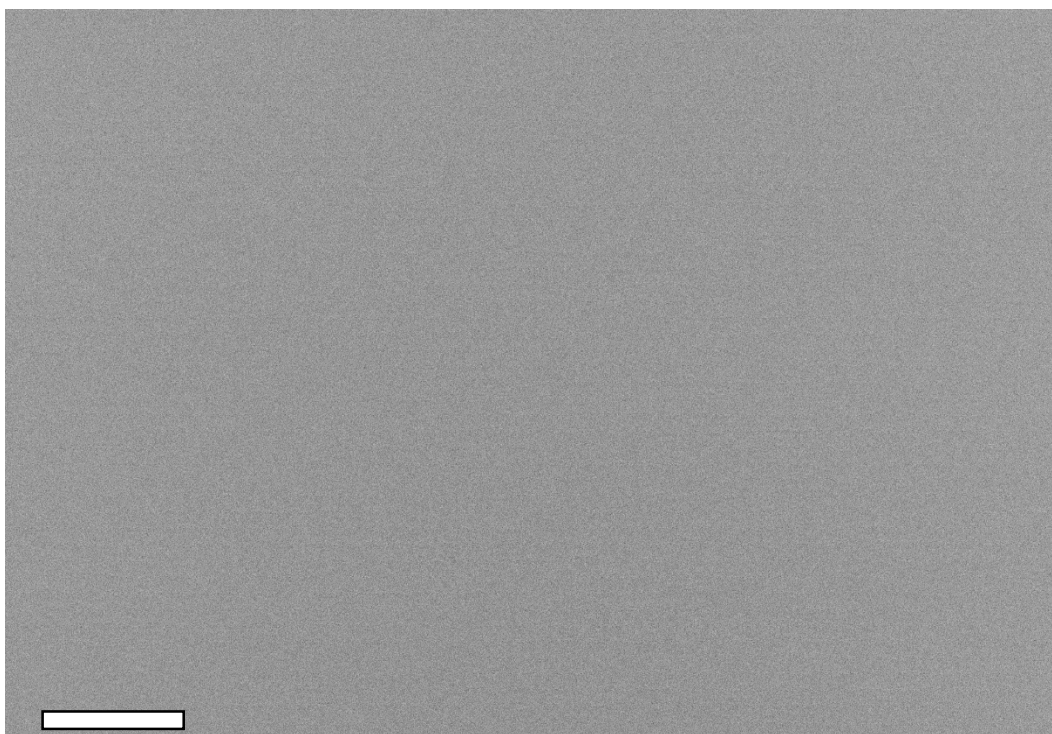


Figure 36: SEM image of the surface of 2% “as-casted” dissolvable silk film (scale = 20  $\mu\text{m}$ ).

### 3.1.3. Fourier Transform Infrared Analysis (FTIR)

FTIR analysis was used to determine the chemical structure of the DSF with or without the incorporation of mefloquine. Characterization of the secondary structure occurred with the use of spectral deconvolution and secondary derivative analysis occurred within the amide I region (1595 – 1705  $\text{cm}^{-1}$ ) of the “as-casted films” with or without mefloquine hydrochloride. Further confirmation of the amorphous structure of the films were the 12 peaks that were detected within the following ranges (side chains: 1,605 – 1,615  $\text{cm}^{-1}$ ;  $\beta$ -sheets: 1,619 – 1,628  $\text{cm}^{-1}$  & 1,697 1,703  $\text{cm}^{-1}$ ; random coil: 1,638 – 1,655  $\text{cm}^{-1}$ ;  $\alpha$ -helix: 1,656 – 1,662  $\text{cm}^{-1}$ ; and  $\beta$ -turns) (Lawrence et al., 2008). **Figures 37 & 38** presents the structural composition of the films. Since the processing of the films did not include procedures that induced crystallinity (e.g. water-annealing, heat, or methanol treatment) both types of films consisted of a much higher random coil composition and minimal  $\beta$ -sheet structure (~40% random coil vs ~18%  $\beta$ -sheet). This corroborates the films ability to readily dissolve within contact of media. When examining the structural differences between the two types of films (with or without mefloquine), significant differences were only observed were composition of  $\beta$ -sheet [ $p(0.037) < (0.05)$ ] and  $\alpha$ -helix [ $p(0.037) < (0.05)$ ]. In the analysis of differences between the different concentrations of silk films (with or without mefloquine), only significant difference observed was for the composition of  $\beta$ -turns [ $p(0.017) < 0.05$ ]. These observations demonstrate that the composition of dissolvable films fabricated are of silk I structure.

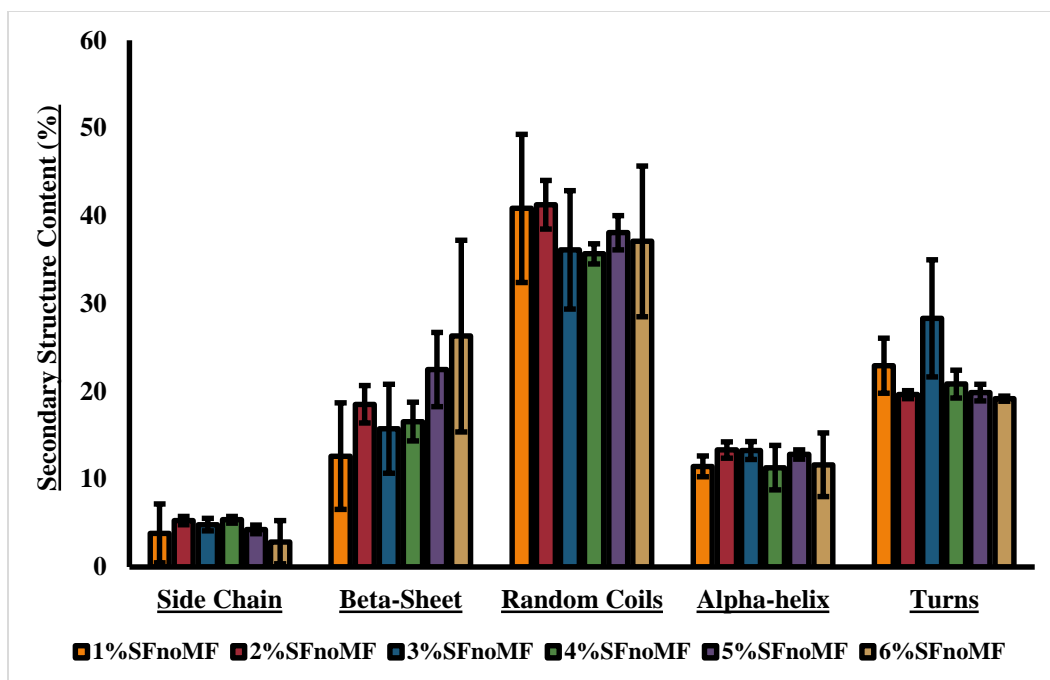


Figure 37: FTIR spectrum of dissolvable silk films (1-6%) without mefloquine hydrochloride.

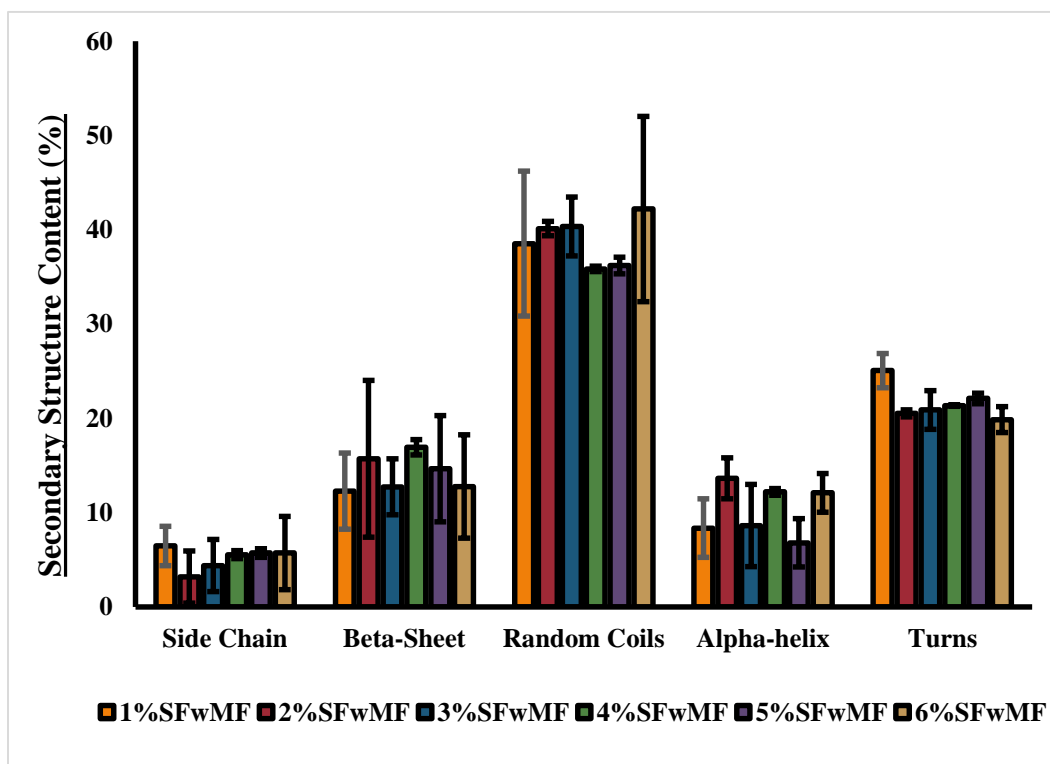


Figure 38: FTIR spectrum of dissolvable silk films (1-6%) with mefloquine hydrochloride.

### 3.2. Disintegration Testing of Silk Films Doped with Blue Food Dye

Silk films were fabricated according to the protocol described in section 2.1.2 and were implemented according to the protocol described in section 2.1.5. The purpose of disintegration testing is to help evaluate the composition (e.g. thickness, mass, porosity, etc.) of the dissolvable polymer and determine how long the hydrophilic polymers disintegrate *in vitro*. It is beneficial to estimate the rate of disintegration of the polymer in the oral mucosa. Criteria of oral disintegration films have not been firmly established/ or regulated. The measures are based on FDA guidelines used to govern oral disintegrating tablets. Using this standard, time requirements for fast-dissolving oral films can vary between 30 seconds to 180 seconds (Preis et al., 2013).

In this study, the films were doped with blue food coloring to provide a visual affect while the films were recorded. Elapsed time was measured from the moment the samples made contact with the selected media. **Figures 39 & 40** show composition of the films during disintegration testing. **Table 11** lists disintegration times for silk films (1% - 6%) in distilled water and phosphate buffer saline while **Figures 41 & 42** illustrate the rate of disintegration of the films in both media. As expected, 1% silk films would fit the criteria of fast dissolving films along with 2% and 3% silk films. Films with silk concentrations of 4% - 6% would be considered for slow release/multilayer films since they failed to dissolve in less than 1 - 1.5 minutes. Upon contact with media, 1% - 3% silk films begin dissolving almost immediately. However, for films with silk concentrations of 4% - 6%, disintegration did not occur until at least 30 – 40

seconds after initial contact with the media. The variation of silk concentration was observed to have a significant effect only on disintegration times. There was no statistical difference in the rate of disintegration between the samples with respect to media used (PBS/diH<sub>2</sub>O).



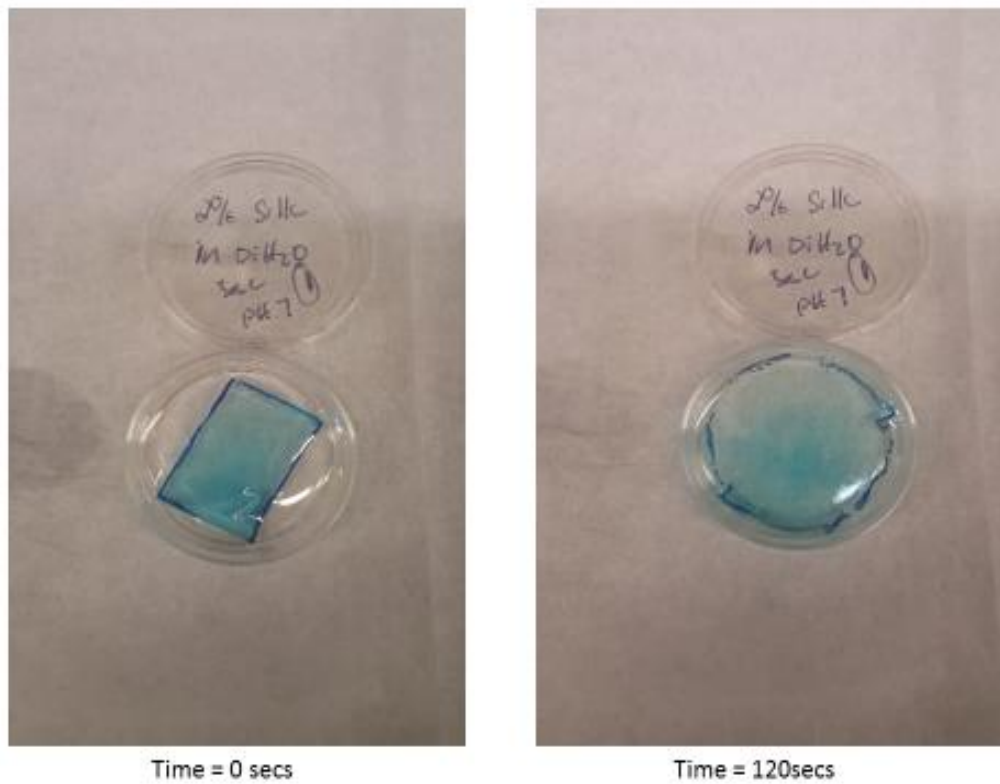


Figure 39: Disintegration Testing of 2% Silk Films Dissolving in Distilled Water (pH = 7).

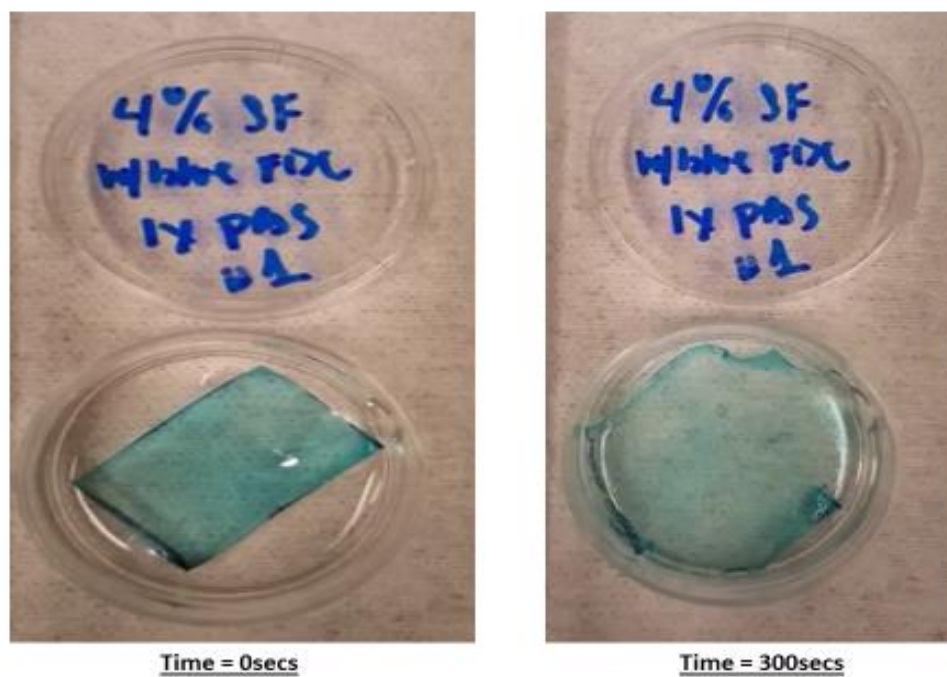


Figure 40: Disintegration Testing of 4% Silk Films Dissolving in PBS (pH=7).

Table 11: Comparison of the disintegration times amongst the different concentration of silk films in media (PBS/DiH<sub>2</sub>O). (N = 3); p ≤ (0.01).

<u>Silk Films (w/v)%</u>	<u>Time (Mins) = PBS</u>	<u>Time (Mins) = DiH<sub>2</sub>O</u>
<b>1% Silk Films</b>	0.14 ± 0.0436	0.0933 ± 0.0115
<b>2% Silk Films</b>	0.49 ± 0.0529	0.03033 ± 0.0476
<b>3% Silk Films</b>	1.267 ± 0.0577	1.4533 ± 0.551
<b>4% Silk Films</b>	2.46 ± 0.1015	3.0033 ± 1.469
<b>5% Silk Films</b>	3.267 ± 0.1779	5.0300 ± 2.9072
<b>6% Silk Films</b>	7.647 ± 0.60807	6.1100 ± 0.0511

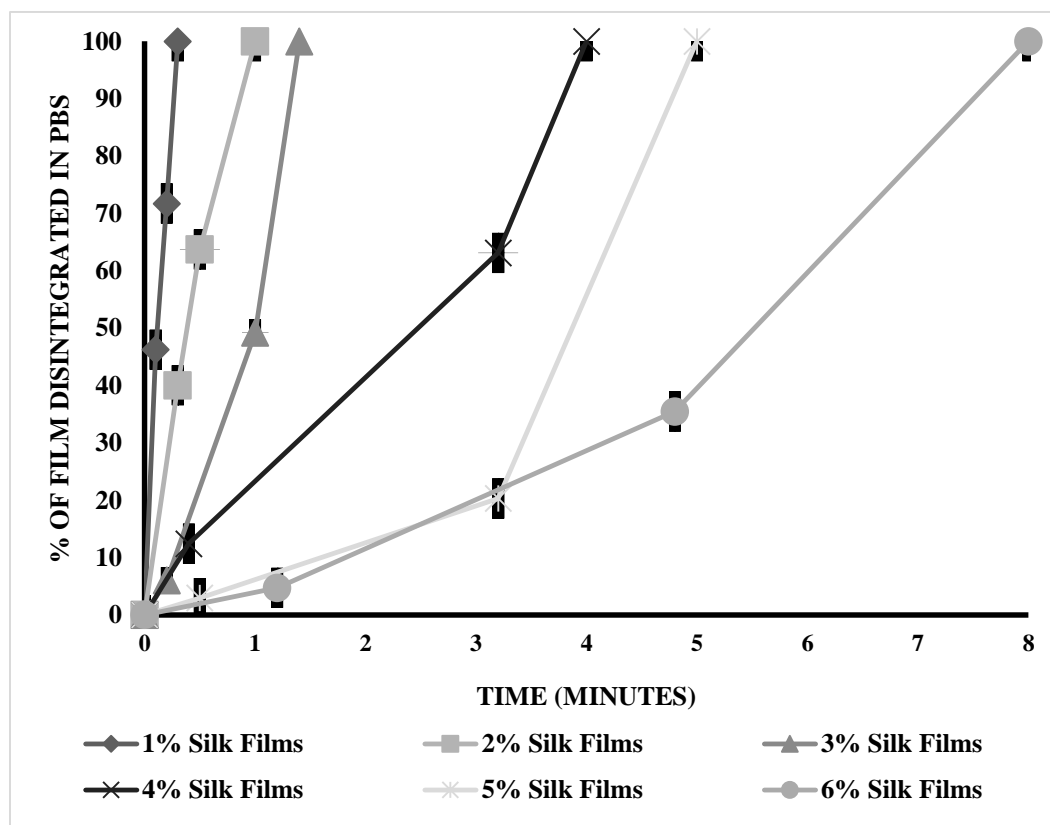


Figure 41: Graph displays the relationship of silk concentration versus percentage of film disintegration in PBS (pH = 7). Error bars represent standard deviation of samples (N=3); p ≤ (0.01).

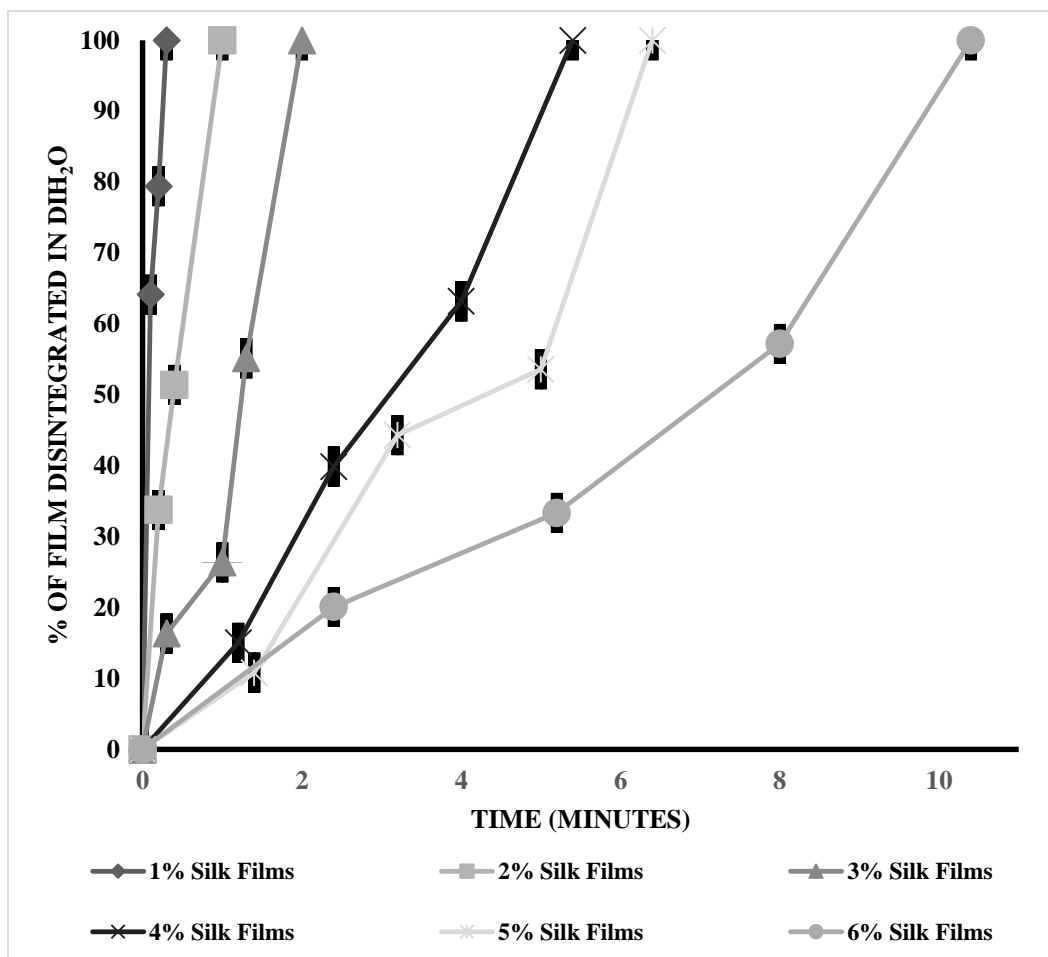


Figure 42: Graph displays the relationship of silk concentration versus percentage of film disintegration in  $\text{DiH}_2\text{O}$  (pH=7). Error bars represent standard deviation of the samples ( $N = 3$ );  $p \leq (0.01)$ .

### 3.3. Drug Loading of Mefloquine Hydrochloride with Dissolvable Silk Films

Section 2.2.2 details how mefloquine hydrochloride was loaded into samples (N=3) as well as the process of measuring drug loading mefloquine (1mg/mL) into the films. **Figures 43 & 44** display the total mass and percentage load of the antimalarial chemotherapeutic incorporated into the dissolvable films. The average drug loading efficiency of mefloquine hydrochloride, across all concentrations, was  $760.76\mu\text{g} \pm 296.451$ . Differences in drug loading efficiency were observed between different silk concentrations but they were not statistically significant. The highest drug load measured in DSF was detected in 4% silk films ( $871.794\mu\text{g} \pm 33.70$ ). A separate study examining protein-mefloquine binding with water insoluble silk films (4% SF w/ MF =  $50\mu\text{g/mL}$ ; data not shown) was conducted and confirms the drug loading efficiency of silk films (~85%). This also determined that concentration of silk films does not have a significant impact on protein – small molecule interaction of the films.

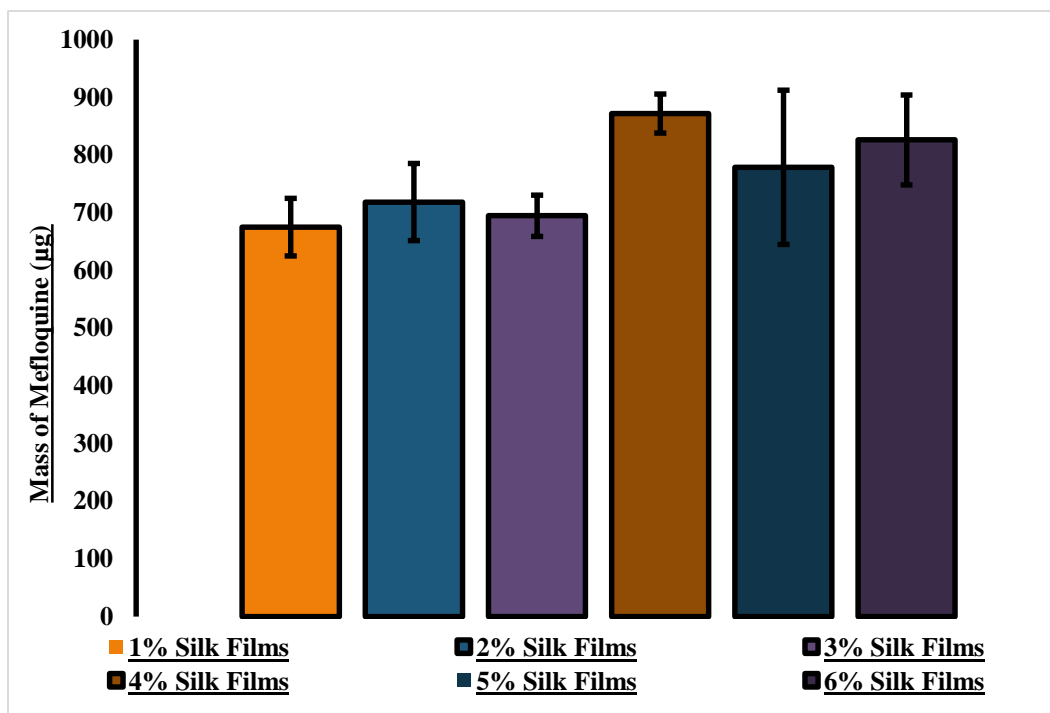


Figure 43: Total mass of mefloquine hydrochloride loaded into dissolvable silk films (1-6%). Error bars represent standard deviation of the samples ( $N = 3$ );  $p(0.124) > (0.05)$ .

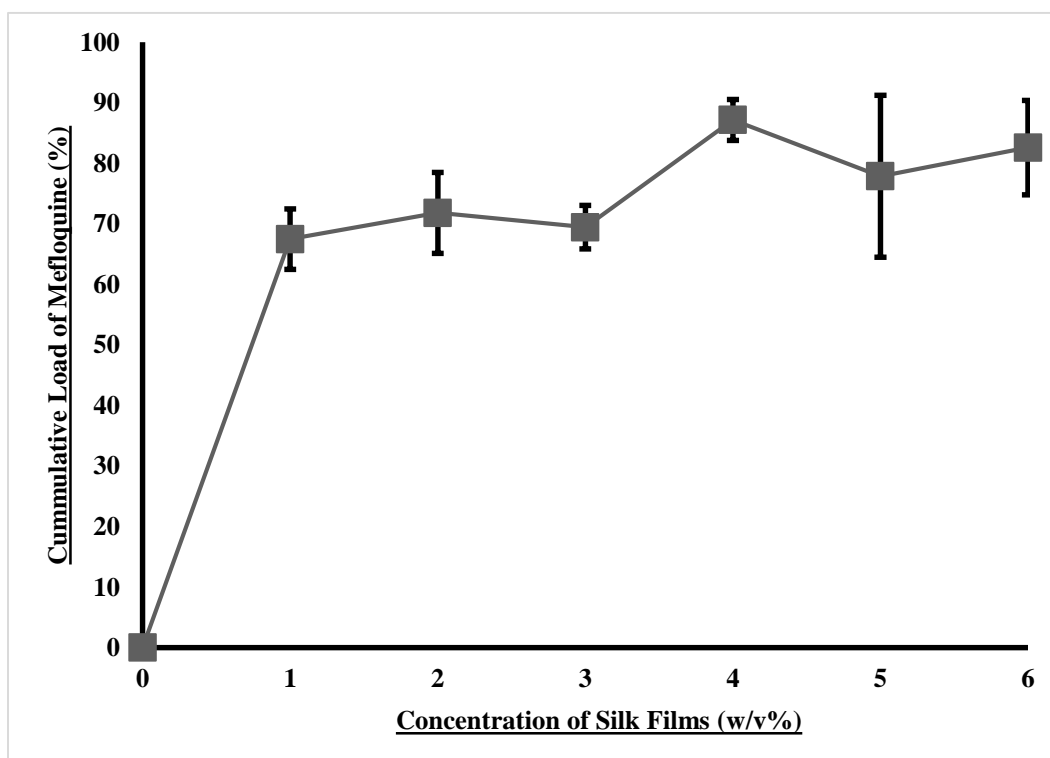


Figure 44: Percentage of mefloquine hydrochloride loaded into dissolvable silk films (1-6%). Error bars represent standard deviation of the samples ( $N = 3$ );  $p(0.124) \geq (0.05)$ .

### **3.4. *In vitro* Dissolution Testing of Dissolvable Silk Films with Mefloquine Hydrochloride**

*In vitro* drug release of the antimalarial drug mefloquine from DSF was evaluated to help determine the diffusion of the antimalarial compound from the films (**Figure 45 & 46**). The total time used to evaluate the rate of release of the small molecule was 30 minutes. The conditions that the samples were exposed to emulated physiological temperature and pH (37°C; phosphate buffered saline - pH = 7). Release profiles for the samples were significantly different especially between 1-3% films and 4-6% films. The highest cumulative rate of release was observed in DSF of 1% (>90%). The lowest cumulative rate of release of mefloquine was observed in DSF of 6% (<35%). This coincides with results detected from disintegration testing of dissolvable films in section 3.2. It should also be noted that each film sample experienced some form of gelation/aggregation in media. This is most likely due to the increased heat and salt content, which may have caused an increase in crystallinity in secondary structure, thereby inducing  $\beta$ -sheet content. Also, as the concentration of silk increased the cumulative release of mefloquine hydrochloride decreased. This decrease was highly significant ( $p < 0.01$ ) for films with silk concentration > 3%. This is corroborated by the increase in the formation of aggregates in media as concentration of silk increased.

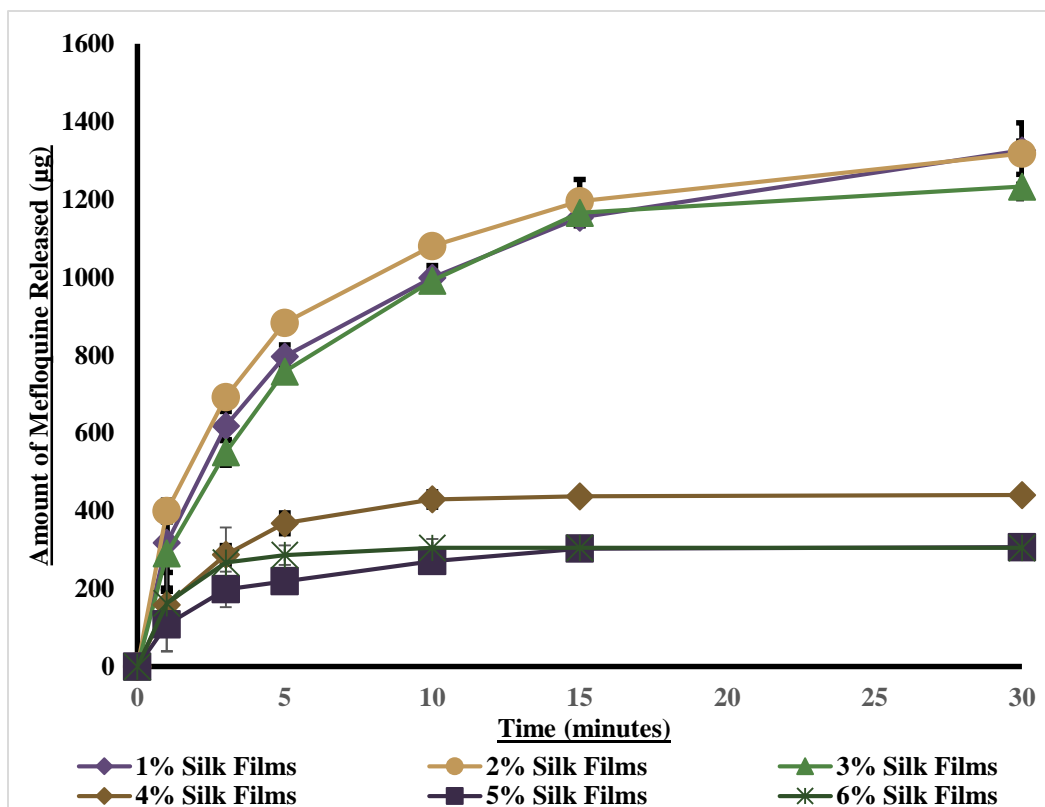


Figure 45: Rate of cumulative mass release of mefloquine from dissolvable silk films. Error bars represent standard deviation of the samples;  $p \leq 0.01$ .

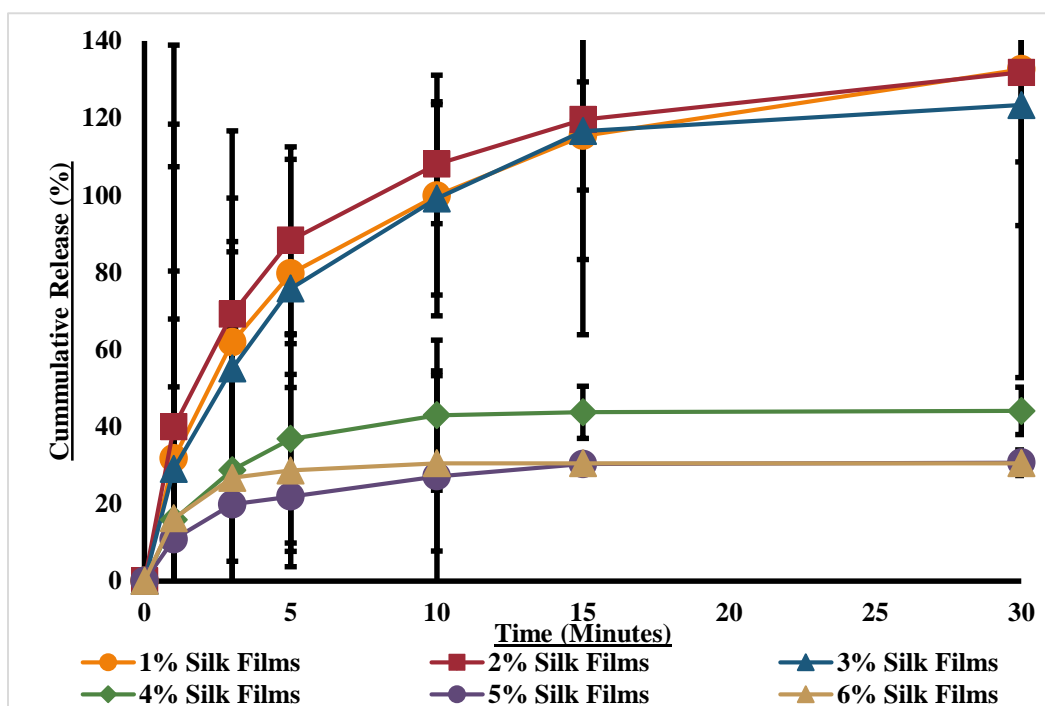


Figure 46: Cumulative rate release (%) of mefloquine from dissolvable silk films. Error bars represent standard deviation of the samples;  $p \leq 0.01$ .

### 3.5. Mechanical Testing of Dissolvable Silk Films

Mechanical properties for silk films were tested on an Instron Universal Testing Instrument (model 3366) as mentioned in section 2.3.1. Tensile testing is one of two forms of mechanical testing that have been suggested in literature as a tool in assessing and characterizing the mechanical properties of OFTs (Preis et al., 2015). Tensile testing helps to determine the robustness of films based on the parameters of ultimate tensile strength (UTS), elastic modulus (stiffness), and strain to failure %. **Figure 47** outlines general characteristics of films based on mechanical properties described earlier. **Figures 48 - 50** display the different mechanical properties measured during tensile testing of the dissolvable films (1 – 6%).

Statistically significant differences were observed among films for all measured mechanical properties (stiffness, UTS, and strain to failure) for all samples examined. There was a significant increase in strain to failure % of the samples as the concentration of silk in the films increased. The highest strain to failure % was observed in 6% silk films. An inverse relationship was detected for UTS and stiffness. 1% silk films exhibited the highest stiffness (378.6 MPa) and ultimate strength (2.8 MPa) while 5% silk films demonstrated the lowest measurement for stiffness (101.8 MPa) and ultimate strength (0.7 MPa). Based on all of the parameters measured in this study and the characteristics listed in **Figure 47**, 1 – 2% silk films can be considered as “hard and brittle polymeric films,” while 3 – 6% silk films can be characterized as “soft & tough polymeric films,” with 3-5% silk films being more suitable based on their features.



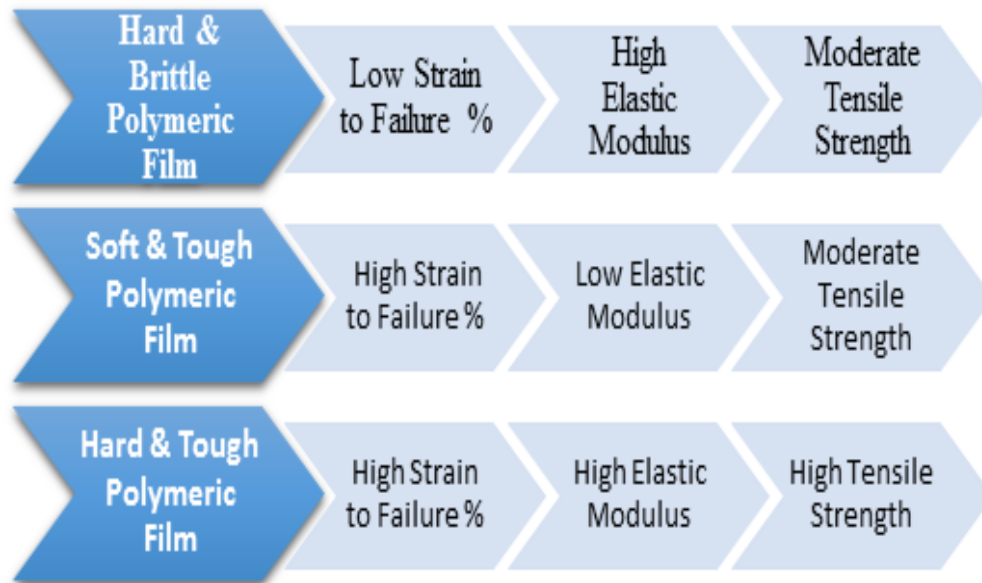


Figure 47: Flow chart of different characterizations of films based on mechanical properties (Kundu et al., 2008).

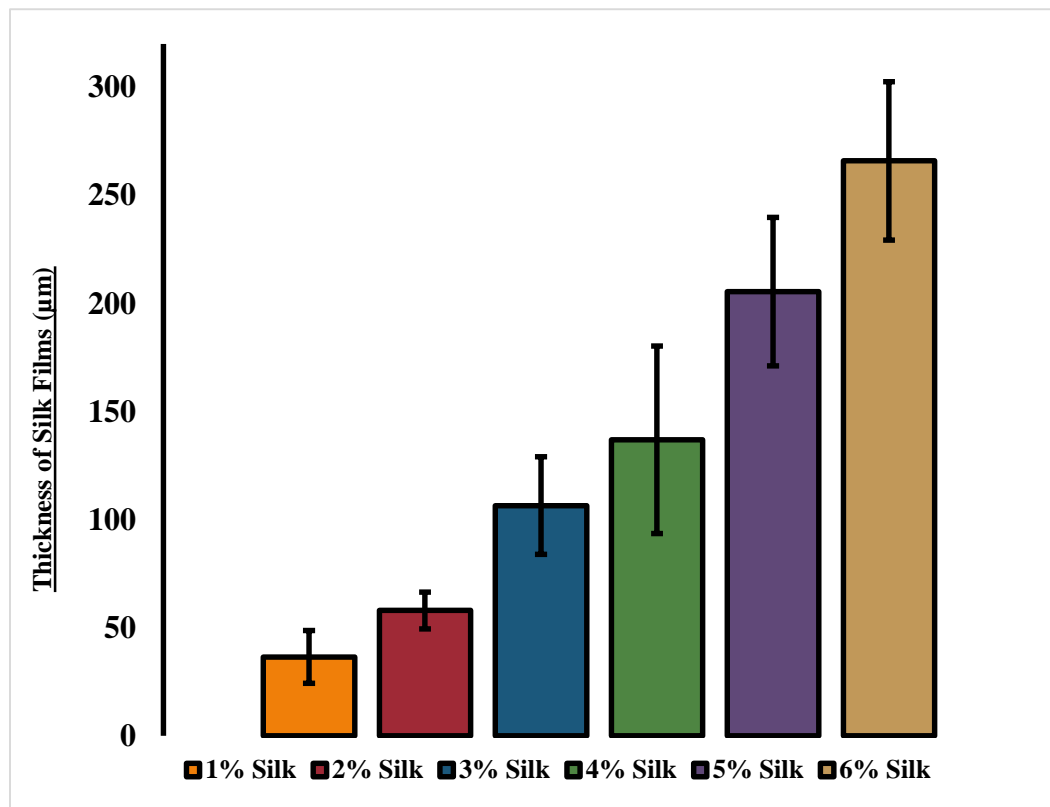


Figure 48: Comparison of concentration of silk films versus thickness. Error bars represent standard deviation of the samples (N = 4)  $p(0.002) \leq 0.01$ .

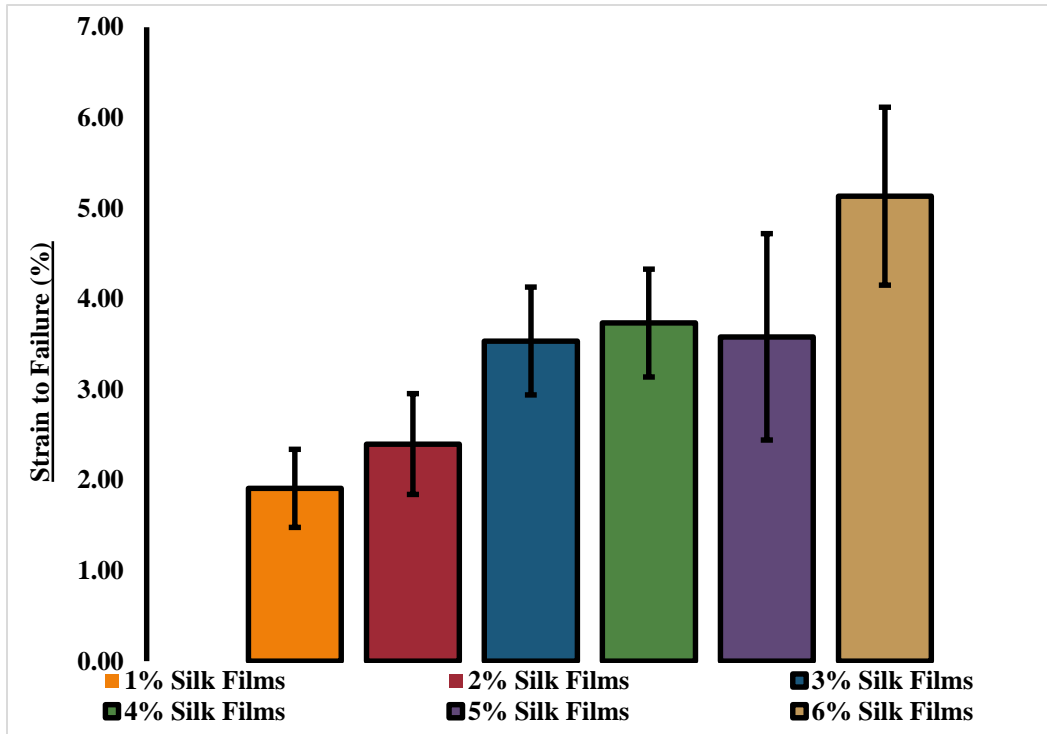


Figure 49: Relationship of silk concentration versus strain to failure of silk films. Error bars represent standard deviation of samples (N=4);  $p(0.01) \leq (0.01)$ .

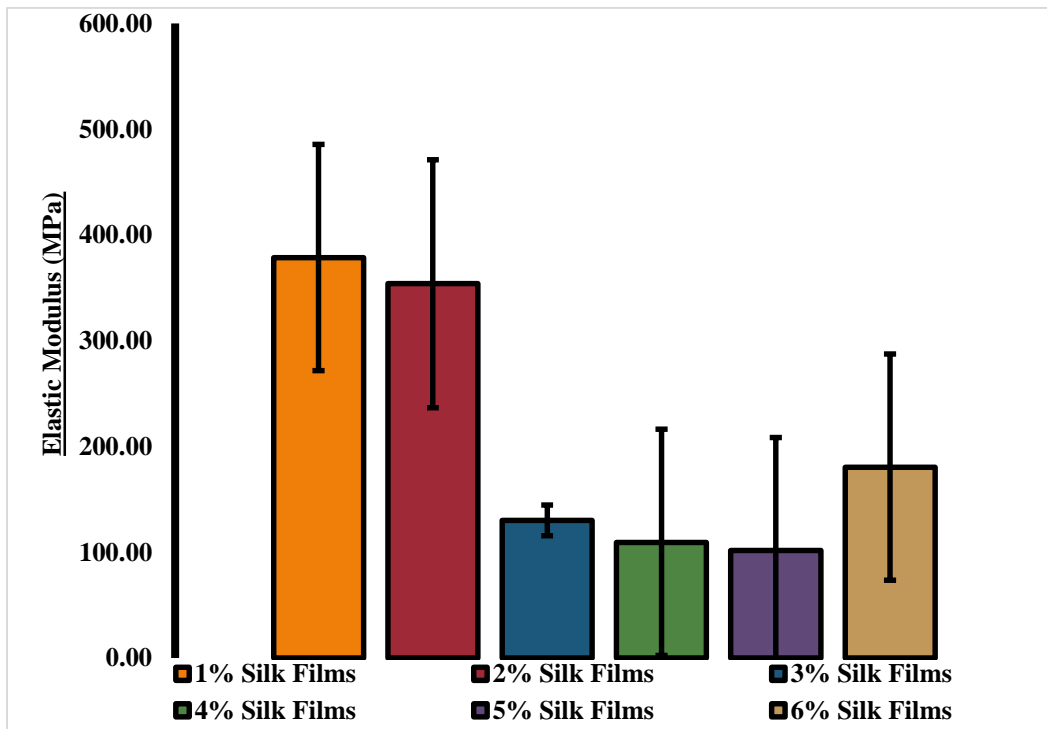


Figure 50: Relationship of silk concentration versus elastic modulus (MPa) of silk films. Error bars represent standard deviation of samples (N=4);  $p(0.008) \leq (0.01)$ .

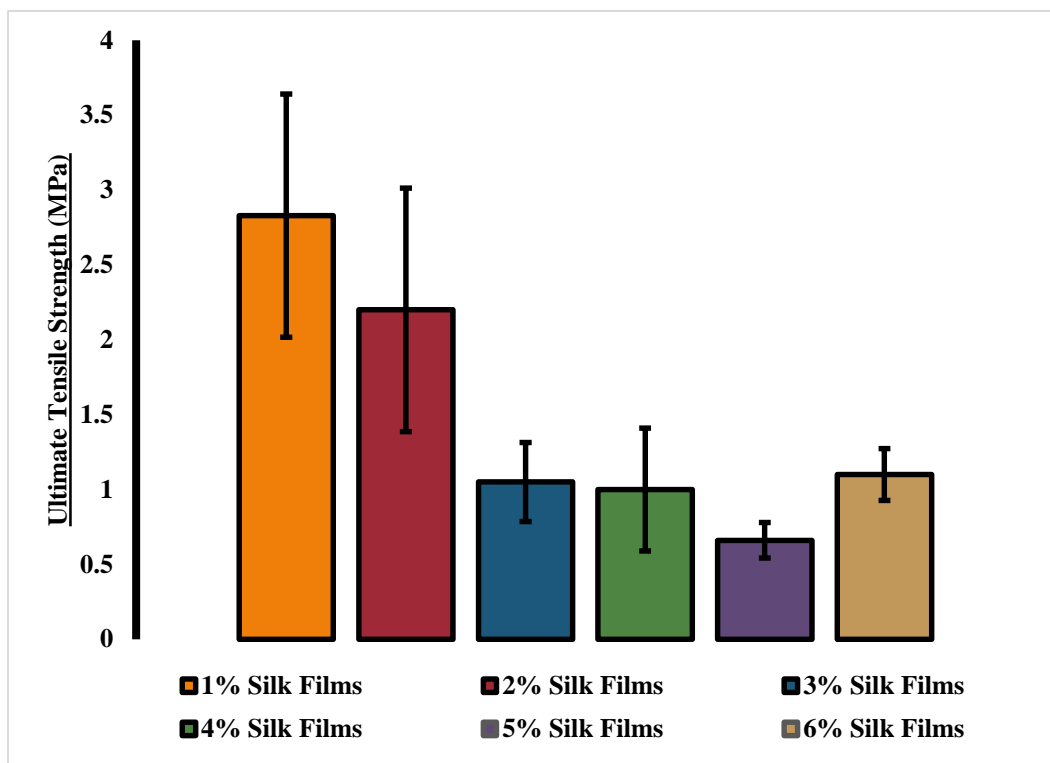


Figure 51: Relationship of silk concentration versus UTS (MPa) of silk films. Error bars represent standard deviation of samples (N=4);  $p(0.006) \leq (0.01)$ .

### 3.6. *In vitro* Cytotoxicity Testing of Silk Films

To investigate the safety of DSF incorporating mefloquine hydrochloride for oral mucosal delivery, cytotoxicity testing was conducted both quantitatively (**Figures 42 – 46**) and qualitatively (**Figures 47 – 49**). For this study, testing was modified from the ISO 10993-5 biological evaluation of medical devices – Part 5: Tests for *in vitro* cytotoxicity. The ISO 10993-5 is the industry standard in evaluating the exposure and biological response of mammalian cells to biomaterials *in vitro*. Evaluation can be applied to assess cell damage, measure cell growth, or cellular metabolism. For this study, cell growth and metabolism was investigated using the mouse fibroblast L292 cell line. Three different test groups were investigated: a) dilution of stock solution of mefloquine hydrochloride (500µg/mL), b) dilution of DSF loaded with mefloquine hydrochloride, and c) dilution of DSF. The mammalian cells were exposed to the extracts for a period of 24 hours at 37°C.

The first test group investigated, L292 cells exposure to stock solution of mefloquine demonstrated cytotoxic effects of the antimalarial chemotherapeutic for concentrations ranging from 62.5µg/mL to 500µg/mL (**Figures 52 & 53**). Investigation of the second test group, DSF loaded with mefloquine hydrochloride, exhibited cytotoxicity at low concentration of silk (1% & 2%) (**Figures 54 & 55**). The final group investigated, DSF without mefloquine, also exhibited cytotoxicity for silk films with concentration of 2% - 6% (**Figures 56 & 57**). These findings do support what was observed from dissolution and disintegration testing of DSFs. DSFs with concentration of silk from 1-3% has a

faster rate of disintegration and would readily release the concentration of mefloquine to mammalian cells. There were a number of issues associated with cytotoxicity study that has impacted the results observed in this study and will be further discussed in section 4.1.4.

### Measuring Cytotoxicity of Mefloquine on L292 Fibroblast Cells

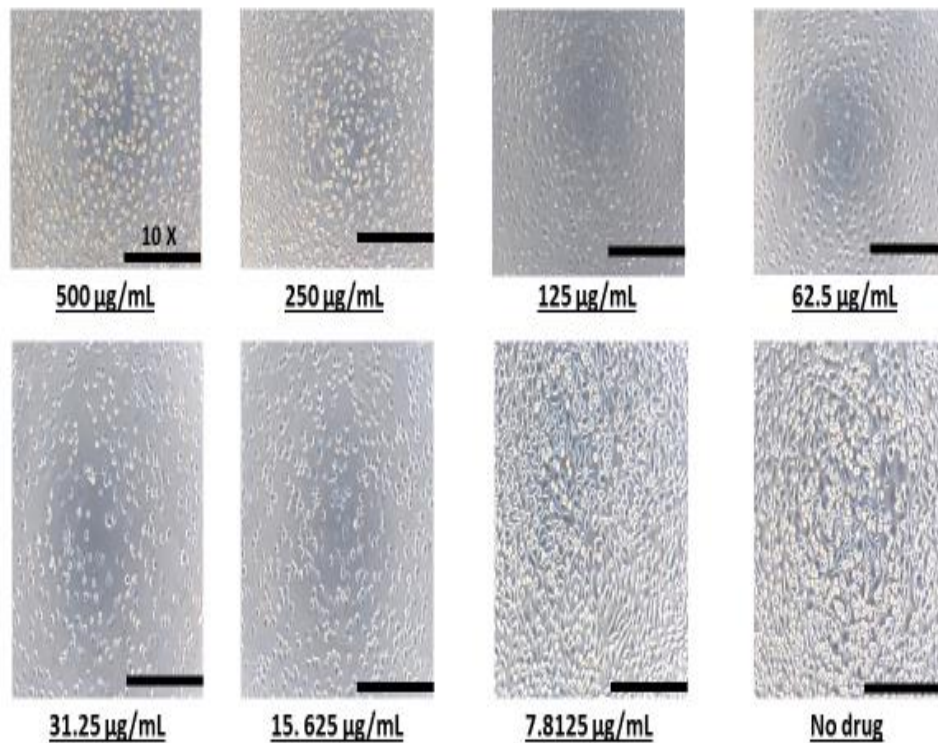


Figure 52: Microscopic images of attachment and proliferation of fibroblasts after exposure to serial dilutions of stock solution of mefloquine hydrochloride (500µg/mL). (Scale bar = 10X magnification).

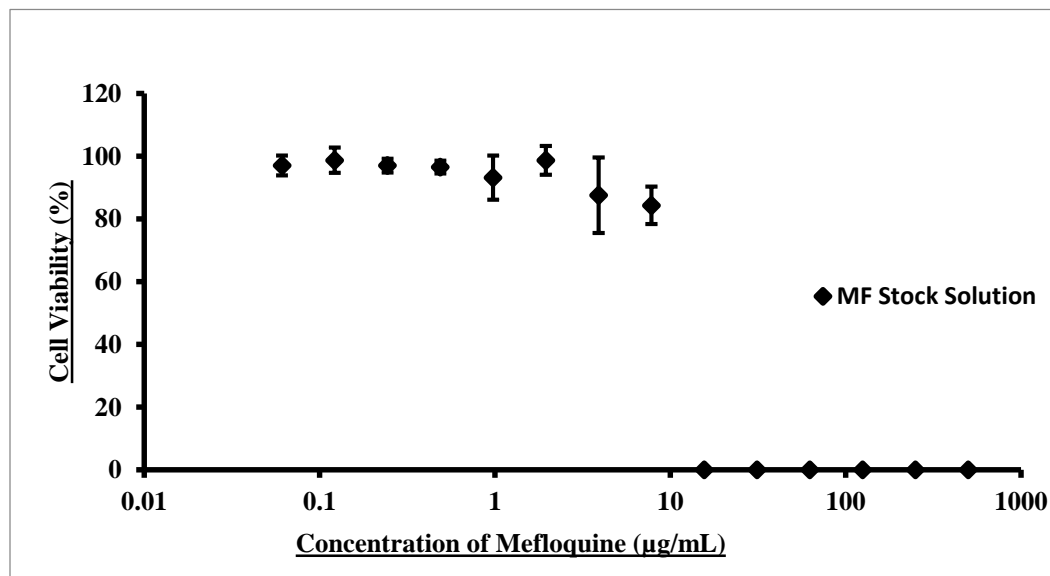


Figure 53: Quantitative assessment of the cell viability from exposure to serial dilutions of mefloquine hydrochloride on fibroblasts (Error bars represent standard deviation of the samples; N=3).

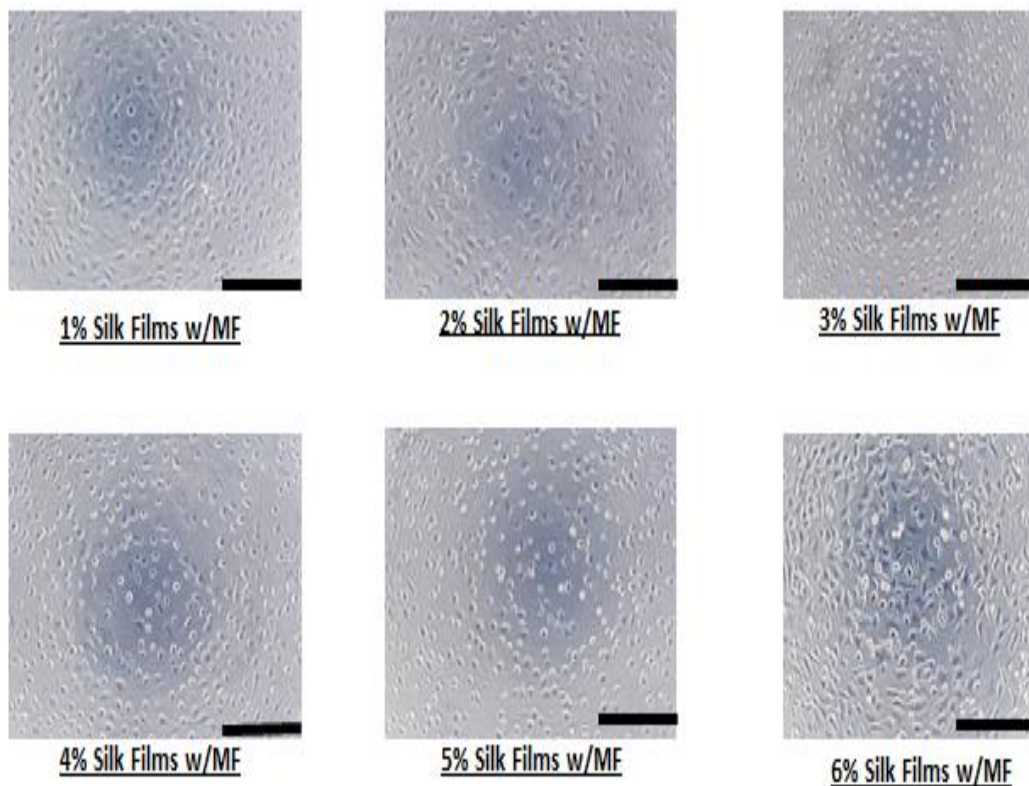


Figure 54: Microscopic images of attachment and proliferation of fibroblasts after exposure to dissolvable silk films (1 – 6%) doped with mefloquine hydrochloride in fibroblasts. (Scale bar = 10X Magnification).

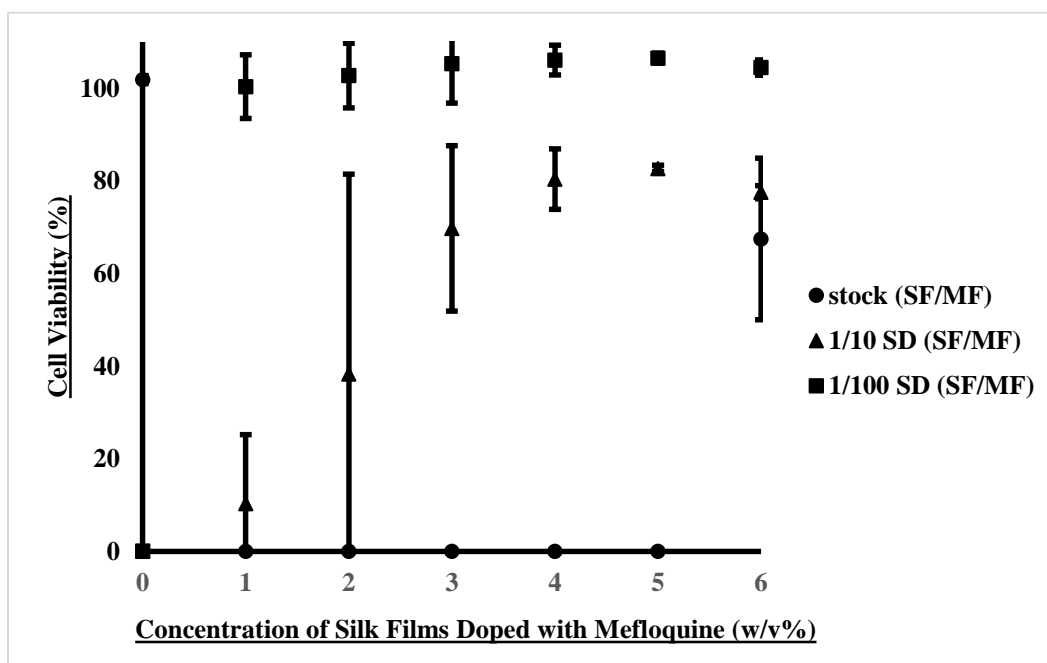


Figure 55: Quantitative assessment of the cell viability from exposure to dissolvable silk films doped with mefloquine hydrochloride on fibroblasts (Error bars represent standard deviation of the samples; N=3).

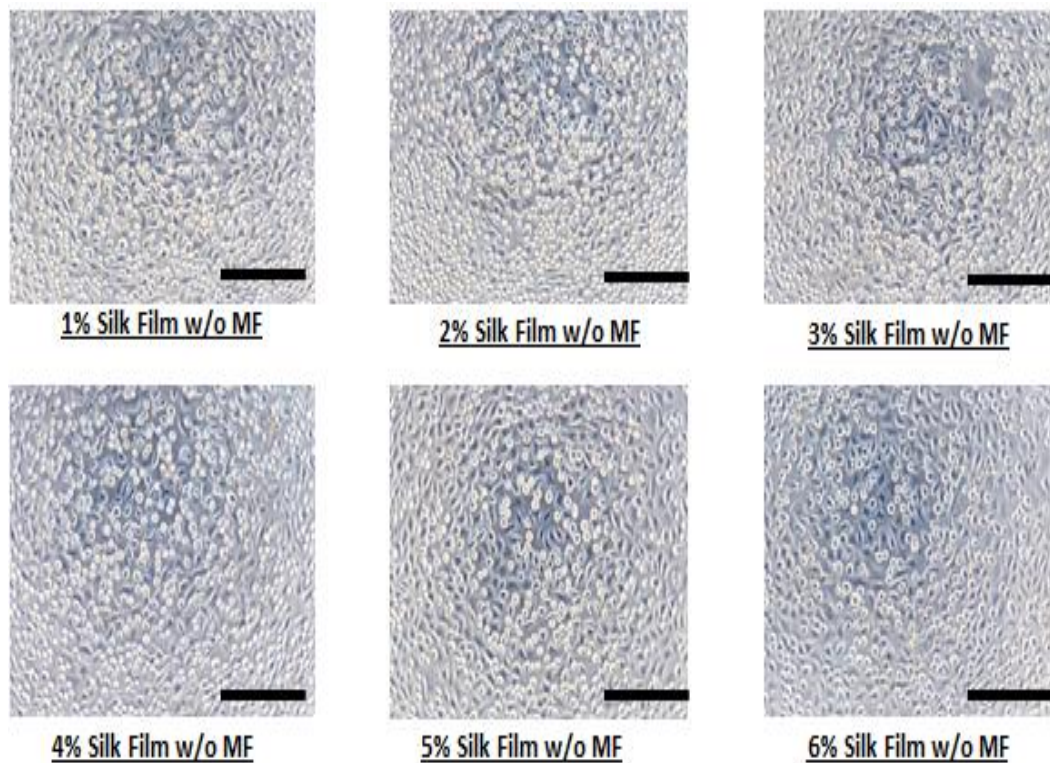


Figure 56: Microscopic images of attachment and proliferation of fibroblasts after exposure to dissolvable silk films (1 – 6%) in fibroblasts. (Scale bar = 10X Magnification).

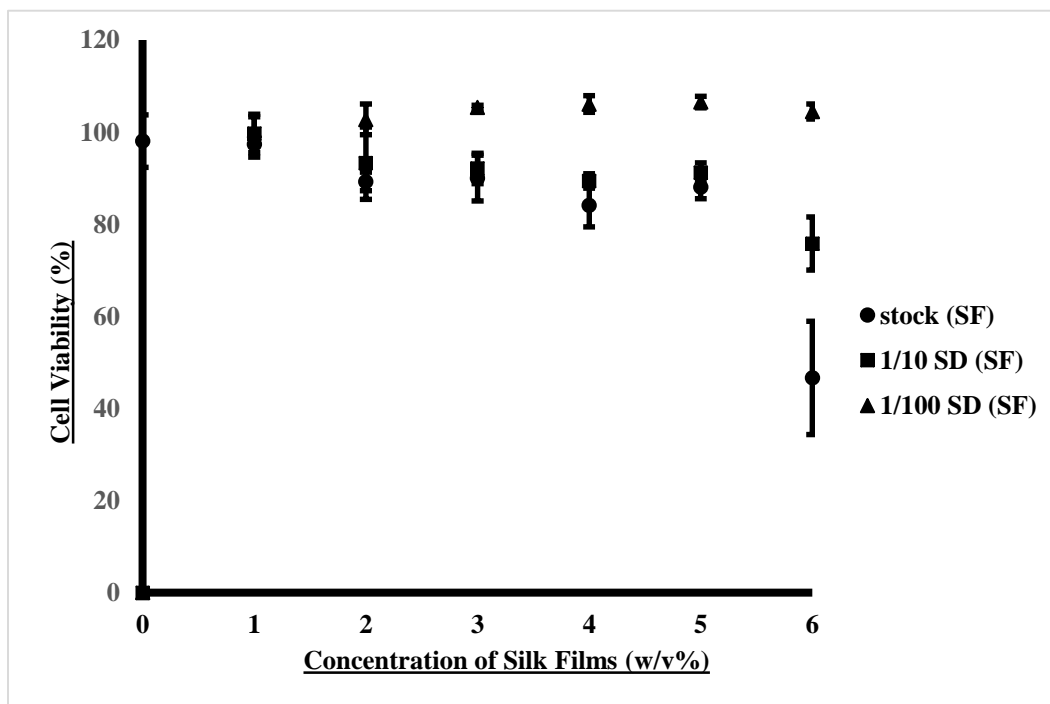


Figure 57: Quantitative assessment of cell viability from exposure of dissolvable silk films on fibroblasts (Error bars represent standard deviation of the samples; N=3).



# **CHAPTER 4: Discussion and Future**

## **Directions**

### **4.1. Discussion**

The goal of this study was to expand the clinical applications of silk films in the delivery of chemotherapeutics from water insoluble films to dissolvable films for oral mucosa delivery. Specifically, this entailed determining whether dissolvable silk films could not only meet the criteria for OFT products on the market, but also serve as a novel application for antimalarial chemotherapeutics using mefloquine hydrochloride as a candidate.

#### **4.1.1. Determining Drug Loading Efficiency of Dissolvable Silk Films**

The goal of this research was to ensure that mefloquine hydrochloride can be readily adsorbed into DSF. As mentioned in section 3.3., a preliminary study was conducted to determine if mefloquine hydrochloride would readily adsorb to silk fibroin protein. This was conducted with the use of water insoluble silk films of 4% (w/v) concentration. That study also showed drug loading greater than 80%. The highest drug load was observed in with 4% silk films. It was also determined that the concentration of silk fibroin in the films did not have a significant impact on the adsorption of mefloquine in films. This was corroborated by analyzing the morphologies of the silk films with the use of SEM imaging and FTIR analysis. In comparison to commercially available OFTs, drug

loading efficiency for products like Listerine Pocketpaks™ are currently unavailable. However, average drug load of commercial OFTs is 25mg. Maximum drug load for dissolvable silk films were not investigated in this study but future studies will investigate the maximum dosage of DSF as well as to determine of dosage similar to tablet formulation of mefloquine hydrochloride could be assessed. The results of this study show that 1 mg of mefloquine hydrochloride did not fully load into the silk films. However, there was still a very high drug loading efficiency of over 80%. Possibility of using a higher concentration of mefloquine stock solution could make drug loading of 1mg attainable.

#### **4.1.2. Determining Rate of Disintegration & Dissolution of Dissolvable Silk Films Doped with Mefloquine Hydrochloride**

Another goal of this research was fabricating DSFs that exhibited a mean cumulative release of ~ 95% for mefloquine hydrochloride as well as meeting the criteria of fast-dissolving films by disintegrating in less than 90 seconds. In this study, cumulative release > 100% was observed for DSFs ranging from 1 – 3% (w/v) while cumulative release for films ranging from 4 – 6% (w/v) was < 50%. This was corroborated by data observed from disintegration testing which will be discussed in further detail shortly. One prime cause for significant differences in rate of drug release of mefloquine detected between the two groups of films (1 – 3% vs 4 – 6% DSFs) is the possible increase in crystallinity induced by exposing the samples in 37°C with PBS. Aggregate formation was observed for all

samples at 37°C temperature compared to room temperature used for disintegration testing (22°C). Karve et al. (2011) determined that as  $\beta$ -sheet formation increased diffusion of small molecule (B-12 vitamin; MW = 1,355.37 g/mol) decreased. For this study, a similar observation was detected for mefloquine hydrochloride (MW = 414.77 g/mol). Water insoluble films with silk concentration > 4% have been studied as a form of slow-releasing films for chemotherapeutic treatment for up to 30 days *in vitro* (Coburn et al., 2015; Seib et al., 2015). This could also explain the low cumulative release of mefloquine from DSFs of 4% and greater within the very short time span of 30 mins.

As mentioned earlier, rate of disintegration for DSFs validated the rate of drug release for mefloquine hydrochloride. 1-3% (w/v) DSFs dissolved in less 90 seconds while max disintegration time of ~7 minutes was observed in 6% (w/v) DSFs (**Table 11**). The general characteristic rule of fabricating and determining the use oral films is that films that dissolve in less than 1 min - 1.5mins *in vitro* or in the oral cavity are considered to be “fast dissolving/orodispersible films” while films outside of this range are considered to be “slow-release” films (Borges et al., 2015; Dixit and Puthli, 2009; Sattar et al., 2014). The best commercial example of this is Listerine PocketPaks™, which dissolves in less than 35s once making contact within the oral cavity. Fabricated films with silk w/v% of 1-3% readily dissolve in media (PBS - pH 7; DiH<sub>2</sub>O - pH 7) within 10 seconds - 1.5 minutes while films with silk w/v% concentration of 4-6% are suited more for slow release *in vitro* since they fail to dissolve in fewer than 1.5 minutes. The study also demonstrated that cumulative release of at least 95% was possible for

DSFs. The discrepancy in data exhibiting cumulative release greater than 100% is attributed to the extraction technique of isolating small molecule from silk fibroin solution however, there may still be some trace silk protein in solution that was inadvertently collected. Future studies could investigate using more sensitive analytical tools such as high performance liquid chromatography equipped with a mass spectrometer for more sensitivity. Also, coming up with an efficient protocol that thoroughly extracts the small molecule from silk solution is needed, especially when examining samples with a UV-spectrophotometer. Finally, determining the mass transfer of mefloquine hydrochloride from DSFs by calculating permeability coefficient (Equation #3), diffusion coefficient (Equation #4), and partition coefficient ( $K_d$ ) (Equation #5) will help elucidate its effect on DSFs rate of diffusion for other small molecules.

$$J = C_0 \cdot P \quad (3)$$

$$D = \frac{P \cdot h}{k_d} \quad (4)$$

$$K_d = V_s \frac{(C_i - C_s)}{V_f C_s} \quad (5)$$

#### **4.1.3. Establishing Robustness of Dissolvable Silk Films for Packaging and Handling**

Another objective for this research was to characterize the mechanical properties of silk films from 1 – 6% (w/v) and determine if the films were as robust as commercially available OFTs. The purpose of characterizing the mechanical properties of OFTs is essential in ascertaining whether DSFs are simply capable of withstanding package and handling associated with the use of

these products. All of the mechanical characteristics investigated for silk films have either focused on films that have been treated (water-vapor, solvent, heat) or films blended with other dissolvable polymers (Kundu et al., 2008). This is the first study to solely focus on “as-casted” silk films and their mechanical robustness as DSFs for oral mucosa delivery.

Comparing mechanical properties of DSFs amongst the different concentration of silk, silk films with concentration of 1% - 2% would be classified as “hard and brittle polymeric films” based on their extremely high elastic modulus and tensile strength. However, when comparing mechanical properties observed for DSFs to mechanical properties of other commercial OFTs, only 6% DSFs (strain to failure% = 5.1%; range = 4.3 – 16%) was within the range reported for OFTs. This highlights a major issue in the regulation of OFTs, the lack of set FDA standards/criteria for OFTs. Only FDA regulations for OFTs are based on regulatory requirements established for formulating oral disintegrating tablets. The selection of instruments for mechanical testing varies, from the use of tensile testing instruments, like the one conducted in this study, to puncture tests which are mostly associated with investigating the characteristics of “soft materials”. Future studies to determine the robustness of DSFs should include folding endurance testing (also known as an “inconvenient stress-test”) and dryness/tack testing. Folding endurance testing involves folding samples at a center area until the film breaks (Dixit and Puthli, 2009). Dryness/tack testing helps determine the tenacity at which a strip adheres to an accessory, like a piece of paper, after it has been pressed into contact with the strip (Nagaraju et al.,

2013). Even though the mechanical properties observed in this study failed to be completely within range of commercially available OFTs, the lack of an industry standard for OFT fabrication prevents us from fully dismissing the robustness of DSFs. Examining individual samples in this study, further studies should investigate increasing the elasticity DSFs for 1 – 3% silk films (fast-dissolving) with the incorporation of plasticizers such as glycerol.

#### **4.1.4. Cytotoxicity Study of Dissolvable Silk Films with Mefloquine**

The final aim of this study, was to determine the safety of DSFs for potential clinical use. As mentioned in section 3.6, ISO 10993-5 is the industry standard in assessing biological response of mammalian cells from exposure to biomaterials for a period of 24hours at temperature of 37°C *in vitro*. Three groups were investigated, mefloquine stock solution, DSFs doped with mefloquine, and DSFs. All three groups exhibited some form of cytotoxicity to the fibroblast cells. However, it is important to indicate a number of issues that may have impacted the results observed in this study. One glaring issue is the cytotoxicity detected both qualitatively and quantitatively for DSFs (**Figures 56 & 57**). One of the main benefits for the use of silk films as a biomaterial is that it has been proven to be biocompatible *in vivo* (Vepari and Kaplan, 2007). One cause for the reduced cell viability for DSFs is most likely due to the formation of aggregates that were possibly transferred to the fibroblasts as a test extract. These aggregates would have caused cells detachment from the wells. This maybe simply due to not thoroughly centrifuging the samples and accidentally pipetting

the aggregates as part of the test extract sample. Another factor in the reduced viability is possible gelation of the silk films (DSFs > 1%) which may have coated the cells and decreased the diffusion of oxygen to the fibroblasts inducing necrosis of the cells. This could explain the reduction in cell viability for 6% DSFs. Similar issues have been observed for dissolution and disintegration testing (sections 3.2 & 3.4).

Evaluating the effects of the free drug and DSFs incorporating, cell death was observed until a 2X dilution of the samples was achieved. It is important realize that in the realm of this study these results should not be indicative of the actual cytotoxicity mefloquine and DSFs incorporating the drug are to fibroblasts. For this study, fibroblasts were exposed to the test extracts for a total of 24 hours. However, proposed clinical exposure of DSFs with mefloquine to the application site will be at a much shorter time period (1 – 1.5 minutes for fast-dissolving films). Since exceptions can be made to ISO 10993-5 for biomaterials used in short-term contact < 4 hours, future studies will look into accessing cytotoxicity of the free drug, DSFs, and DSFs incorporating mefloquine for time periods similar to their disintegration times (20 seconds to 10 minutes). The goal will be to show that DSFs are indeed biocompatible and can be applied for clinical use.

## **4.2. Future Directions**

### **4.2.1. Stability Testing of Dissolvable Silk Films**

One future prospect for this study is use of this drug in an areas plagued by malaria. Most of the locations are in regions that are hot with relatively high humidity where access to storage facilities equipped with refrigeration is limited. Examining the stability of newly fabricated DSFs with mefloquine according to the International Conference on Harmonisation of Technical Requirements for Registration of Pharmaceuticals for Human Use (ICH) guideline Q1A(R2) would be essential to determine its efficacy in these areas. The purpose of stability testing is to demonstrate the quality of DSFs with mefloquine due to the exposure to certain environmental factors such as temperature, humidity, and light. This will also for the determination of DSFs shelf-life and recommended storage (ICH, 2003). **Table 12** lists the testing conditions recommended by the ICH to help assess the stability for DSFs.



Table 12: Conditions for stability testing according to ICH. \*It is up to the applicant to decide whether long term stability studies are performed at  $25 \pm 2^\circ\text{C}/40\% \text{ RH}$  or  $30^\circ\text{C} \pm 2^\circ\text{C}/35\% \text{ RH} \pm 5\% \text{ RH}$ . \*\*If  $30^\circ\text{C} \pm 2^\circ\text{C}/35\% \text{ RH} \pm 5\% \text{ RH}$  is the long-term condition, there is no intermediate condition.

Study	Storage Conditions	Min. time period covered by data at submission
<b>Long term*</b>	$25^\circ\pm 2^\circ\text{C}/40\% \text{ RH} \pm 5\% \text{ RH}$ or $30^\circ\pm 2^\circ\text{C}/35\% \text{ RH} \pm 5\% \text{ RH}$	12 months
<b>Intermediate**</b>	$25^\circ\pm 2^\circ\text{C}/65\% \text{ RH} \pm 5\% \text{ RH}$	6 months
<b>Accelerated</b>	$40^\circ\pm 2^\circ\text{C}/$ not more than (NMT) 25% RH	6 months

#### 4.2.2. Effects of Degumming Time and Fabrication of Silk Films

This current study examined the various concentration of DSF from 1% to 6% w/v. One of the consistent factors between these concentrations are their degumming times which was 30minutes. Previous work on water insoluble films have fabricated films using this 30minutes as the degumming time of choice (Chiu et al., 2014; Coburn et al., 2015; Hines and Kaplan, 2013; Seib et al., 2015). A future aim would be to compare the disintegration times, mechanical testing, and rate of release of 30 minute boiled films to 45 minute and 60 minute boiled films. Pritchard et al in 2013 examined the effects that various degumming times (10 minutes, 30 minutes, 60 minutes, and 90 minutes) had on water insoluble films. As the degumming time of silk fibroin protein increased the molecular weight decreased while the rate of release from films increased over time. Future work can compare the rate of release, the mechanical properties, and the rate of disintegration of DSFs at various degumming times.

#### 4.2.3. Perfusion Studies of Silk Films with Oral Mucosa Models

Another aspect that should be considered is the use of models to investigate the perfusion rate of oral dissolving silk films. Development of perfusion cells have been used to study the absorption rate of small molecules like nicotine *in vitro*. Tissues from human biopsies and cadavers have also been used to study permeation of small molecules *in vitro*. Porcine models have also been used in studies due to histological characteristics that resemble human oral mucosal tissue (Sattar et al., 2014). **Table 13** is a list of small molecules and

proteins that have been studied with the use of porcine models for oral transmucosal drug delivery. There have also been cell culture lines created as an *in vitro* model for studying permeation of small molecules and proteins with the use of OFTs. One promising cell line in particular, EpiOral, is a three-dimensional tissue culture model which was derived from healthy human buccal keratinocytes (Sattar et al., 2014). Future work could investigate the absorption rate of the silk films with any of these models.

Drug	Type of study	Authors
(D-Ala <sup>2</sup> , D-Leu <sup>5</sup> )-enkephalin	In vitro	Lee and Kellaway (2000)
(D-Pen <sup>2</sup> , D-Pen <sup>5</sup> )-enkephalin	In vitro	Yuan et al. (2011)
5-aza-2'-deoxycytidine	In vitro	Mahalingam et al. (2007)
Acyclovir	In vitro	Shojaei et al., (1998)
Antipyrine	In vitro	Kulkarni et al. (2011)
Atenolol HCl	In vitro	Jacobsen (2001)
Bupivacaine	In vitro	Kulkarni et al. (2011)
Buserelin	In vivo	Hoogstraate et al. (1996)
Buspirone	In vitro	Birudaraj et al. (2005)
Caffeine	In vitro	Nicolazzo et al. (2004)
Calcitonin (salmon)	In vitro	Oh et al. (2011)
Carbamazepine	In vitro	Giannola et al. (2005)
Carvedilol	In vitro	Cappello et al. (2006)
Celecoxib	In vitro	Cid et al. (2012)
Chlorpheniramine maleate	In vitro	Sedhar et al. (2008)
Diazepam	In vitro	Meng-Lund et al. (2014)
Diclofenac sodium	In vitro	Miro et al. (2009)
Didanosine	In vitro	Ojewole et al. (2012)
Dideoxycytidine	In vitro	Shojaei et al., (1999)
Diltiazem hydrochloride	In vitro	Hu et al. (2011)
Domperidone	In vitro	Palem et al. (2011b)
Donazepil hydrochloride	In vitro	Caon et al. (2014)
Endomorphin-1	In vitro	Bird et al. (2001)
Felodipine	In vitro	Palem et al. (2011a)
Fentanyl	In vitro	Diaz Del Consuelo et al. (2005)
Flecainide	In vitro	Deneer et al. (2002)
Galantamine hydrobromide	In vitro	De Caro et al. (2008)
	In vivo	Giannola et al. (2010)
Insulin	In vitro	Das et al. (2012)
Lamotrigine	In vitro	Mashru et al. (2005b)
Lercanidipine hydrochloride	In vitro	Charde et al. (2008)
Methimazole	In vitro	De Caro et al. (2012)
Metoprolol	In vitro	Nielsen and Rassing (2000)
	In vivo	Holm et al. (2013)
Morphine hydrochloride	In vitro	Senel et al. (1998)
Naltrexone hydrochloride	In vitro	Giannola et al. (2007)
	In vivo	Campisi et al. (2010)
Nicotine	In vitro	Nair et al. (1997)
Nicotine hydrogen tartrate	In vitro	Hu et al. (2011)
Nimesulide sodium	In vitro	Maffei et al. (2004)
Nortestosterone	In vivo	Claus et al. (2007)
Oestradiol	In vitro	Nicolazzo et al. (2004)
	In vivo	Claus et al. (2007)
Omeprazole	In vitro	Figueiras et al. (2009)
Ondansetron hydrochloride	In vitro	Mashru et al. (2005a)
Phenylephrine	In vitro	Rao et al. (2011)
Phenytoin sodium	In vitro	Adeleke et al. (2010)
Pioglitazone	In vitro	Palem et al. (2011a)
Pituitary adenylate cyclase-activating polypeptide	In vitro	Langoth et al. (2005)
Pravastatin sodium	In vitro	Shidhaye et al. (2010)
Progesterone	In vitro	Jain et al. (2008)
Propranolol HCl	In vitro	Lee and Choi (2003)
Risperidone	In vitro	Heemstra et al. (2010)
Rizatriptan benzoate	In vitro	Avachat et al. (2013)
Ropinirole	In vitro	De Caro et al. (2012)
Salbutamol sulphate	In vitro	Puratchikody et al. (2011)
Saquinavir	In vitro	Rambharose et al. (2014a)
Sotalol	In vitro	Deneer et al. (2002)
Sumatriptan succinate	In vitro	Prasanna et al. (2011)
Tacrine	In vitro	Gore et al. (1998)
Tenofovir	In vitro	Rambharose et al. (2014b)
Testosterone	In vitro	Nielsen and Rassing (2000)
	In vivo	Claus et al. (2007)
Thiocolchicoside	In vitro	Artusi et al. (2003)
Transforming growth factor-beta	In vitro	Senel et al. (2000)

Table 13: Drugs studied with porcine models for oral transmucosal drug delivery (Sattar et al., 2014).

# BIBLIOGRAPHY

Ashton, Michael, Trinh Ngoc Hai, N D Sy, D X Huong, N Van Huong, N T Niêu, and L D Công. 1998. "Artemisinin Pharmacokinetics Is Time-Dependent during Repeated Oral Administration in Healthy Male Adults." *Drug Metabolism and Disposition: The Biological Fate of Chemicals* 26 (1): 25–27.

Borges, Ana Filipa, Cláudia Silva, Jorge F J Coelho, and Sérgio Simões. 2015. "Oral Films: Current Status and Future Perspectives II-Intellectual Property, Technologies and Market Needs." *Journal of Controlled Release* 206. Elsevier B.V.: 108–21. doi:10.1016/j.jconrel.2015.03.012.

Borges, Ana Filipa, Cláudia Silva, Jorge F.J. Coelho, and Sérgio Simões. 2015. "Oral Films: Current Status and Future Perspectives." *Journal of Controlled Release* 206. Elsevier B.V.: 1–19. doi:10.1016/j.jconrel.2015.03.006.

Campisi, G, C Paderni, R Saccone, O Di Fede, a Wolff, and L I Giannola. 2010. "Human Buccal Mucosa as an Innovative Site of Drug Delivery." *Current Pharmaceutical Design* 16 (6): 641–52. doi:10.2174/138161210790883778.

Chiu, B, J Coburn, M Pilichowska, C Holcroft, F P Seib, a Charest, and D L Kaplan. 2014. "Surgery Combined with Controlled-Release Doxorubicin Silk Films as a Treatment Strategy in an Orthotopic Neuroblastoma Mouse Model." *British Journal of Cancer* 111 (June). Nature Publishing Group: 1–8. doi:10.1038/bjc.2014.324.

Coburn, Jeannine M., Elim Na, and David L. Kaplan. 2015. "Modulation of Vincristine and Doxorubicin Binding and Release from Silk Films." *Journal*

- of Controlled Release* 220. Elsevier B.V.: 229–38.  
doi:10.1016/j.jconrel.2015.10.035.
- Dixit, R. P., and S. P. Puthli. 2009. “Oral Strip Technology: Overview and Future Potential.” *Journal of Controlled Release* 139 (2). Elsevier B.V.: 94–107.  
doi:10.1016/j.jconrel.2009.06.014.
- Dow, Geoffrey S, Thomas H Hudson, Maryanne Vahey, and Michael L Koenig. 2003. “The Acute Neurotoxicity of Mefloquine May Be Mediated through a Disruption of Calcium Homeostasis and ER Function in Vitro.” *Malaria Journal* 2: 14. doi:10.1186/1475-2875-2-14.
- Feucht, Cynthia, and Dilip R. Patel. 2011. “Principles of Pharmacology.” *Pediatric Clinics of North America* 58 (1): 11–19.  
doi:10.1016/j.pcl.2010.10.005.
- Ghosh, a., M. J. Edwards, and M. Jacobs-Lorena. 2000. “The Journey of the Malaria Parasite in the Mosquito: Hopes for the New Century.” *Parasitology Today* 16 (5): 196–201. doi:10.1016/S0169-4758(99)01626-9.
- Greenwood, Brian M, David a Fidock, Dennis E Kyle, Stefan H I Kappe, Pedro L Alonso, Frank H Collins, and Patrick E Duffy. 2008. “Review Series Malaria : Progress , Perils , and Prospects for Eradication” 118 (4).  
doi:10.1172/JCI33996.1266.
- Hines, Daniel J., and David L. Kaplan. 2013. “Characterization of Small Molecule Controlled Release from Silk Films.” *Macromolecular Chemistry and Physics* 214 (2): 280–94. doi:10.1002/macp.201200407.
- Hoffmann, Eva Maria, Armin Breitenbach, and Jörg Breitreutz. 2011.

- “Advances in Orodispersible Films for Drug Delivery.” *Expert Opinion on Drug Delivery* 8 (3). Taylor & Francis: 299–316.  
doi:10.1517/17425247.2011.553217.
- ICH. 2003. “ICH Topic Q1A (R2) - Stability Testing of New Drug Substances and Products.” *International Conference on Harmonization*, no. February: 24. doi:10.1136/bmj.333.7574.873-a.
- “Karbawang, J and White, N.J., 1990, Clinical Pharmacokinetics of Mefloquine.pdf.” n.d.
- Krettli, Antoniana U., and Louis H. Miller. 2001. “Malaria: A Sporozoite Runs through It.” *Current Biology* 11 (10): 409–12. doi:10.1016/S0960-9822(01)00221-4.
- Kundu, Joydip, Chinmoy Patra, and S. C. Kundu. 2008. “Design, Fabrication and Characterization of Silk Fibroin-HPMC-PEG Blended Films as Vehicle for Transmucosal Delivery.” *Materials Science and Engineering C* 28 (8). Elsevier B.V.: 1376–80. doi:10.1016/j.msec.2008.03.004.
- Lawrence, Brian D., Fiorenzo Omenetto, Katherine Chui, and David L. Kaplan. 2008. “Processing Methods to Control Silk Fibroin Film Biomaterial Features.” *Journal of Materials Science* 43 (21): 6967–85.  
doi:10.1007/s10853-008-2961-y.
- Lu, Q, B Zhang, M Li, B Zuo, D L Kaplan, Y Huang, and H Zhu. 2011. “Degradation Mechanism and Control of Silk Fibroin.” *Biomacromolecules* 12: 1080–86. doi:10.1021/bm101422j.
- Lu, Qiang, Xiaoqin Wang, Xiao Hu, Peggy Cebe, Fiorenzo Omenetto, and David

- L. Kaplan. 2010. "Stabilization and Release of Enzymes from Silk Films." *Macromolecular Bioscience* 10 (4): 359–68. doi:10.1002/mabi.200900388.
- Lu, S, X Wang, Q Lu, X Hu, N Uppal, F G Omenetto, and D L Kaplan. 2009. "Stabilization of Enzymes in Silk Films." ... 10: 1032–42 ST – Stabilization of enzymes in silk f. doi:10.1021/bm800956n.
- Lu, Shenzhou, Xiaoqin Wang, Qiang Lu, Xiaohui Zhang, Jonathan a. Kluge, Neha Uppal, Fiorenzo Omenetto, and David L. Kaplan. 2010. "Insoluble and Flexible Silk Films Containing Glycerol." *Biomacromolecules* 11 (1): 143–50. doi:10.1021/bm900993n.
- MacPherson, G. G., M. J. Warrell, N. J. White, S. Looareesuwan, and D. a. Warrell. 1985. "Human Cerebral Malaria. A Quantitative Ultrastructural Analysis of Parasitized Erythrocyte Sequestration." *The American Journal of Pathology* 119 (3): 385–401. doi:10.1002/jmor.1051840203.
- Madhav, N V Satheesh, Ashok K Shakya, Pragati Shakya, and Kuldeep Singh. 2009. "Orotransmucosal Drug Delivery Systems: A Review." *Journal of Controlled Release : Official Journal of the Controlled Release Society* 140 (1): 2–11. doi:10.1016/j.jconrel.2009.07.016.
- Mashru, R. C., V. B. Sutariya, M. G. Sankalia, and P. P. Parikh. 2008. "Development and Evaluation of Fast-Dissolving Film of Salbutamol Sulphate." *Drug Development and Industrial Pharmacy*, September. Taylor & Francis. <http://www.tandfonline.com/doi/abs/10.1081/DDC-43947?journalCode=iddi20#.Vvs-h0KOhF0.mendeley>.
- Nagaraju, T, R Gowthami, M Rajashekar, S Sandeep, M Mallesham, D Sathish,



- and Y Shravan Kumar. 2013. "Comprehensive Review on Oral Disintegrating Films." *Current Drug Delivery* 10 (1): 96–108. doi:10.2174/1567201811310010016.
- P. J. Rosenthal. 2001. *Anti- Malarial Chemotherapy: Mechanisms of Action, Resistance, and New Directions in Drug Discovery. Journal of Chemical Information and Modeling*. Vol. 53. doi:10.1017/CBO9781107415324.004.
- Patel, Viralkumar F., Fang Liu, and Marc B. Brown. 2011. "Advances in Oral Transmucosal Drug Delivery." *Journal of Controlled Release* 153 (2). Elsevier B.V.: 106–16. doi:10.1016/j.jconrel.2011.01.027.
- Preis, Maren, Joerg Breitzkreutz, and Niklas Sandler. 2015. "Perspective: Concepts of Printing Technologies for Oral Film Formulations." *International Journal of Pharmaceutics* 494: 578–84. doi:10.1016/j.ijpharm.2015.02.032.
- Preis, Maren, Miriam Pein, and Jörg Breitzkreutz. 2012. "Development of a Taste-Masked Orodispersible Film Containing Dimenhydrinate." *Pharmaceutics* 4 (4): 551–62. doi:10.3390/pharmaceutics4040551.
- Preis, Maren, Christina Woertz, Peter Kleinebudde, and Jörg Breitzkreutz. 2013. "Oromucosal Film Preparations: Classification and Characterization Methods." *Expert Opinion on Drug Delivery* 10 (9): 1303–17. doi:10.1517/17425247.2013.804058.
- Rockwood, D N, R C Preda, T Yucel, X Wang, M L Lovett, and D L Kaplan. 2011. "Materials Fabrication from Bombyx Mori Silk Fibroin." *Nat Protoc* 6 (10): 1612–31. doi:10.1038/nprot.2011.379.
- Rogers, W O, a Malik, S Mellouk, K Nakamura, M D Rogers, a Szarfman, D M

- Gordon, a K Nussler, M Aikawa, and S L Hoffman. 1992. "Characterization of Plasmodium Falciparum Sporozoite Surface Protein 2." *Proceedings of the National Academy of Sciences of the United States of America* 89 (19): 9176–80. doi:10.1073/pnas.89.19.9176.
- Santos-Magalhães, Nereide Stela, and V. C F Mosqueira. 2010. "Nanotechnology Applied to the Treatment of Malaria." *Advanced Drug Delivery Reviews* 62 (4-5). Elsevier B.V.: 560–75. doi:10.1016/j.addr.2009.11.024.
- Sattar, Mohammed, Ossama M. Sayed, and Majella E. Lane. 2014. "Oral Transmucosal Drug Delivery - Current Status and Future Prospects." *International Journal of Pharmaceutics* 471 (1-2). Elsevier B.V.: 498–506. doi:10.1016/j.ijpharm.2014.05.043.
- Saunders, David L., Eric Garges, Jessica E. Manning, Kent Bennett, Sarah Schaffer, Andrew J. Kosmowski, and Alan J. Magill. 2015. "Safety, Tolerability, and Compliance with Long-Term Antimalarial Chemoprophylaxis in American Soldiers in Afghanistan." *American Journal of Tropical Medicine and Hygiene* 93 (3): 584–90. doi:10.4269/ajtmh.15-0245.
- Seib, F. Philipp, Jeannine Coburn, Ilona Konrad, Nikolai Klebanov, Gregory T. Jones, Brian Blackwood, Alain Charest, David L. Kaplan, and Bill Chiu. 2015. "Focal Therapy of Neuroblastoma Using Silk Films to Deliver Kinase and Chemotherapeutic Agents *in Vivo*." *Acta Biomaterialia* 20. Acta Materialia Inc.: 32–38. doi:10.1016/j.actbio.2015.04.003.
- Seib, F. Philipp, and David L. Kaplan. 2013. "Silk for Drug Delivery

- Applications: Opportunities and Challenges.” *Israel Journal of Chemistry* 53 (9-10): 756–66. doi:10.1002/ijch.201300083.
- Seib, F. Philipp, Manfred F. Maitz, Xiao Hu, Carsten Werner, and David L. Kaplan. 2012. “Impact of Processing Parameters on the Haemocompatibility of Bombyx Mori Silk Films.” *Biomaterials* 33 (4). Elsevier Ltd: 1017–23. doi:10.1016/j.biomaterials.2011.10.063.
- Shah, Sonia. 2010. *The Fever: How Malaria Has Ruled Mankind for 500,000 Years*. 1st ed. New York: Sarah Crichton Books.
- Shretta, Rima, and Prashant Yadav. 2012. “Stabilizing Supply of Artemisinin and Artemisinin-Based Combination Therapy in an Era of Wide-Spread Scale-Up.” *Malaria Journal* 11 (1). Malaria Journal: 399. doi:10.1186/1475-2875-11-399.
- SINDEN, R. E., and R. H. HARTLEY. 1985. “Identification of the Meiotic Division of Malarial Parasites.” *The Journal of Protozoology* 32 (4): 742–44. doi:10.1111/j.1550-7408.1985.tb03113.x.
- Skórska, Agnieszka, Jan Sliwiński, and Barbara J Oleksyn. 2006. “Conformation Stability and Organization of Mefloquine Molecules in Different Environments.” *Bioorganic & Medicinal Chemistry Letters* 16 (4): 850–53. doi:10.1016/j.bmcl.2005.11.016.
- Syafruddin, Ryo Arakawa, Kiyoshi Kamimura, and Fumihiko Kawamoto. n.d. “Penetration of the Mosquito Midgut Wall by the Ookinetes of *Plasmodium Yoelii Nigeriensis*.” *Parasitology Research* 77 (3): 230–36. doi:10.1007/BF00930863.

- TORII, MOTOMI, KEI-ICHIRO NAKAMURA, KLAUS P. SIEBER, LOUIS H. MILLER, and MASAMICHI AIKAWA. 1992. "Penetration of the Mosquito ( *Aedes Aegypti* ) Midgut Wall by the Ookinetes of *Plasmodium Gallinaceum*." *The Journal of Protozoology* 39 (4): 449–54.  
doi:10.1111/j.1550-7408.1992.tb04830.x.
- Turley, Susan M. 2009. "Routes of Administration and the Drug Cycle." *Understanding Pharmacology for Health Professionals, Fourth Edition*.
- Vepari, Charu, and David L. Kaplan. 2007. "Silk as a Biomaterial." *Progress in Polymer Science (Oxford)* 32 (8-9): 991–1007.  
doi:10.1016/j.progpolymsci.2007.05.013.
- Weber, J L. 1988. "Molecular Biology of Malaria Parasites." *Experimental Parasitology* 66 (2): 143–70.
- World Health Organisation. 2014. "World Malaria Report 2014."  
doi:10.1007/s00108-013-3390-9.